A NOVEL METHOD FOR METAL RECOVERY FROM ZINC FUMING SLAGS

by

Fengxiang He

B. Eng., Kunming University of Science and Technology, P. R. China, 1985
M. Eng., Kunming University of Science and Technology, P. R. China, 1988

A THESIS SUBMITTED IN PARTIAL FULFILLMENT OF
THE REQUIREMENTS FOR THE DEGREE OF
MASTER OF APPLIED SCIENCE

in

THE FACULTY OF GRADUATE STUDIES
DEPARTMENT OF METALS AND MATERIALS ENGINEERING

We accept this thesis as conforming
to the required standard

THE UNIVERSITY OF BRITISH COLUMBIA

November 2000

In presenting this thesis in partial fulfilment of the requirements for an advanced degree at the University of British Columbia, I agree that the Library shall make it freely available for reference and study. I further agree that permission for extensive copying of this thesis for scholarly purposes may be granted by the head of my department or by his or her representatives. It is understood that copying or publication of this thesis for financial gain shall not be allowed without my written permission.

Department of METALS AND MATERIALS

The University of British Columbia
Vancouver, Canada

Date Feb. 28, 2001

ABSTRACT

In typical zinc & lead production operations, lead blast furnace slags and zinc leaching residues are usually fumed to recover zinc metal. Regardless of the fuming methods employed, the tail slag from zinc fuming furnaces still contains about 3 per cent or more zinc and some trace amounts of elements such as lead, indium and germanium.

Although by traditional measures the contents of Zn, Pb, and the rarer elements In and Ge are very low, in absolute terms there is still the potential to extract considerable value from these remaining metals. As well, the elimination of these heavy metals from the slag would go even further in ensuing that the slags can be used as cement additives, landfill, roadbed material, etc. without environmental ramifications.

A new electrochemical process, similar to the Hall-Héroult process in aluminum production, has been proposed for the recovery of metal values from this slag. Based on thermodynamic analysis and F*A*C*T calculations, copper melt was chosen as the cathode because it significantly decreases the activity of zinc while increasing the activity of iron. The results of synthetic slags (24.4 pct-Fe 39 pct-SiO_2 17 pct-CaO 6 pct-Al_2O_3 2 pct-Zn) at 1250 °C revealed that 1) even without passing a direct current, a certain amount of zinc was diffused into the copper melt by the predicted thermodynamic driving force; 2) zinc was continuously deposited into the copper melt by electrochemical reaction when the voltage difference between the electrodes was 4 volts or greater. The effects of temperature and basicity on the process have also been studied. By the results of Fe^{2+}/Fe^{3+} analysis and SEM examinations, possible reaction mechanism have also been suggested. The as-received ***Cominco*** tail slags were also examined by electrolysis.

TABLE OF CONTENTS

LIST OF FIGURES

LIST OF TABLES

ACKNOWLEDGMENT

I would like to acknowledge the help of the many people who with their direct and indirect help and advice have contributed to the project.

First, my thanks to Dr. Ray Meadowcroft, for providing me the opportunity to work with him in UBC. His advise, expertise and encouragement throughout the project have made it both a memorable and enjoyable learning experience.

I would also like to thank ***Cominco Research***, especially Dr. Mike Fairweather and Greg Richards, for their help of chemical analysis and detailed discussions.

Mr. Peter Musel, has provided invaluable support in form of building the experimental apparatus and helping in running experiments, to keep the project moving forward. His support and companionship is greatly acknowledged and will be cherished for a long time. Thanks are also due to many faculty, staff and fellow graduate students in the Department of Metals and Materials Engineering.

Financial support for this work by the ***Natural Sciences and Engineering Research Council of Canada*** (NSERC) and ***Cominco Research*** is gratefully acknowledged.

1. INTRODUCTION

The tail slags of interest in this research are generated from the slag fuming furnaces in zinc & lead production operations. The slag is basically a silicate, which contains about 30 pct-Fe, 30 pct-SiO_2, 17 pct-CaO, 3 pct-ZnO, 0.05 pct-Pb and some trace Cd, In, and Ge. A typical zinc & lead producer such as ***Cominco*** has an output of 160,000 tonnes of this slag annually.[1] The concentration of zinc in this slag is usually higher than the 3% published value due to the fuming operations being difficult to maintain at the optimum conditions.

Although by traditional measurements the contents of Zn, Pb, and the rarer elements Cd, In and Ge are very low, in absolute terms there is still the potential to extract considerable metal values from these remaining metals. As well, the elimination of these heavy metals from the slag would go even further in ensuring that the slags can be used as cement additives, landfill, roadbed material, etc. without environmental ramifications.

Conventional pyrometallurgical methods[2-7] for zinc-bearing slags and residues are not suitable for tail slag treatment because 1) the zinc content is too low to be recovered economically; 2) there are some problems, such as iron metal formation and slag foaming, that will occur if the zinc content in slag drops too much. On the other hand, if a hydrometallurgical route[8,9] is employed, a substantial portion of iron dissolution will impede its further application. Therefore, a new method is needed for the further treatment of the zinc fuming tail slag.

2. COMINCO TAILING SLAG AND CHARACTERIZATION

Cominco operates a large integrated lead-zinc smelter in Trail, British Columbia, Canada. An overview of the metallurgical circuit of Trail Operations is given in Figure 1.The zinc plant is a typical roast-leach-electrowinning process with an integrated pressure leaching facility providing approximately 20% of Trail's zinc production. Most of the zinc plants around the world are stand-alone operations and have adopted hydrometallurgical processes for the treatment of the residues from weak acid leaching. Invariably, these processes incorporate a hot acid leach to dissolve the zinc ferrites, which are formed during concentrate roasting. Iron is precipitated and rejected from the circuit as either jarosite, goethite or hematite. Cominco has taken a different approach. Instead of hydrometallurgical processing, weak acid leach residues are treated pyrometallurgically in the lead smelter. Zinc is recovered in a slag-fuming step, where it is vaporized into the gas phase and collected as fume, and is returned to the zinc plant.

After the commissioning of the Kivcet process for the production of lead in 1996, the production capacity was expanded to 290,000 t/y and 120,000 t/y for zinc and lead respectively. Consequently, the output of tailing slag from the slag fuming furnaces will be in the order of 500-600 tonnes per day. The tailing slag, exiting at roughly 1200 °C and water quenched to a particle size of less than 4 mm, is the residue of the process. It is called "residue" because by traditional measures the contents of Zn, Pb, and the rarer elements In and Ge are too low to be worth recovering.

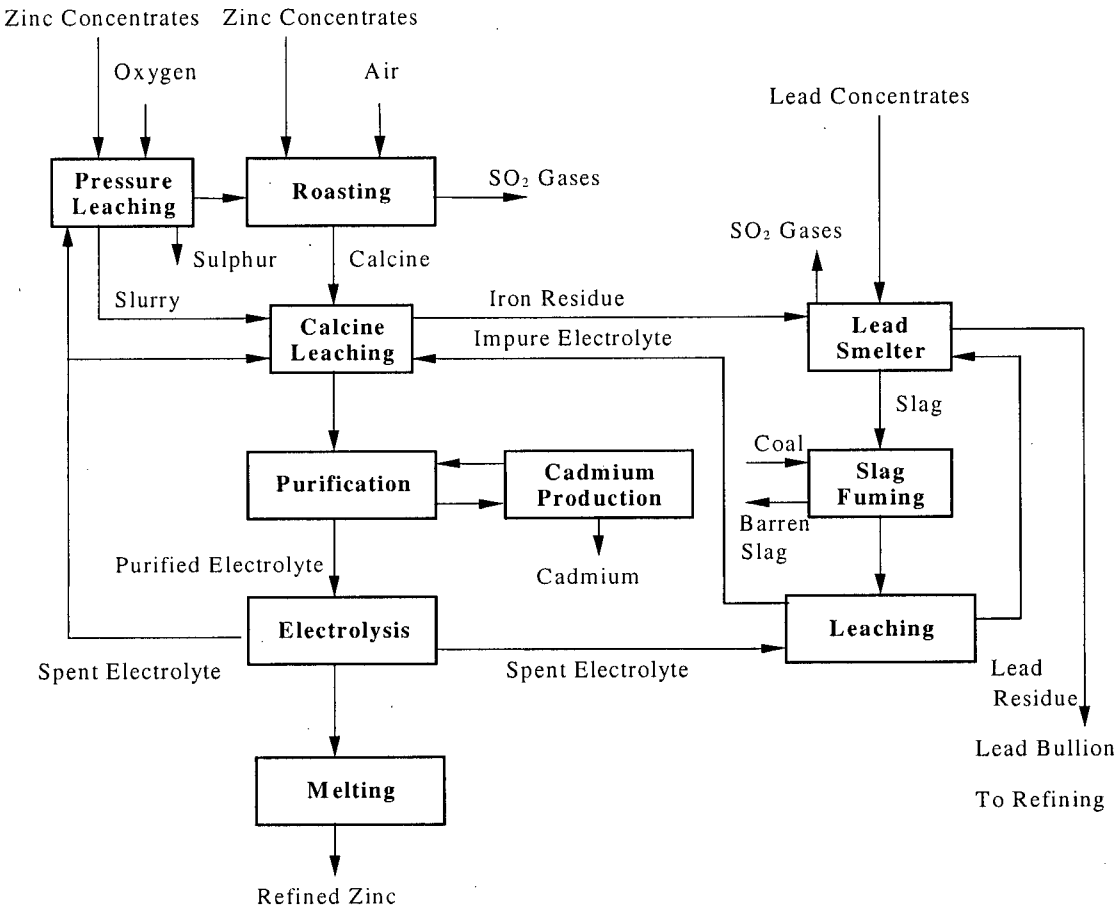

Fig. 1 — Overview of *Cominco*'s Trail Operations[9]

The slag fumer may be either a batch or continuous operation. Generally, the tailing slag from continuous operation has a higher zinc content than that from a batch operation[3,10]. An average of 2.38 percent Zn was obtained from publications for tailing slags from batch operations.

For this study, as-received slag samples from ***Cominco*** were sent to both ***Cominco*** and ***IPL*** (International Plasma Lab Ltd., Vancouver, B.C. Canada) for chemical composition analysis. Results are summarized in Table I.

Table I. Chemical Composition of *Cominco* Fumer Slag - Fe^{2+}/Fe^{3+}

By *Cominco* Research						
Wt.(%)	**Fe**	**SiO_2**	**Al_2O_3**	**CaO**	**Cu**	**Zn**
	28.9	**28.6**	**2.8**	**18.2**	**0.26**	**4.6**

By *IPL*(International Plasma Lab Ltd.)							
Wt.(%)	**Fe^{2+}**	**Fe^{3+}**	**SiO_2**	**Al_2O_3**	**CaO**	**Cu**	**ZnO**
	27.45	**2.87**	**30.82**	**3.05**	**17.45**	**0.36**	**5.7**

The results from the two analyzers(***Cominco*** and ***IPL*** respectively) are in agreement. Both of the results showed that the zinc content was about 5%, which is much higher than 2.38% - the average value from publication. The iron valence analysis indicated that about 90% of the iron existed in the ferrous state; in other words, the slag was produced under very strong reduction conditions, as would be expected in the fuming operation.

The as-received ***Cominco*** tail slag was also analyzed using SEM, BSE, EDS and XRD to identify the particle size distribution and species present in the slag. It was observed that the slag particles were heterogeneous, and that the maximum dimension of most of the slag particles was less than 3 mm (Figure 2). The many cracks inside the slag particles indicate that it is very porous due to the water-quench operation. Almost all the slag particles present in the polished sections were grey, dull minerals, with very poor reflectivity. Almost no crystals were found in the slag section examinations (Figure 3). As confirmed by XRD analysis, the slag was in a glassy state (Figure 4).

Very shiny, bright spots were observed in the cross section samples (Figure 5, 6, 7). BSE and EDS examination shown that they are lead alloy particles – lead alloyed with antimony, copper, iron and arsenic (Figure 8).

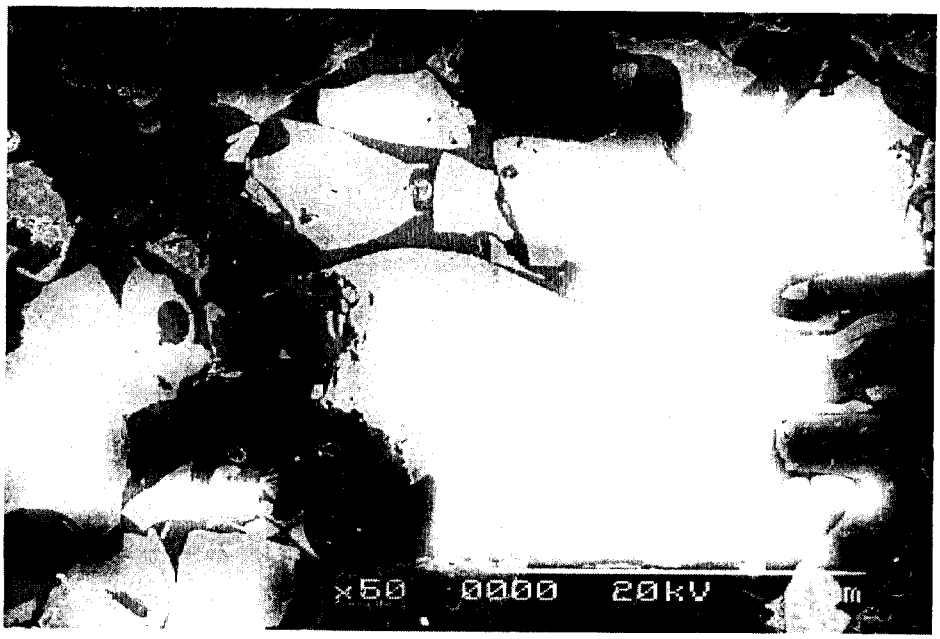

Fig. 2 —General view of as-received Cominco tail slag (SEM, magnification 50, accelerating voltage 20kV) shows the particle size distribution

Fig. 3 — Close-up shows the as-received Cominco tail slag is homogeneous (SEM, magnification 800, accelerating voltage 20kV). Confirmed by XRD, it is in a glassy state.

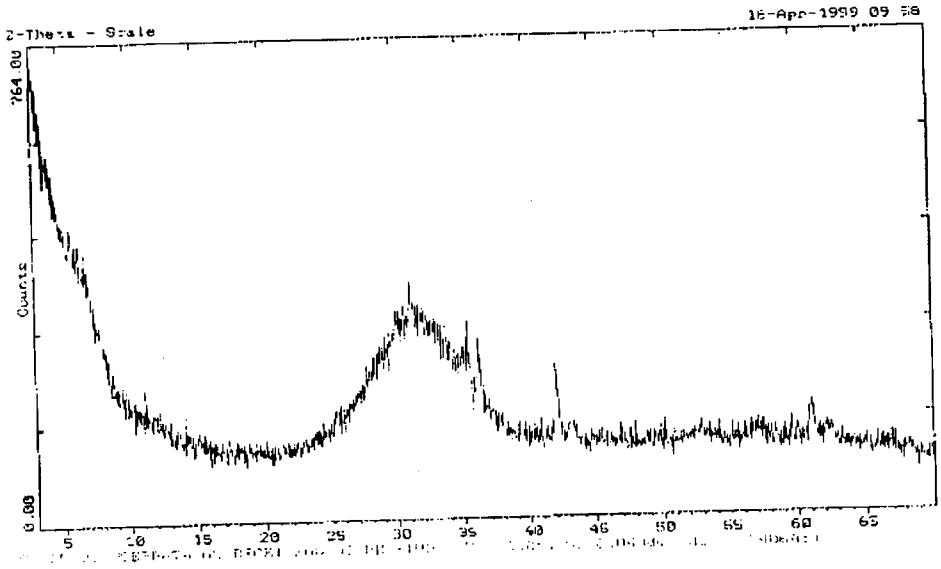

Fig. 4 — X-ray diffraction pattern of Cominco tail slag showing it is in a glassy state

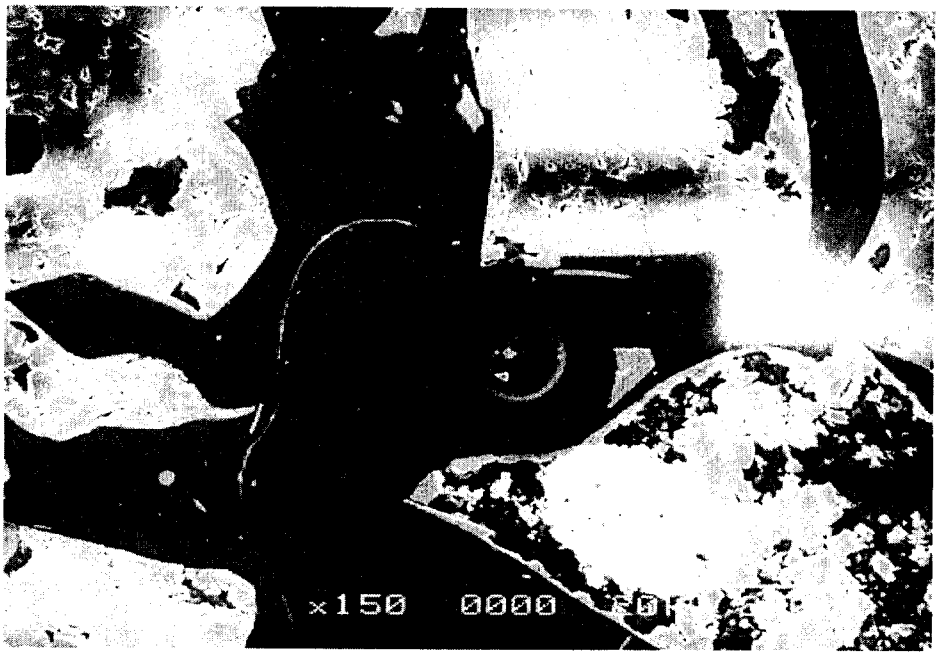

Fig. 5 — Cracks and white beads in as-received Cominco tail slag(SEM, magnification 150, accelerating voltage 20kV)

Fig. 6 — Another white bead in Cominco tail slag (SEM, magnification 100, accelerating voltage 20kV)

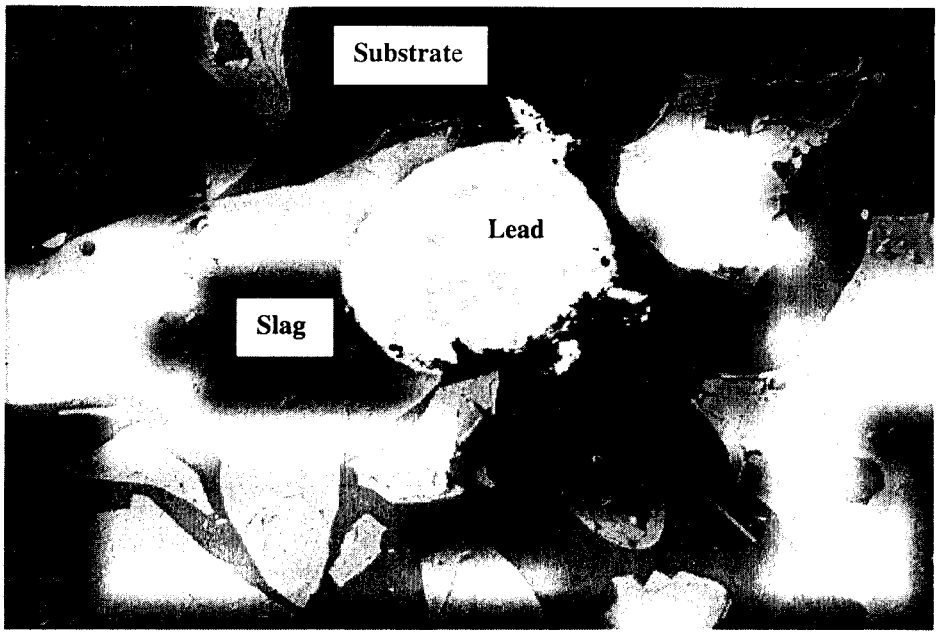

Fig. 7 — BSE examination of Figure 6 showing Lead alloy particles existing in Cominco tail slag (BSE, magnification 100, accelerating voltage 20kV)

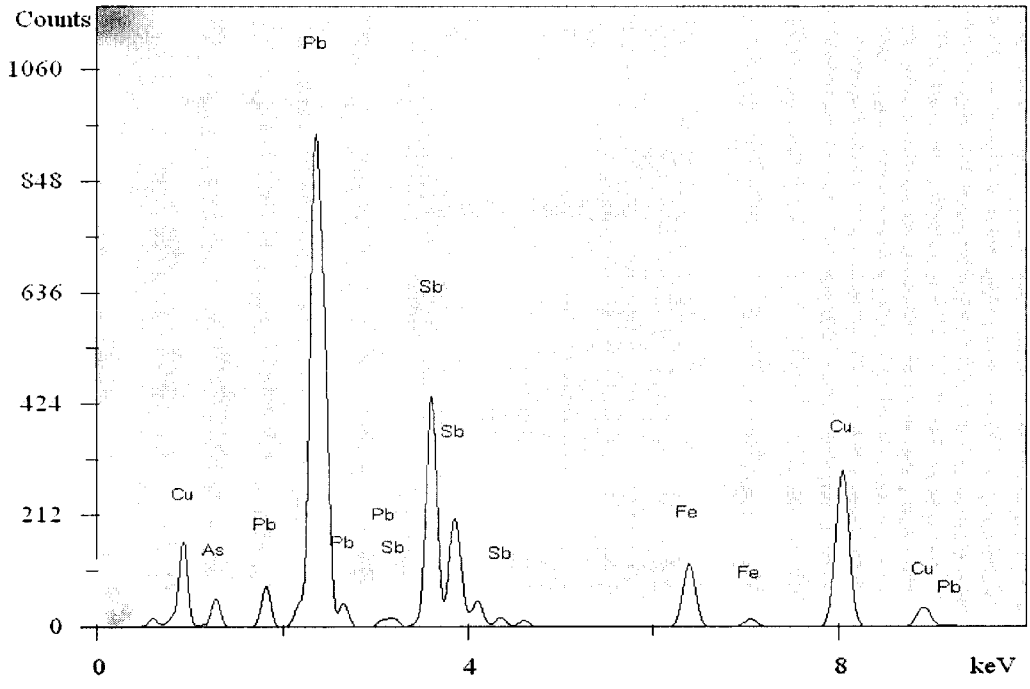

Fig. 8 — EDS(Energy Dispersive Spectrum) examination of the white spot in Figure 5 indicated it is an alloy of Pb, Sb, Fe, Cu, As and some other elements

It was observed that some dendrites precipitate out from the slag matrix as individual crystals with very sharp edges (Figure 9), although this was not common. EDS examination showed that this was iron oxide (Figure 10, 11), which might be magnetite. Other researchers[11,12] also found that dendrites of magnetite exist in slow cooled fuming slags. Our research indicated that the quantity of this phase is very small, which is in agreement with the fact that the percentage of ferric iron is only about 10% and the slag is in a glassy state.

Iron was present in various forms in the fuming slags. Some of the iron was alloyed into the metal lead bead, and as mentioned above, some of the iron existed in dendritic magnetite; however, most of the iron was in the slag matrix, primarily as ferrous iron.

Fig. 9 — Dendrites exist in as-received Cominco tail slag (BSE, magnification 988, accelerating voltage 15kV)

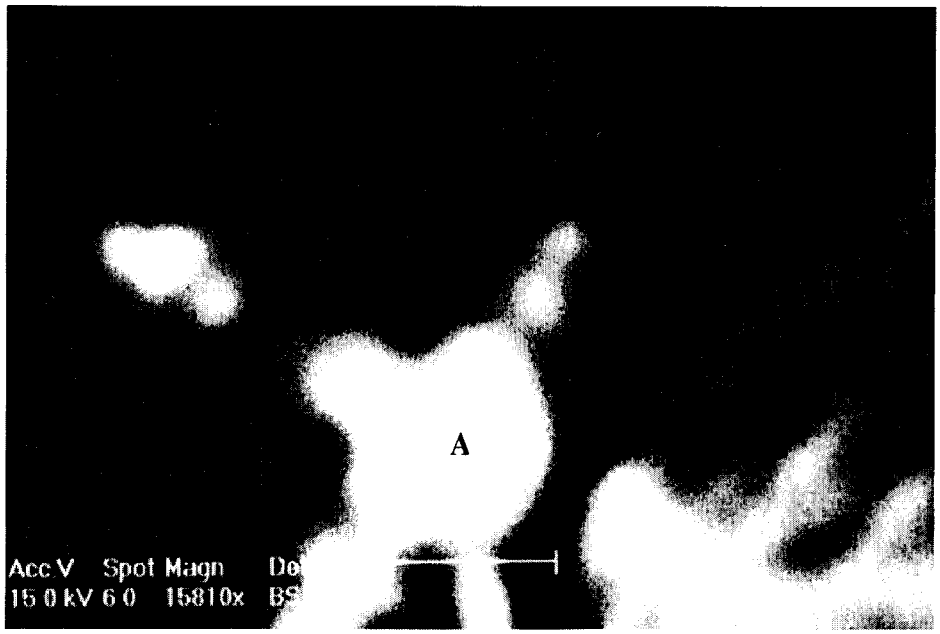

Fig. 10 — Close-up of a dendrite in previous picture (BSE, magnification 1581, accelerating voltage 15kV). Spot A is the point for EDS examination of Figure 11.

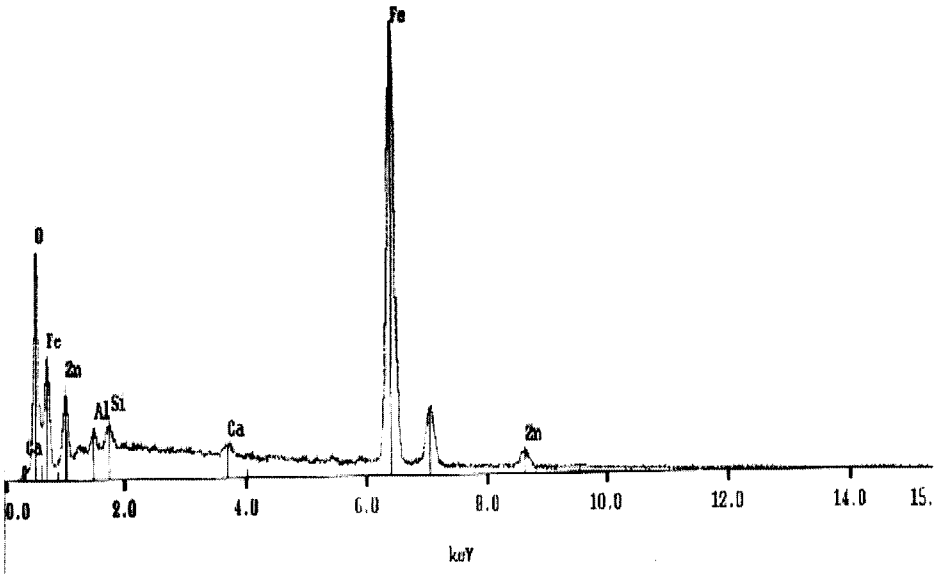

Fig. 11 — EDS examination of the dendrites shown it is mainly iron oxides

3. LITERATURE SURVEY

3.1. Pyrometallurgical Processes for Zinc-bearing Slags and Residues

In the non-ferrous smelting industry, the development of new processes such as flash smelting and the Kivcet process has been focused on methods to intensify the extraction of non-ferrous metals. One of the disadvantages of these processes is the corresponding slag usually contains relatively higher metal content. Consequently, slag treatment is an inevitable step for metal recovery from these slags. Slag treatment is usually carried out by a pyrometallurgical process. Depending on the physical-chemical properties of the metals of interest, they are either fumed and collected as dust, or settled into the metal phase at quiescent conditions. Many furnace types are used including: 1) water-jacketed fuming furnaces for tin smelting slags; 2) electrical resistance furnaces for copper smelting slags; 3) Ausmelt furnace for tin, lead smelting slags.

Both the melting and boiling temperatures for zinc metal are very low, only 419.5 °C and 907 °C respectively. This is the main reason why zinc-bearing slags are treated by fuming processes. As iron reduction is unavoidable when the zinc content in the slag is too low, say below 1%, iron metal could form and the slag will become foaming. There are several fuming methods in commercial operation in the world, as described below.

- Water-jacketed Fumer

The zinc fuming process conducted in a rectangular, water-jacketed furnace is the most common method for lead blast furnace slag treatment (Appendix I). The first commercial development of the process was made by the Anaconda Copper Mining Co. and the Consolidated Mining and Smelting Co. in the 1920's[13-15]. The first furnace was blown in at the Anaconda Smelter, East Helena, Montana in December 1927. The process has changed little in the intervening decades.

Lead blast furnace slags contain 11 to 18 pct Zn normally are reduced to 1.5 to 2.5 pct Zn in a fuming cycle of about 3 hours including 30 minutes for charging and tapping. The recovery of zinc from the slag is 85 to 90 pct and requires 1 to 2 kg coal per kg zinc (3.3 to 6.5 kg-moles C per kg-mol Zn). Recovery of lead is always near 100 pct. In addition the fume contains traces of tin, indium, cadmium, sulfur, chlorine, and fluorine.

Since its inception, slag fuming has undergone little general alternation. The major developments—blast preheat, continuous fuming with fuel oil, and fuming with natural gas—have been implemented at individual plants but have not been adopted widely.

According to the publication of Snelgrove and Taylor[7], when slag fuming is part of the circuit to recover zinc, it is not necessary to produce as clean a slag as would be the case when the zinc content is too low, say less than 10%, for economic recovery.

- Ausmelt Fumer

The Ausmelt process was named "Siromelt" at the very beginning of its development for the smelting of tin concentrates in the early seventies[11] by ***CSIRO*** (Commonwealth Scientific and Industrial Research Organization), an Australian organization. In 1980, the main researchers left ***CSIRO*** to form Ausmelt, to commercially develop and market the technology. The process involves injecting fuel, either gaseous or liquid, through a lance into a molten bath of slag or concentrate. The injection of large volumes of gases results in extremely fast rates of reaction due to enhanced mass transfer rates. The presence of large volumes of gases also provides for excellent fuming conditions, which helps in the removal of volatile species such as lead, zinc, and cadmium. Since the mid-eighties, the process had found successful commercial applications. A summary of the commercial plants in operation is given in Appendix II. After Ausmelt treatment, the final tail slag contains about 4 per cent of zinc, as shown in Table II.

Table II. Zinc Content in Slag after Ausmelt Treatment[2]

	QSL Slag		**ISP Slag**		**Zinc Leach Residues**			
					Pre			After
	Pre	After	Pre	After	Goethite	Primary	Jarosite	
Zn%	13 - 15	5 - 7	6 - 8	2 - 3	13	22	5	3 - 4

- Waelz Kiln Fumer

Waelz kilns are by far the major process technology used for treating neutral leach residues. In fact, there are more than 30 Waelz kilns in operation around the world, with the majority in the former USSR[16].

E. Dedolph at Kaslo, B.C., Canada[16] in 1909 was the first person to suggest the use of a rotary kiln for the volatilization of zinc and lead. The Lurgi Group of companies in Germany acquired the patent and developed the process. The first large scale Waelz plant was started in 1925 at Kayser, Lünen, Germany for the treatment of lean zinc ores.

The Waelz process is performed in a long, slightly inclined and refractory-lined rotary kiln. The feed mixture is comprised of zinc bearing materials, fluxed, if necessary, and coke. Depending on the feed basicity, the addition of a conditioner, e.g. limestone or sand, is needed to maintain a genuine Waelz motion of the charge at all times. The feed mixture is slowly moved down by the kiln rotational speed and heated up by the off-gas stream leaving the kiln counter-current to the material flow. After drying and preheating, the charge enters the reduction zone in which the iron and zinc oxides are reduced by coke or carbon mono-oxide. At bed temperatures of up to 1200 °C, zinc is vaporized. The dust laden gases enter a spacious dust chamber, where coarse particles are settled out, then to a surface or water evaporation cooler and finally, to a baghouse or electrostatic precipitator in which the Waelz oxide is collected. After treatment, the zinc content in the slag can be as low as 2 per cent.

- Enviroplas^{TM} Process Fumer

The Enviroplas^{TM} process has been developed by Mintek located in Randburg, South Africa[6].This technology uses high temperature DC-arc electric furnaces which permit the Zn vapor to be recovered as a directly saleable metal product (i.e. Prime Western Zn) in a conventional lead splash condenser.

A 5.6 MVA pilot-plant, including a 5.6 MVA power supply, two plasma-arc furnaces, and an ISP (Imperial Smelting Process) lead-splash condenser, was successfully commissioned at Mintek in 1994. About 600 t of lead blast furnace slag was processed through the demonstration plant at feed rates of 1 to 3 t/h. Zinc fuming rates of 120 to 180 kg/h were achieved. Disposable slags were produced that contained less than 1.5 percent zinc and less than 0.2 per cent lead. The zinc condensing efficiency was about 80 per cent, and Prime Western grade zinc was produced consistently.

Some of the main points of zinc bearing slags and residues fuming are summarized below:

1. If the zinc content is below 10%, slag fuming is unlikely to be economical,
2. The water-jacketed furnace is still the most popular furnace in the world,
3. Ausmelt is a new technology which has achieved wide application,
4. The Waelz kiln is mainly used for zinc leaching residues treatment,
5. No matter what method is used, the tail slag contains about 3 per cent zinc,

6. The reduction of zinc to consistently low levels, i.e., 1 wt.% or lower, could not be achieved because of foaming of slags, which is also accompanied by the formation of iron,
7. Some valuable metals, such as silver and indium, which are common in zinc & lead concentrate, are only partially recovered by fuming processes.

3.2. Properties of Zinc Fuming Slags

3.2.1. Resistance of zinc fuming slags

1. Pure Oxides

The measurement of the electrical conductance of pure liquid oxides and of molten silicates has contributed substantially in clarifying the ionic nature of these melts. The electrical conductivity of slags is an important factor in the design of electric smelting furnace, where heat is produced by electric current according to the formula I^2R. The smelting furnace is not an arc furnace, like the steelmaking unit, but is a resistance furnace with the electrodes dipping into the slag, which forms the resistance.

Table III shows the electrical conductivity of some pure liquids at temperature just above the melting point of each oxide.[17,18] If the fusion of the network oxides gives rise to highly associated liquids held together by strong covalent bonds, the ionic conductivity is expected to be small. It is seen from Table III that the specific conductivity K of SiO_2, B_2O_3 and GeO_2 at their melting temperature is less than 10^{-5} ohm^{-1} cm^{-1}. Other crystalline oxides such as As_2O_3 and P_2O_5, by analogy, are expected to exhibit low conductivity also. Ferrous iron oxide exhibits the highest conductance among the melts, while CaO, MgO, Al_2O_3, TiO_2, and Cr_2O_3 also have relatively higher values. Solid FeO is known to be a *p*-type (positive hole) semiconductor deficient in Fe. The high specific conductivity of FeO at the melting temperature of 1370 °C, the absence of a marked change of

conductance on fusion and the positive temperature coefficient, indicate that a similar mechanism is applicable in the melt.

Table III. Electrical Conductivity of Pure Oxides

Oxide	T °C	K, ohm^{-1} cm^{-1}
SiO_2	1710	10^{-5}
B_2O_3	450	$<10^{-6}$
GeO_2	1115	$<10^{-5}$
Al_2O_3	2050	15
CaO	2580	40
MgO	2800	35
TiO_2	1650	10
Cr_2O_3	2275	65
FeO	1370	122

2. Conductivity of Nonferrous Smelting Slags

❖ Ionic vs nonionic conduction

Publications dealing with the conductance of molten slags can be traced in the literature back to the first decade of the last century. Authors who made important contributions in this field were Aiken[19], Doelter[20], Sauerwald and Neuendorff[21], and Farup *et al.*[22]

who measured the electrical conductivity of melts both in the $CaO-SiO_2$ system and in the $CaO-Al_2O_3-SiO_2$ system. Wejnarth[23] measured the electrical conductivity of various silicates in $FeO-SiO_2$ and $FeO-CaO-MnO-Al_2O_3-SiO_2$ systems. Martin and Derge[24] investigated extensively the conductance of molten blast furnace slags as a function of both slag temperature and composition.

Molten wustite, FeO, was found by Inouye *et al.*[25] to exhibit electronic conduction, presumably because of the ability of the iron cation to alter valency giving a *p*-type semiconduction. This phenomenon was also remarked on by Simnad, Derge, and George[26] and by Dukelow and Derge[27] when studying the systems $FeO-SiO_2$ and $FeO-MnO-SiO_2$ with the extent of electronic conduction dropping as the MnO or SiO_2 contents of the melts increased.

Perhaps the most pertinent previous work in the system $FeO-CaO-SiO_2$ is that of Dickson and Dismukes[28] who determined current efficiencies and transference numbers in the melts containing from 38 to 90 percent FeO at ratios of lime to (lime + silica) of 0 to 0.6. The anode current efficiency, determined by Dickson and Dismukes[28] for $FeO-CaO-SiO_2$ system and by Dukelow and Derge[27] for $FeO-MnO-SiO_2$, as shown in Figure 12 and 13 respectively, can reach a magnitude of 90 percent. The higher the silica content is, the higher the current efficiency will be.

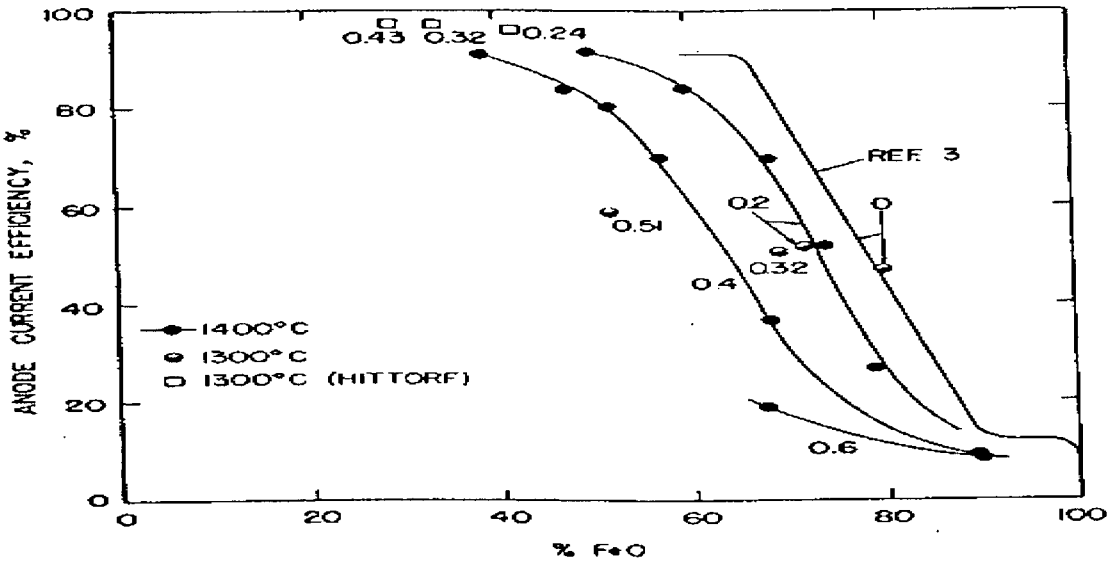

Fig. 12 — Anode current efficiency as a function of melt composition for FeO-CaO-SiO_2 melt. Number associated with individual curves and points correspond to different values of pce CaO/(pct CaO + pct SiO_2) [28].

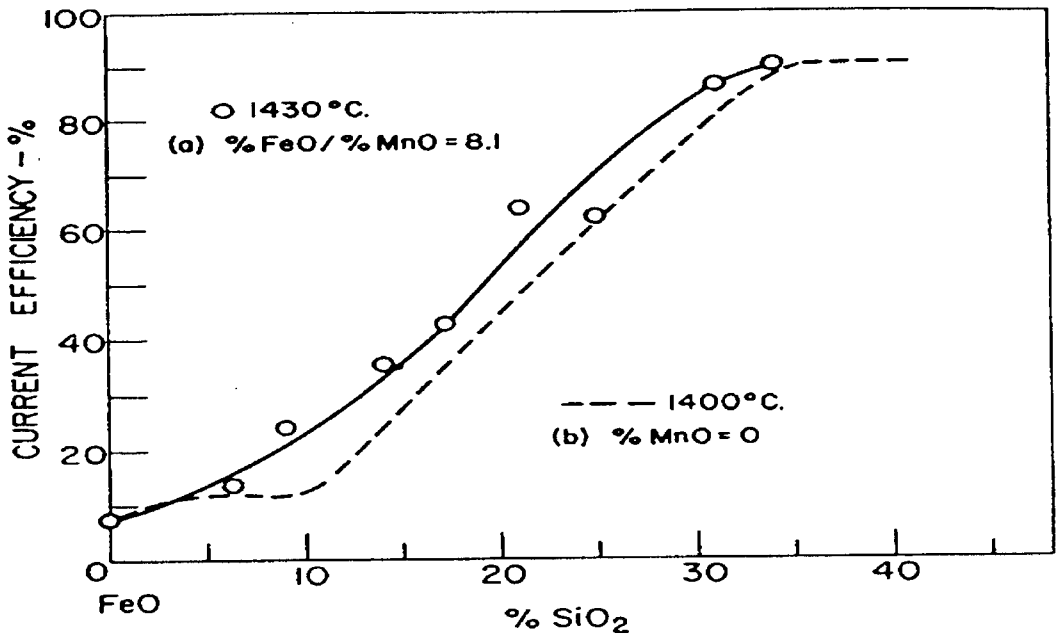

Fig. 13 — Current efficiency of FeO-MnO-SiO_2 melts: (a) pct FeO/pct MnO = 8.1, (b) pct MnO = 0 [27].

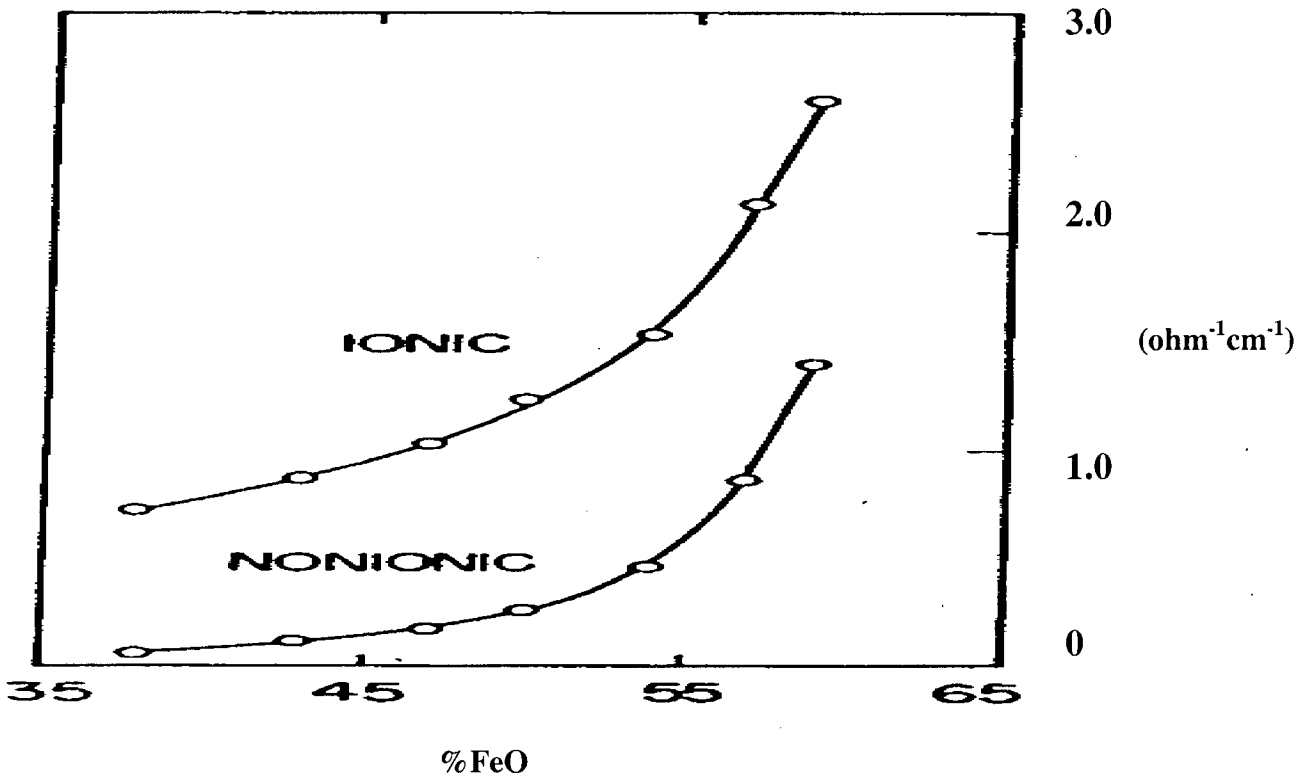

Fig. 14 — Ionic and nonionic conductance in melts having a pct CaO/(pct CaO + pct SiO_2) ratio of 0.4 [28]

As indicated in Figure 12, for melts of a fixed proportion of CaO and SiO_2, an addition of FeO causes a decrease in the fraction of current that is conducted by ions. In order to consider the effect of FeO additions on the magnitude of ionic and nonionic conduction separately, conductivity values - obtained by interpolating data reported by Wejnarth[23]- were multiplied by the fractions of ionic and nonionic conduction indicated by current efficiency in Figure 12, and the results were presented in Figure 14. Increasing pct FeO, therefore, increases both ionic and nonionic conductivity although the relative value of nonionic conductivity increases more sharply, which Dukelow and Derge[27] have reported to be the case for the simple binary system FeO-SiO_2.

Experiments have shown [28,29] some general trends between electrical conductivity and viscosity: high viscosity is associated with low conductivity and an increase in SiO_2 and Al_2O_3 concentrations increases viscosity and diminishes conductivity in most cases. Some authors, such as Martin *et al.*[24] and Hejja[30], tried to establish a relationship between these two phenomena, but did not succeed. Although both properties depend on the quantity and type of the ions in the melt, viscosity is related to the flow of fluid arrays while conductance is subject to the migration of ions; they are two different phenomena.

Goto *et al.* [31,32] studied the relationship between the partial conductance of ionic species and their respective diffusivity and suggested that the ionic conductance of a species could be estimated from the Nernst-Einstein equation, when the tracer diffusivity of the species was known.

$$k = \frac{n_i (z_i e)^2}{\sigma T f t_i} D_i^{tr}$$

Where k: the conductivity in $A \cdot V^{-1} \cdot cm^{-1}$

D_i^{tr} : the tracer diffusivity of an ionic species I in $cm^2 \cdot sec^{-1}$

n_i, z_i and t_i: concentration, valency and transference number of the ionic species, respectively

e: the unit charge (1.6×10^{-19} A·sec)

σ: Boltzmann constant (1.38×10^{-23} $V \cdot A \cdot sec^{\circ}K^{-1}$)

T: the absolute temperature

f: the correlation factor of successive jumps of the tracer

However, the measured tracer diffusivities by these authors did not agree with the diffusivities estimated from the conductivities by the Nernst-Einstein equation, which suggests that in molten slags, in which there are strong interionic forces, the Nernst-Einstein equation becomes less valid, due to different ionic mechanisms influencing the diffusivity and the electrical conductivity.[33]

❖ Temperature dependence

The temperature dependence of electrical conductivity can be expressed by the Arrhenius Law (which, in conductivity measurements, has been named by some authors the Rasch-Hinrichsen Law[29]):

$$k = A\exp\left(-\frac{E}{RT}\right)$$

or

$$\ln k = \ln A - \frac{E}{RT}$$

Where k: specific electrical conductivity ($ohm^{-1}\,cm^{-1}$);

E: activation energy ($J\,mole^{-1}$);

R: 8.31441 ($J\,mole^{-1}\,K^{-1}$) gas constant;

A: constant

T: temperature, K

Figure 15 shows the electrical conductivity of various slags as a function of temperature. It can be seen that slags of higher SiO_2 and/or Al_2O_3 content, thus of lower conductivity, are more sensitive to temperature; *i.e.*, they exhibit larger temperature coefficients. This is in contrast to slags of higher FeO content, which generally have higher conductivities and small temperature coefficients.

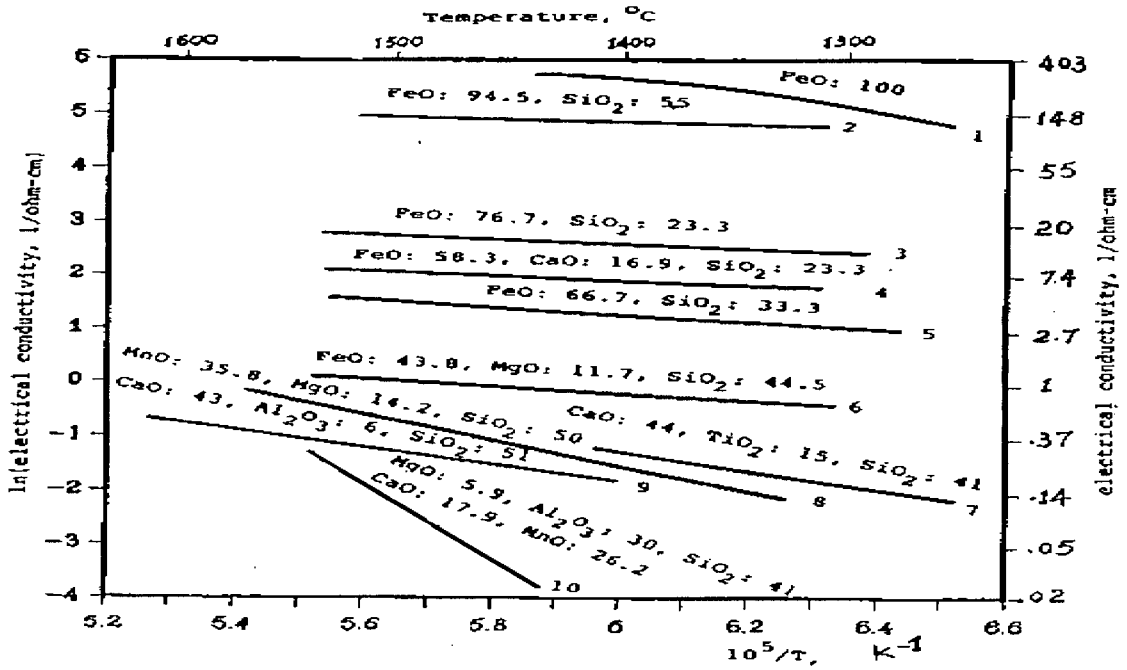

Fig. 15 — Electrical conductivity vs temperature [33]

❖ Composition dependence

Since the fifties, there has been much research work on the structure of slags. It is now well accepted that molten slag acts as an electrolyte in which most of the metal oxides exist in the form of cations. Some high-valence oxides, such as SiO_2, $Al2O_3$, form

complex arrays called tetrahedra (the smallest ones are SiO_4^{-4} and AlO_4^{-5} tetrahedra, respectively) by attracting oxygen ions, O^{-2}, from low-valence oxides. Experiments using high energy X-ray diffraction have proved the existence of such tetrahedra. Masson[34] developed polymerization models to describe the behavior of slags. The ionic theory of slags and the polymerization models can be used to estimate qualitatively the effect of composition on the electrical conductivity. However, it is not possible to derive quantitative equations from these theories. This can be attributed to the complexity of the phenomena involved in slag conductance.

Based on the assumption that high ionization occurs in the melts, and that an addition of basic metal oxides does not change appreciably the structure of the slag, Jiao and Themelis[33] developed a formula for the conductivity of nonferrous smelting slags (copper and nickel electric smelting):

$$\ln k = a + bX_{FeO} + c(X_{CaO} + X_{MgO}) \qquad [1]$$

where k: electrical conductivity, ohm-1cm-1;

a: constant;

b, c: concentration coefficients;

X_{FeO}, X_{CaO}, X_{MgO}: mole fractions in the slag.

The constant a and the coefficients b, c in Eq. [1] were estimated from a multiple linear regression analysis of the experimental data by Inouye[25], Fontana *et al.*[35], Hejja[30], and Victorovich *et al.*[36]. The resulting correlation for slags at 1400 °C is:

$$\ln k = -5.21 + 9.92X_{FeO} + 5.94(X_{CaO} + X_{MgO})$$

The main components of zinc fuming slag are SiO_2, FeO, CaO and Al_2O_3, which, when added together, constitutes about 90 percent of the tail slag. The above formula might be applicable to zinc fuming slag. Calculation from this formula gives a conductivity value of about 0.4 ohm^{-1} cm^{-1} at 1400 °C.

The results indicated that, in the range of slag chemistries of interest in this study, at 1250 °C, 1)the ionic conduction should be roughly 90 percent(Based on the published results for ferro-silicate slags and the silica content on ***Cominco Tail Slag***), 2)the specific conductance is about 0.5 ohm^{-1} cm^{-1} (Estimated from the composition of ***Cominco Tail Slag*** and Jiao's equation).

3.2.2. Activities of ZnO and FeO in zinc fuming slags

Zinc is a major impurity in lead smelting and reports essentially to the iron silicate slag. Slag from the smelting of lead can contain up to 20 percent zinc as an oxide. An understanding of the lead smelting process, of the subsequent fuming process for the recovery of zinc and of the development of new zinc smelting process, such as the **Warner Process** (Appendix IV)[37-39], and the **High Pressure Liquid Zinc Extraction Process** (HPLZEP) (AppendixV)[40], is enhanced by a knowledge of the activity coefficient behavior of zinc oxide in smelting slags. Because the vapor pressure of zinc is relatively high at smelting temperatures, a variety of methods were employed by previous researchers to overcome the experimental difficulties associated with the determination of zinc oxide activity in molten slags. Those methods include:

- Equilibration of slag with CO-CO_2-(N_2) containing fixed p_{Zn} [41, 42]
- Solid-state oxygen concentration cell, Fe-FeO(slag)/ZrO_2/Ni-NiO to determine activity of FeO; then equilibrium of Ag-Zn with iron-saturated slag [43]:

$$ZnO + Fe = FeO + Zn$$

- Solid-state oxygen concentration cell, Pt/Ni·NiO/ZrO_2·MgO/Slag(l)/Fe/Pt and equilibrium of Cu-Zn with iron-saturated slag[44]
- Equilibrium between slag and iron-saturated Cu-Zn-Fe[40]
- Fitting of plant zinc-fuming data to thermodynamic model[43]

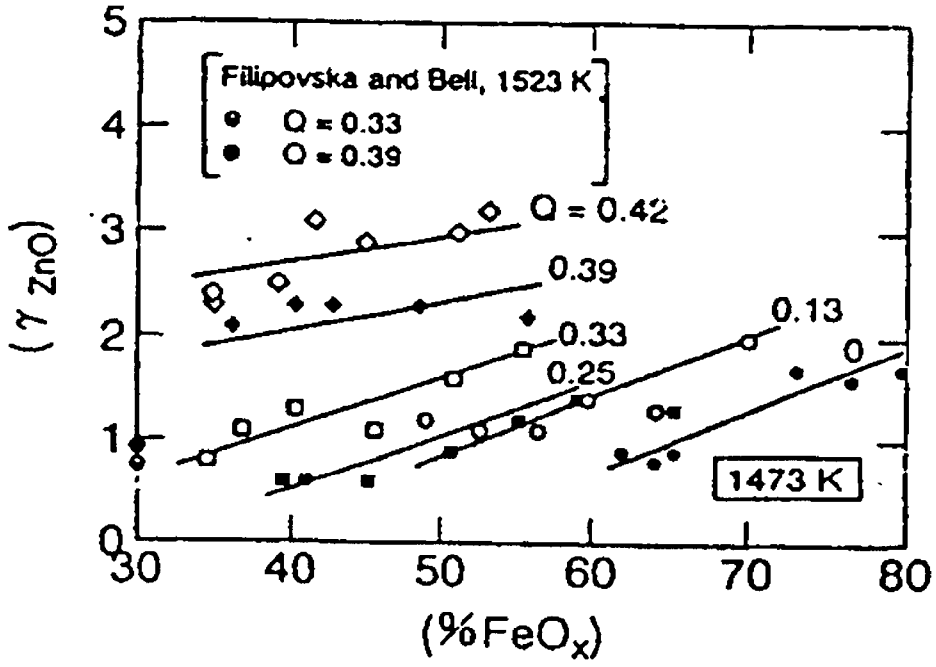

Fig. 16 — Activity coefficient of ZnO in slag coexisting with Cu-Zn-Fe (iron-saturated) alloy with zinc content of more than 1% at 1523k[40] (Q = %CaO/(%CaO + %SiO_2))

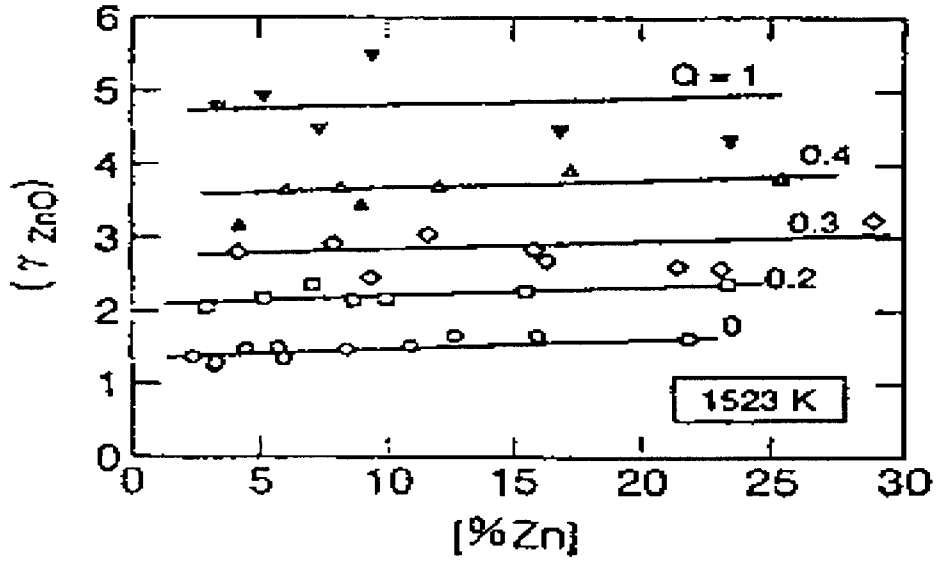

Fig. 17 — Activity coefficient of ZnO in slag equilibrated with Cu-Zn-Fe (iron-saturated) alloy with zinc content of less than 1% at 1473k[40]

With the objective of developing a new zinc smelting process, many studies have been done by Japanese researchers[40, 45, 46] on the activity of zinc in the molten Cu-Zn-Fe ternary system, activity measurements in liquid Cu-Zn-X (X = Pb, Ag and Au) ternary alloys and the equilibrium between $CaO-SiO_2-FeO_x$ slag and Cu-Zn-Fe (iron-saturated) alloys. Figure 16 and 17 summarize the activity coefficient of ZnO in slag equilibrated with Cu-Zn-Fe (iron-saturated) alloy. When the zinc content is above 1 percent, the zinc activity coefficient is nearly independent of zinc concentration but dependent on slag basicity Q ($Q = \%CaO/(\%CaO + \%SiO_2)$). The higher the basicity of the slag, the higher the zinc activity coefficient. A similar relationship between slag basicity and zinc activity coefficient was also obtained by Yoichi Takeda.[44] When the zinc content is less than one percent, as shown in Figure 17, the zinc activity coefficient still could be maintained as high as 2 to 3 if the slag basicity Q ($Q = \%CaO/(\%CaO + \%SiO_2)$) is about 0.4.

Industrial ISP slag and zinc fuming tail slag have a slag basicity of about 0.4. The zinc oxide activity coefficient in this slag, from researchers listed above, is between 2.5 to 3.5 at 1250 °C. An average value of 3.0 should be suitable for the zinc oxide activity coefficient.

Iron oxides constitute 30 to 35 percent of the zinc fuming slag with more than 90 per cent as ferrous. This is one of the concerns in the zinc fuming operation and this research. The best operation would be the lowest iron reduction and the highest zinc reduction. As iron oxides and zinc oxide coexist in the slag, when the system reaches chemical reaction equilibrium, both of reactions (1) and (2) will reach equilibrium and have the same

oxygen potential pO_2. The activity coefficient of FeO not only depends on the standard free energy of formation of FeO and ZnO, but also depends on their mole fractions in the slag, which can be calculated from equation (4).

$$Zn_{(g)} + \frac{1}{2}O_2 = ZnO_{(s)} \quad (1)$$

$$a_{ZnO} = K_1 a_{Zn}\, pO_2^{0.5} = \gamma_{ZnO} N_{ZnO}$$

$$Fe_{(s)} + \frac{1}{2}O_2 = FeO_{(s)} \quad (2)$$

$$a_{FeO} = K_2 a_{Fe}\, pO_2^{0.5} = \gamma_{FeO} N_{FeO}$$

$$FeO_{(s)} + Zn_{(g)} = ZnO_{(s)} + Fe_{(s)} \quad (3)$$

$$\frac{\gamma_{ZnO}}{\gamma_{FeO}} = K\left(\frac{N_{FeO}}{N_{ZnO}}\right)\left(\frac{a_{Zn}}{a_{Fe}}\right) \quad (4)$$

Table IV. The standard free energy of formation for FeO and ZnO reactions [47]

Reaction	ΔG^0/J	ΔG^0/J 1250 °C
$Fe_{(s)} + \frac{1}{2}O_2 = FeO_{(s)}$	-259,431 + 62.51T	-164228
$Zn_{(g)} + \frac{1}{2}O_2 = ZnO_{(s)}$	-482,571 –43.27TlogT + 344.43T	-167745

Filipovska[48] measured ferrous oxide activities of slags containing 3-8 mole % zinc. When compared with the results of Bodsworth[48] at 1265 °C for zinc free slag, it was concluded that the addition of zinc oxide slightly increases the activity of ferrous oxide in these slags. The phase diagrams for the ZnO-SiO_2 and FeO-SiO_2 systems suggest that the

interaction is slightly more negative in the $ZnO\text{-}SiO_2$ system. This would be borne out by their data. The activity coefficient of ferrous oxide γ_{FeO} increases almost linearly with slag basicity, which was defined as lime:silica ratio $(\frac{CaO}{SiO_2})$ by the author. The effect of Al_2O_3 additions is also to raise γ_{FeO} for a given lime:silica ratio, and this increase is greater as the lime:silica ratio rises. For the slag of interest in this research, the mole fractions of FeO and ZnO are about 0.288 and 0.0351 respectively, the activity coefficient of FeO is about 1.4, which means that the activity of FeO is about 0.4.

3.3. Electrolysis in Molten Silicates

Pyrometallurgical methods for metal production usually contain a step of carbon reduction, which employs carbon as the reductant to reduce metal oxide into its elemental form. The starting temperature needed for the reducing reaction is indicated by the Ellingham diagram, corresponding to the temperature at the point of intersection between the lines of the formation of oxide and the combustion of carbon. This temperature for some reactive metals is so high that it is nearly impossible to reduce them by carbon or other known reducing agent in an economical operation. It is also not practical to electrorefine those metals in aqueous solution since hydrogen gas will evolve before metal is deposited. Molten salt electrolysis is one the solutions for solving this puzzle. Aluminum production is a good example of extracting reactive metals by molten salt electrolysis.

Aluminum occurs in the earth's crust to the extent of 7.3 wt.% in about 250 different minerals, and its abundance is only exceeded by oxygen and silicon. Owing to its chemical reactivity, it is never found in nature as an element, but always as a compound in an oxidized state. In 1808, H. Davey[49] first isolated, by an electrothermic-electrochemical method, small amounts of an Al-Fe alloy, which he called aluminum. On April 23rd, 1886, P. L. Héroult in France, and independently C. M. Hall in the U.S.A. on July 9th of the same year, applied for the registration of a patent for aluminum production by electrolysis of a molten solution of alumina in cryolite. This process was named Hall-Héroult process and it still dominates the production of aluminum.

Electrolysis in silicate melts has been studied by many researchers.[27, 28, 50-52] Dickson and Dismukes[28] measured the current efficiency at an iron anode during the electrolysis of FeO-CaO-SiO_2 melts contained in an iron crucible, and studied the Hittorf transference-number in the same furnace with some modification. Their results indicated that the anode current efficiency could be as high as 90 percent if the melt was of relatively higher silica and lower FeO contents. Dukelow and Derge[27], examining the FeO-MnO-SiO_2 melts at about 1400 °C, also got an anode current efficiency of 90 percent while the silica content in the melt was more than 33 percent. The partial replacement of MnO with FeO in FeO-MnO-SiO_2 melts or CaO with FeO in FeO-CaO-SiO_2 melts did not have much effect on the current efficiency.

Larson and Eagar[50] studied the electrolysis of titanate slags with a targeted composition of 20%CaO, 15%MgO, and 65%TiO_2 heated by plasma by the following electrode reactions:

$$CO_{(g)} + O^{2-}{}_{(slag)} = CO_{2(g)} + 2e^-$$

$$TiO_{2(g)} + 4e^- = Ti_{(metal)} + 2O^{2-}$$

A transferred arc plasma makes it feasible for reactions to occur at the plasma/slag interface. The solid anode material, such as graphite, does not have to take part in the reaction. Contamination by the anode material is thus avoided. Titanium metal was deposited at the cathode (the bottom of the containment crucible) in solid dendrites. Although titanium made from this process is expected to contain oxygen at levels that will greatly impair the metal's ductility and probably make it brittle, the cost of

production of titanium metal by this technique was estimated to be USD2-3 per pound, which is much cheaper than USD6-10 per pound for the conventional method.

Perhaps the most pertinent previous work to the electrolysis contemplated in this work is a patent done by Shell Int Research, where metals have been recovered from a complex metal halide using a liquid metal cathode. The metals electrorefined include Ti, Hf, Ta, Al, Zr, W Nb, V, Mo, In, and Ag using cathodes selected from Zn, Cd, Sn, Pb, In, Bi and Ga.[51] There has also been work on the recovery of silver, gallium and other trace metals from fly ash, but this work started with the conversion of these metals to the halide by mixing with $AlCl_3$ in an alkali halide melt.[52]

4. SCOPE AND OBJECTIVES

As stated in section 3.2.1, the resistance of zinc fuming tail slag should be under 1 ohm^{-1} cm^{-1}, which may be low enough to permit reasonable voltage and current parameters in a commercial cell. Also, a relatively high current efficiency can be expected because the silica content in zinc fuming tail slag is more than 30%. Therefore, an electroreduction process, which is similar to the Hall-Héroult process in aluminum production, was proposed for the treatment of this slag.

The iron content in the slag is sufficiently high that it might be deposited at the cathode also while zinc is electrolyzing from the zinc tail slag. Since the solubility of iron in copper at the working temperature of 1250 °C is only about 5% but zinc can dissolve into a copper melt with any proportion at the same temperature, a small amount of iron in copper should reach a high iron activity. So, by introducing copper as the cathode, it behaves as a "getter' for the electrowinning of heavy metals from a slag of this nature. A patent search indicates that there is no prior art using copper for this purpose although there is work done by Shell International Research of a somewhat similar nature where metals have been recovered from a complex metal halide using a liquid metal cathode.[51]

Before starting the experimental work, it is necessary to quantify the thermodynamic driving force provided by using copper as the cathode. The calculation can be done manually, based on the thermodynamic data (such as the iron and zinc metal/oxide concentrations, interaction coefficients in metal/slag phases) from publications. Because

FACT[53,54], a thermodynamic software, has a quite good data base for zinc smelting slags, it was used for this calculation.

The experimental trials in this research are divided into three sections. Firstly, the design of experimental set-up and the electrolyzing cell, and estimation of some of the electrolyzing parameters are the main task for this research. Since there is no previous work related to this project, all the experimental trials need to start from the beginning. All the details, such as the selection of electrode materials and crucibles, the design of the mechanism for the controlling of the electrode positions, the construction of the furnace for conducting the experiments and the conceiving of the methods for sampling and analysis, had to be realized. Secondly, some parameters, such as the cell voltage, the intensity of current flow, and the time duration for the electrorefining also need to be estimated before the scheduling of the experiments. The last part, also the most important part, is the implementing of the electrorefining experiments for both of the synthetic slags and the as-received ***Cominco*** slags under different conditions.

The main output of this research should clarify the effectiveness of the electrolysis on the recovery of zinc and other metals of interest, by employing copper as the cathode and passing current through the slag. Another output of this research is the estimation of the zinc fuming slag conduction mechanism: ionic or electronic, by data obtained from the electrorefining runs.

5. "FACT" CALCULATION OF THE ACTIVITIES OF ZINC AND IRON

Most waste oxides and non-ferrous slags suitable for fuming operations usually contain oxides of several elements, i.e., SnO, ZnO, PbO, As_2O_3, etc, in addition to a significant amount of iron oxides. The aim of the fuming operation is to reduce the volatile oxides and collect them as a pure product (metal) or a mixture of oxides. In typical zinc and lead production operations, lead blast furnace slags and zinc leaching residues are usually fumed to recover zinc metal. The conventional zinc fuming operations from lead blast furnace slags are carried out at temperatures in the range of 1200 to 1300 °C, which is lower than the melting point of iron (pure iron melts at 1536 °C). This implies that iron will tend to form as solid particles in the melt. The formation of solid iron is usually associated with operational problems like the formation of accretions, foaming of slag, and contamination of fumes. Therefore, the objective of most fuming operations is to prevent the formation of significant amounts of metallic iron. In typical slag fuming operations with lead blast furnace slags, iron tends to form at zinc and lead contents of 1.5-2.5 wt.% and 0.1-0.5 wt.% respectively.[11] One of the ways to determine the end point of the reducing operation would be the detection of the formation of the first traces of metallic iron in the melt, a part of which may report in the fumes.

There are many commercial processes for fuming operation available, such as Water-jacketed Fumer fuming[3-5], Waelz Kiln fuming[16], Ausmelt Furnace fuming[2] and Enviroplas Process fuming[6]. Regardless of the fuming methods employed, all the published papers seems to agree that the tail slag from zinc fuming furnaces still contains about 3% zinc and some trace amounts of elements such as lead, indium and germanium,

based on data obtained from production lines[3]. As shown in Table V, all of the chemical analysis results of three Cominco tail slag samples, which were done independently by ***Cominco*** Research, Trail, British Columbia and ***IPL*** (International Plasma Laboratory Ltd., Vancouver, B. C.), indicated that the zinc oxide content was actually close to 6 percent for Cominco tail slag produced by its water-jacketed fumer.

Table V. Chemical composition of *Cominco* Tail Slag

	Fe **Wt.(%)**	**SiO_2** **Wt.(%)**	**Al_2O_3** **Wt.(%)**	**CaO** **Wt.(%)**	**ZnO** **Wt.(%)**	**Cu** **Wt.(%)**	**Σ**
***Cominco* 1**	28.9	28.6	2.8	18.2	5.7	0.26	84.46
***Cominco* 2**	28	28.1	2.6	17.6	5.6	0.38	82.28
IPL	30.32	30.82	3.05	17.45	5.7	0.36	87.61

As will be mentioned in section 5.1.2, at a working temperature of about 1250 °C, the solubility of iron in a copper melt is only about 6.5 weight percent but zinc can dissolve into a copper melt and form a binary alloy at any proportion. The difference in the solubility of iron and zinc in copper melt indicates the interaction between iron and copper is weaker than that between zinc and copper. This is reasonable since the difference of electronegativity is 0.3 between Cu and Zn, and 0.1 between Cu and Fe, as indicated in Table VI.

Table VI. The Pauling Electronegativity of Some Elements[55]

Element	Copper (Cu)	Iron (Fe)	Zinc (Zn)
Electronegativity	**1.9**	**1.8**	**1.6**

In a molten copper melt, copper atoms repel iron atoms somewhat while they attract zinc atoms. If the concentrations of iron and zinc in a copper melt are the same, the activity of iron should be much larger than that of zinc. This is the key reason why copper was chosen as the cathode material. By reducing the activity of zinc while maintaining a higher activity of iron, it should be possible to extract zinc from the slag without the formation of solid iron.

By introducing a copper melt at the bottom of a crucible then putting slag on the top of copper, the activity of zinc could be decreased and that of iron could be increased. This forms an extra thermodynamic driving force, which favors zinc and mitigates against iron depositing into the copper melt. A thermodynamic software package, F*A*C*T, was used to compute the activity of each component in the metal alloy system and the slag system, and the phase equilibrium between slag and copper. A notable feature of the package is that it contains thermodynamic databases for over 5000 compounds and allows user to do calculation for nonferrous smelting slags.

For the conceived electrorefining experiments, about 200 grams of slag and 150 grams of copper were used in each run. So, 150 grams of copper was used as the base of activity calculation for both the Cu-Zn binary system and the Cu-Zn-Fe ternary system.

5.1. Cu–Zn Binary System

In the electrorefining process, any metal ion that deposits into the copper melt will increase the concentration gradually. At the same time, the activity of this metal in the copper melt will increase also. It is of interest to calculate the activity evolution with metal concentration in the metal and the slag until a new equilibrium is reached.

A brief summary of the calculations are presented in Figure 18, 19 and 20. Figure 18 shows the activity changes when there is 0.5 to 5 grams of zinc deposited in the copper melt at 1250 °C. The same calculation results for iron in copper melt are illustrated in Figure 19. The activity of copper is nearly constant in both the Zn-Cu and the Fe-Cu system while zinc and iron activities increase with increasing concentrations, but the magnitude is different. A dimensionless activity ratio, defined as:

$$l_{Me} = \frac{\text{Activity of iron } a_{Fe} \text{ in Cu-Fe melt}}{\text{Activity of zinc } a_{Zn} \text{ in Cu-Zn melt}}$$

was introduced to describe this difference, which was graphically presented in Figure 20. As we can see, at 1250 °C in a binary copper melt, the activity ratio is about 330 when there is 0.5 gram of zinc and iron respectively. This ratio decreases while the metal concentration increases, to a value of 160 when five grams of metal are deposited in copper.

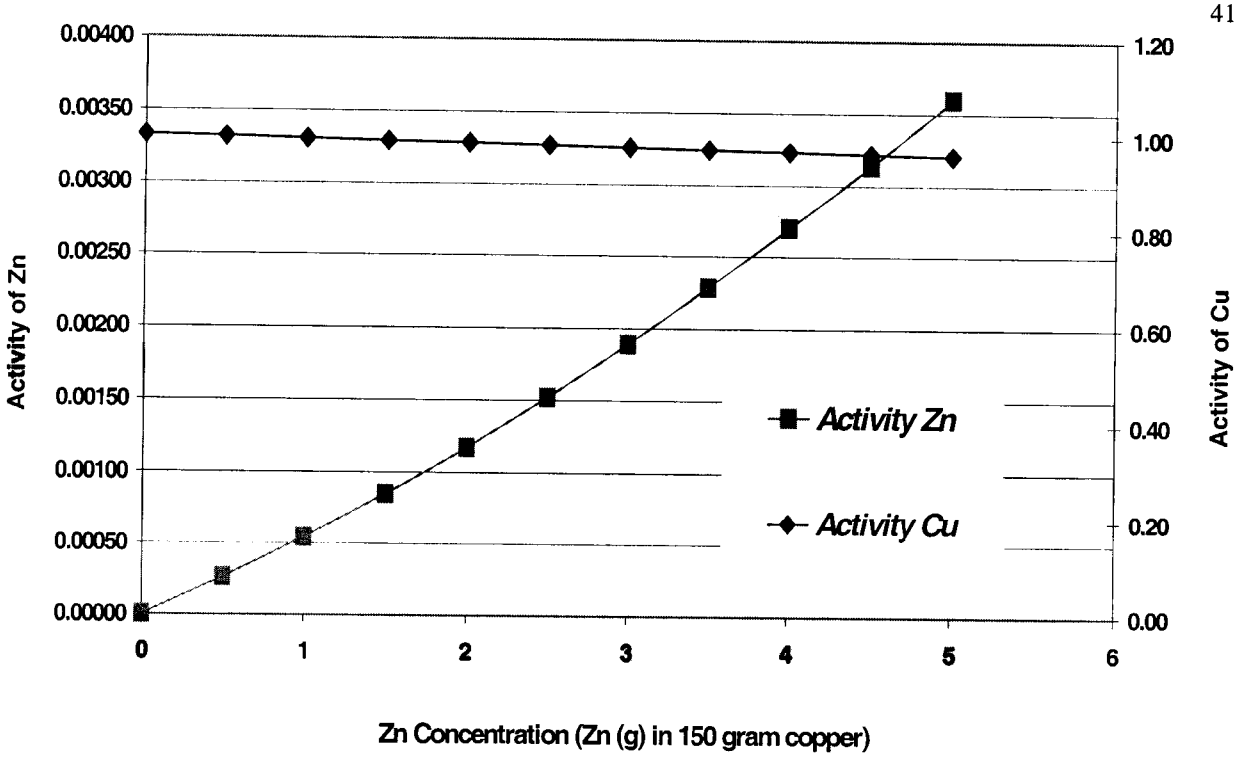

Fig. 18 — The activity of zinc in binary Cu-Zn melt at 1250 °C

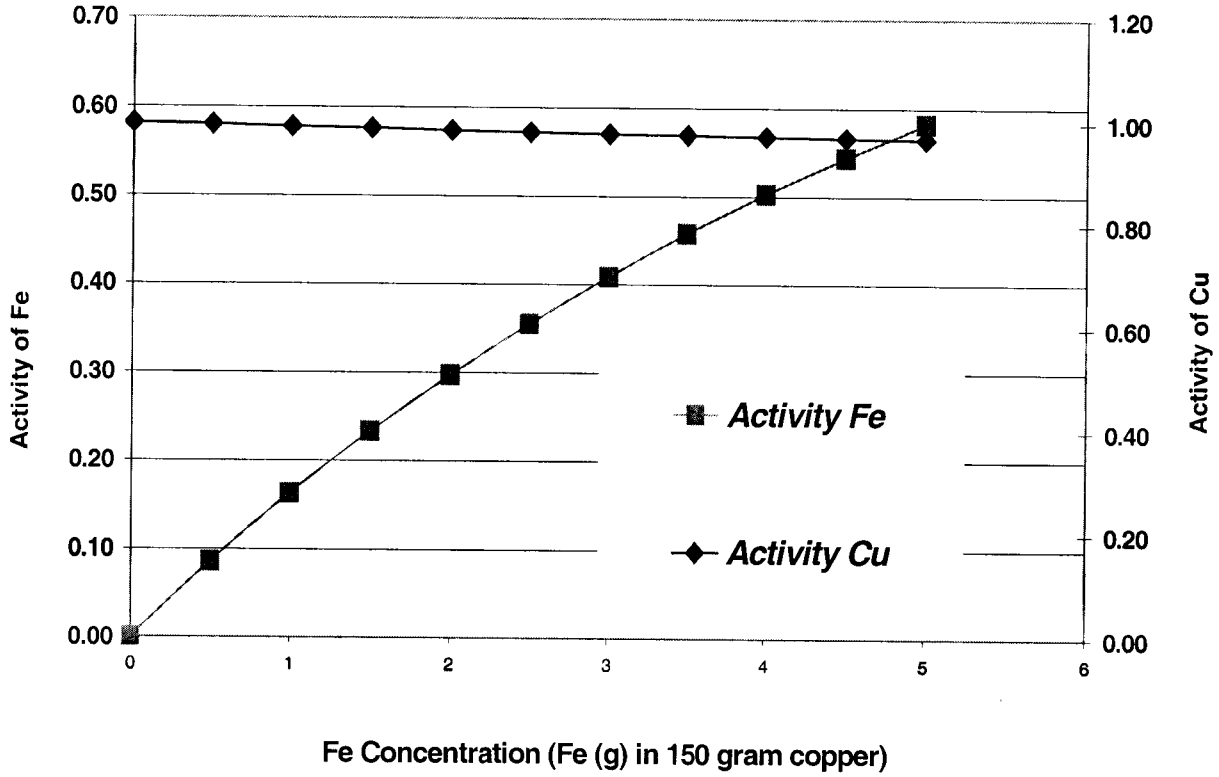

Fig. 19 — The activity of iron in binary Cu-Fe melt at 1250 °C

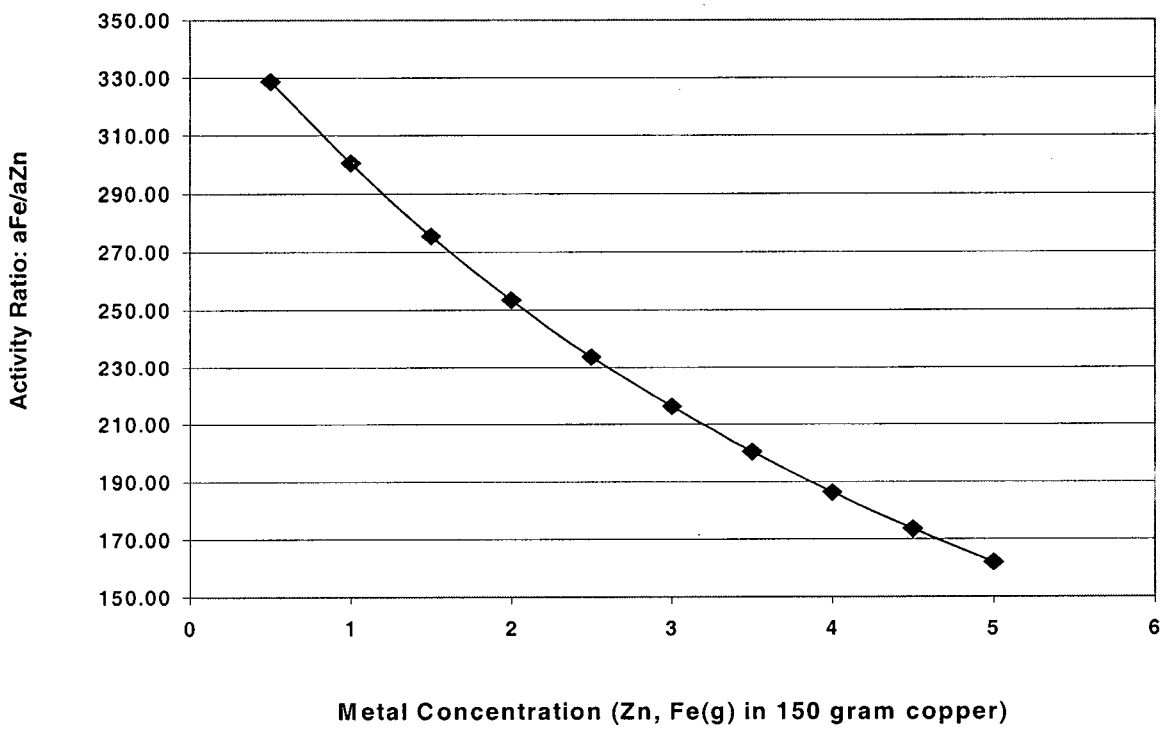

Fig. 20 — The activity ratio: a_{Fe}/a_{Zn} in binary copper melt at 1250 "C

5.2. Cu-Zn-Fe Ternary System

When a third element is added into a binary copper melt, the activity of each element will change accordingly. The magnitude of this change depends on the intensity of interaction between those elements. The stronger the attraction of this element to other elements, the lower the activity of this element will be, and the more likely there will some intermetallic compounds form.

When copper contains 0.5 percent of zinc and iron respectively, as seen from Figure 21, the activity of iron is much larger than that of zinc. The same relation continues when their corresponding amount increase. The activity ratio - iron activity to zinc activity, is almost the same as that of the binary system.

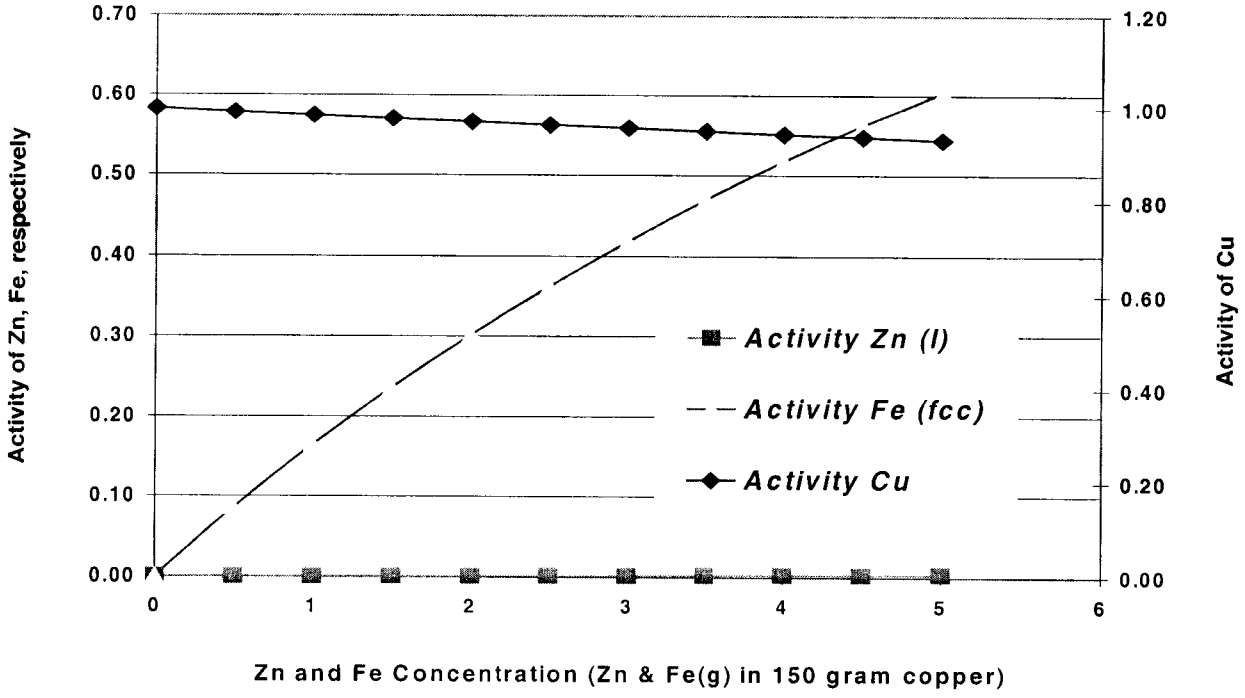

Fig. 21 — The activities of zinc and iron in Zn-Fe-Cu ternary system at 1250 °C

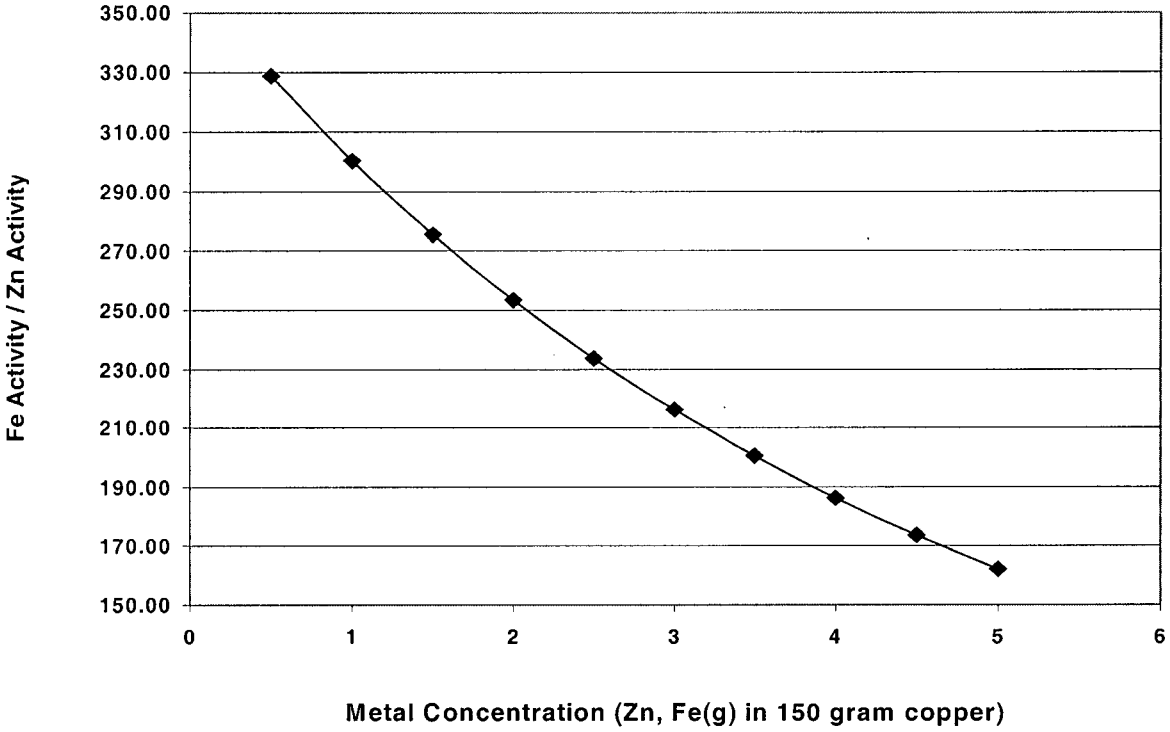

Fig. 22 — The activity ratio – a_{Fe}/a_{Zn} in Cu-Zn-Fe ternary melt at 1250 °C

5.3. Synthetic Slag

A synthetic slag was made from pure chemicals, with a proportion of each component as indicated in Table VII, which was based on the main components in the ***Cominco*** tail slag.

Because an extra amount of carbon is introduced into the zinc fumer, the operating atmosphere in the fuming furnace is usually very reducing. Usually, more than eighty percent of the iron in the fuming tail slag is in the ferrous form[3-5].

Metal iron powder and Fe_2O_3 were mixed according to the reaction:

$$Fe + Fe_2O_3 = 3FeO$$

to make ferrous iron. Although the amount of metal iron required by stoichimety for 295 gram Fe_2O_3 (to make 1000 gram synthetic slag) is 103.16 gram, 105 grams of iron was put into the mixture so that if air was involved in the furnace and any small amount of iron was oxidized into iron oxide, the status of iron in the final slag should be FeO.

Table VII shows the chemical composition of the synthetic slag (FACT + Al_2O_3). The six percent of alumina results from the melting of the slag in a fireclay crucible at 1250 °C.

Table VII. Composition of Synthetic Slag (by Calculation)

	Fe	Fe_2O_3	FeO	CaO	SiO_2	Al_2O_3	ZnO
Chemicals (gram)	**105**	**295**	--	**230**	**370**		**30**
Synthetic Slag (wt.%)	**--**	**0.4346**	**35.726**	**20.976**	**33.744**	**6.3839**	**2.7360**

When the zinc oxide concentration in the synthetic slag is increased over a small range, its activity increases also, as seen in Figure 23. However, the activity of iron oxide is nearly constant because the size of the ZnO increase is so small that it has a negligible effect on the FeO mole fraction, and the interaction between ZnO and FeO is also negligible.

Again, the activity ratio is defined as follows and is plotted out, as shown in Figure 24.

$$l_{MeO} = \frac{\text{Activity of iron oxide } a_{FeO} \text{ in slag}}{\text{Activity of zinc oxide } a_{ZnO} \text{ in slag}}$$

When the zinc oxide concentration in the synthetic slag decreases to about two percent, the activity ratio increases but only slightly. However, when the ZnO concentration is below 1.5 percent, the activity ratio increases from about 60 at 1.5 wt.% ZnO to 250 at 0.5 wt.% ZnO. Obviously, the lower the concentration of ZnO in slag, the more difficulty will be the reduction of ZnO from this slag.

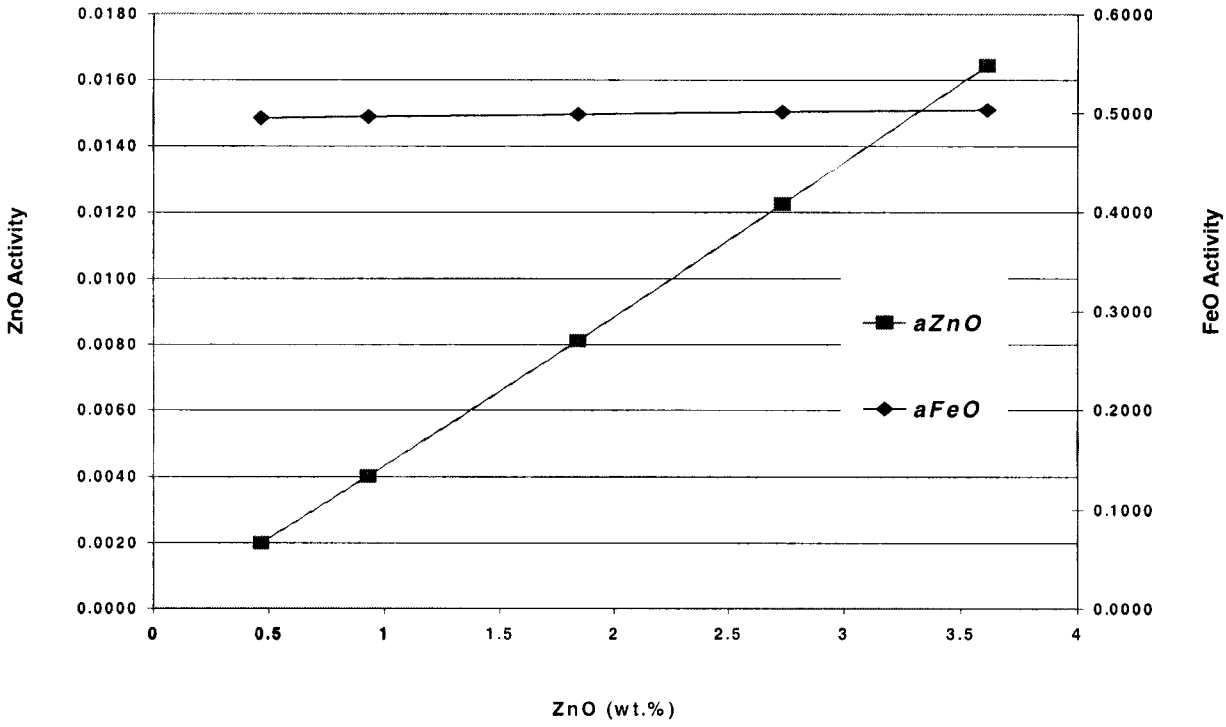

Fig. 23 — The effect of ZnO concentration on the activities of ZnO and FeO in synthetic slag (1250 °C)

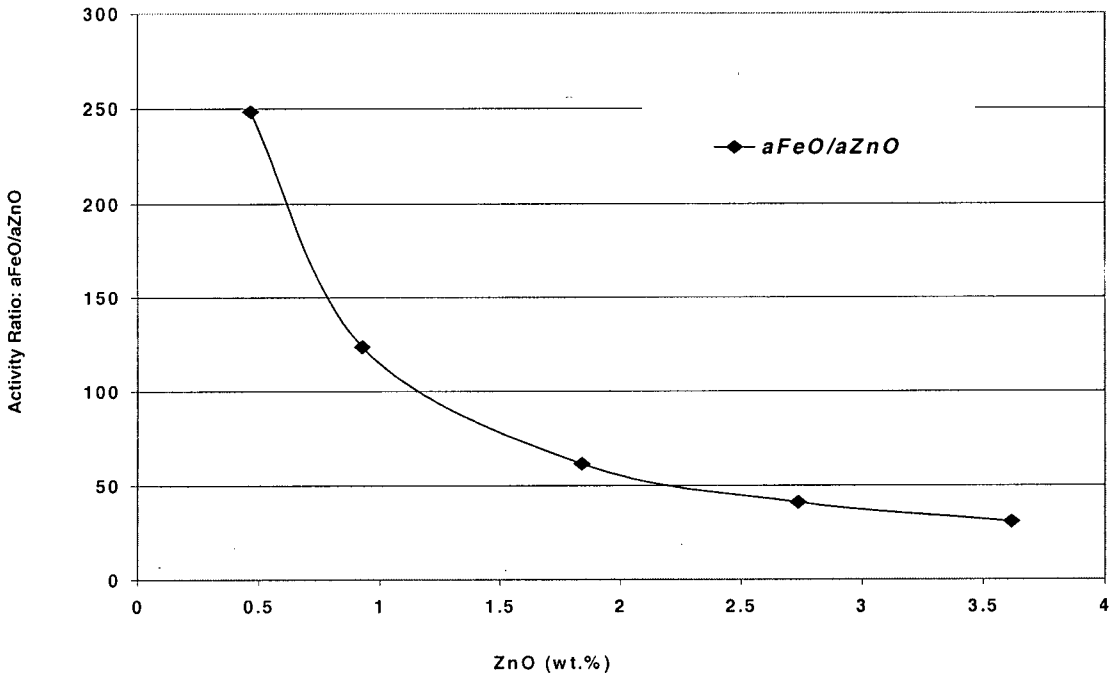

Fig. 24 — The effect of ZnO concentration on the activity ratio a_{FeO}/a_{ZnO} at 1250°C

The synthetic slag is a mixture of oxides. When a certain proportion of chemicals are mixed and melted at 1250 °C, all of the following reactions may possibly take place:

$$FeO_{(S)} = Fe_{(Me)} + 0.5O_2$$

$$Fe_{(Me)} + Fe_2O_{3(S)} = 3FeO_{(S)}$$

$$Fe_2O_{3(S)} = 2FeO_{(S)} + 0.5O_2$$

$$ZnO_{(S)} = Zn_{(Me)} + 0.5O_2$$

$$ZnO_{(S)} + FeO_{(S)} = Zn_{(Me)} + Fe_2O_{3(S)}$$

When the system reaches equilibrium, there should be a fixed oxygen potential and also a fixed ratio of Fe^{3+}/Fe^{2+}. By F*A*C*T calculation, the synthetic slag at equilibrium at

1250 °C, has an oxygen potential of 0.2323×10^{-9}, with Fe_2O_3 at 0.4344 percent, and FeO at 35.71 percent. When 200 gram of this slag is equilibrated with 150 gram of copper, two phases coexist. The weight of copper phase increases due to dissolution of some of the iron and zinc. The zinc content in the copper melt is almost three time that of iron. The oxygen potential of the slag phase will increase to 0.2829×10^{-7}, Fe_2O_3 increases to 1.4454 percent and FeO decreases to 34.595 percent (Table VIII).

Table VIII. The Composition and Phase Equilibrium among Metal and Slag Phases

Phase	*FeO*	*Fe_2O_3*	*CaO*	*SiO_2*	*Al_2O_3*	*ZnO*	*Cu_2O*	*P_{O2}*
Synthetic Slag (grams)	**71.427**	**0.8688**	**41.938**	**67.465**	**12.763**	**5.470**	**0.068**	**0.2323×10^{-9}**
Slag (199.88 grams) (wt.%)	**34.595**	**1.4454**	**20.988**	**33.764**	**6.3877**	**2.1174**	**0.7026**	**0.2829×10^{-7}**
	Cu	**Fe**	**Zn**					
Copper (150.19 grams) (wt.%)	**99.086**	**0.25126**	**0.66315**					

It is clear that the lower the activity ratio of FeO/ZnO in slag and the higher the activity ratio of Fe/Zn in copper, the more zinc and the less iron will be in the copper at equilibrium. Methods which can favor those ratios will definitely improve the efficiency of copper as a zinc "getter". If some of the ferrous iron oxide is oxidized into ferric oxide, the FeO activity in slag will decrease. So, it is also of interest to calculate the effect of Fe_2O_3 concentration on the activity changes of iron oxides and zinc oxides, the distribution of iron and zinc between the slag phase and copper phase. Figure 25 and 26 illustrated the results of this calculation. Because Fe_3O_4 will precipitate from the slag melt at an Fe_2O_3 content of about 3 per cent, the amount of ferrous oxide that can be oxidized into ferric oxide is very limited. Also, when the amount of Fe_3O_4 in the slag increases, the viscosity of slag will increase and the solubility of copper in the slag will increase. The conclusion is that it is not desirable to decrease the ferrous activity by oxidizing some amount of it into the ferric form.

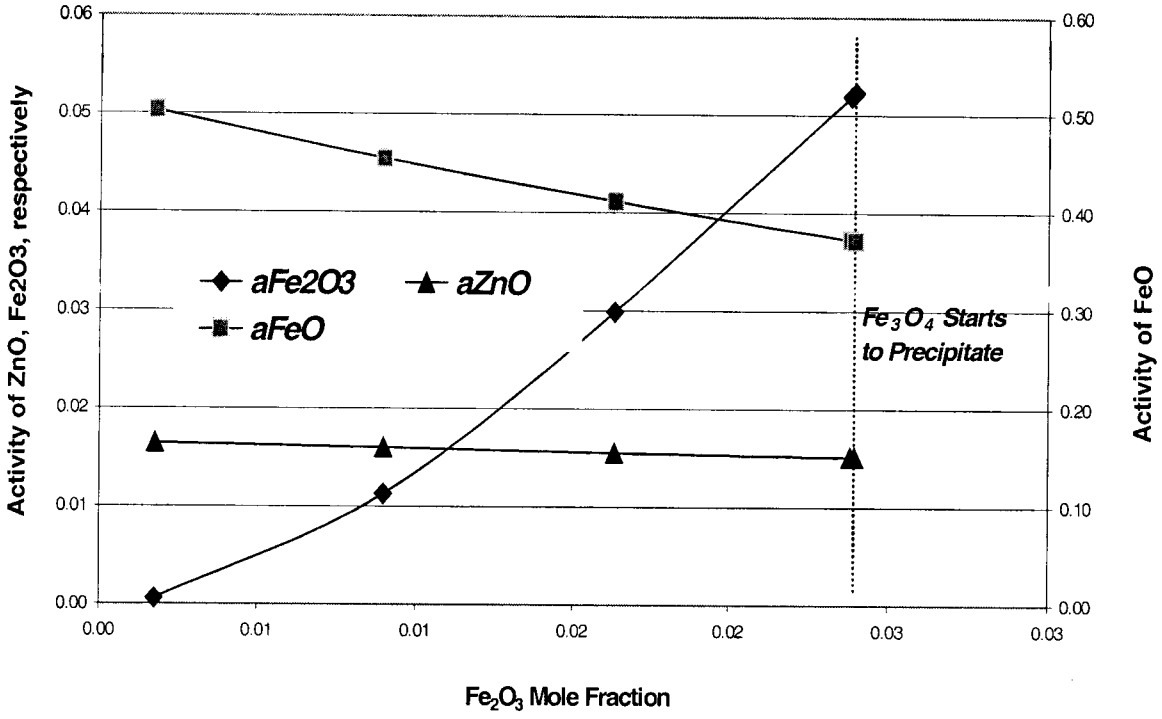

Fig. 25 — The effect of Fe_2O_3 mole fraction on the activities of ZnO, FeO and Fe_2O_3 in synthetic slag (N_{Zn} = 0.03) at 1250 °C

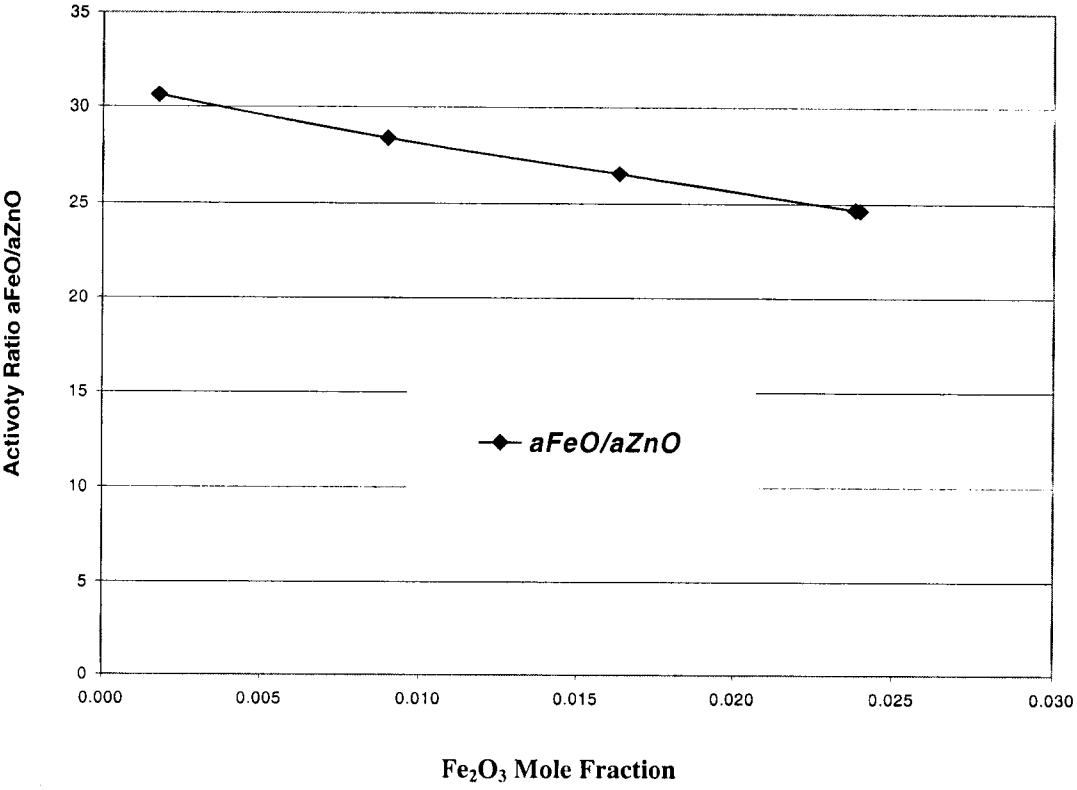

Fig. 26 — The effect of Fe_2O_3 mole fraction on the activity ratio aFeO/aZnO (N_{Zn} = 0.03)

6. EXPERIMENTAL DESIGN AND METHODS

6.1. Experimental Apparatus

A schematic diagram of the apparatus used in the experiments is shown in Figure 27. The various sections of the apparatus are discussed individually in greater detail below.

6.1.1. Crucible

The basicity of zinc fuming slag is usually around 1, which means that it is almost a neutral material. Both synthetic slags and fuming slags are not very corrosive at a working temperature of around 1250 °C. Alumina crucibles have been widely employed by researchers for their experimental work on zinc fuming, activity measurements of zinc fuming slags or lead blast furnace slags. Since the molten slag and copper will be air-quenched for the final slag and copper samples, each crucible can be used for only one experiment. Fireclay crucibles were tested with fuming and synthetic slags to see if they could be used to replace the much more expensive alumina crucibles. Initial experimental trials using a fireclay crucible with a fairly small curvature at the bottom resulted in significant corrosion due to the porous character of the crucible. Each crucible lasted for about 30 minutes. This led to the consideration of a denser fireclay crucible. After testing, this kind of crucible was found to perform satisfactorily, and was thus employed for all subsequent experiments.

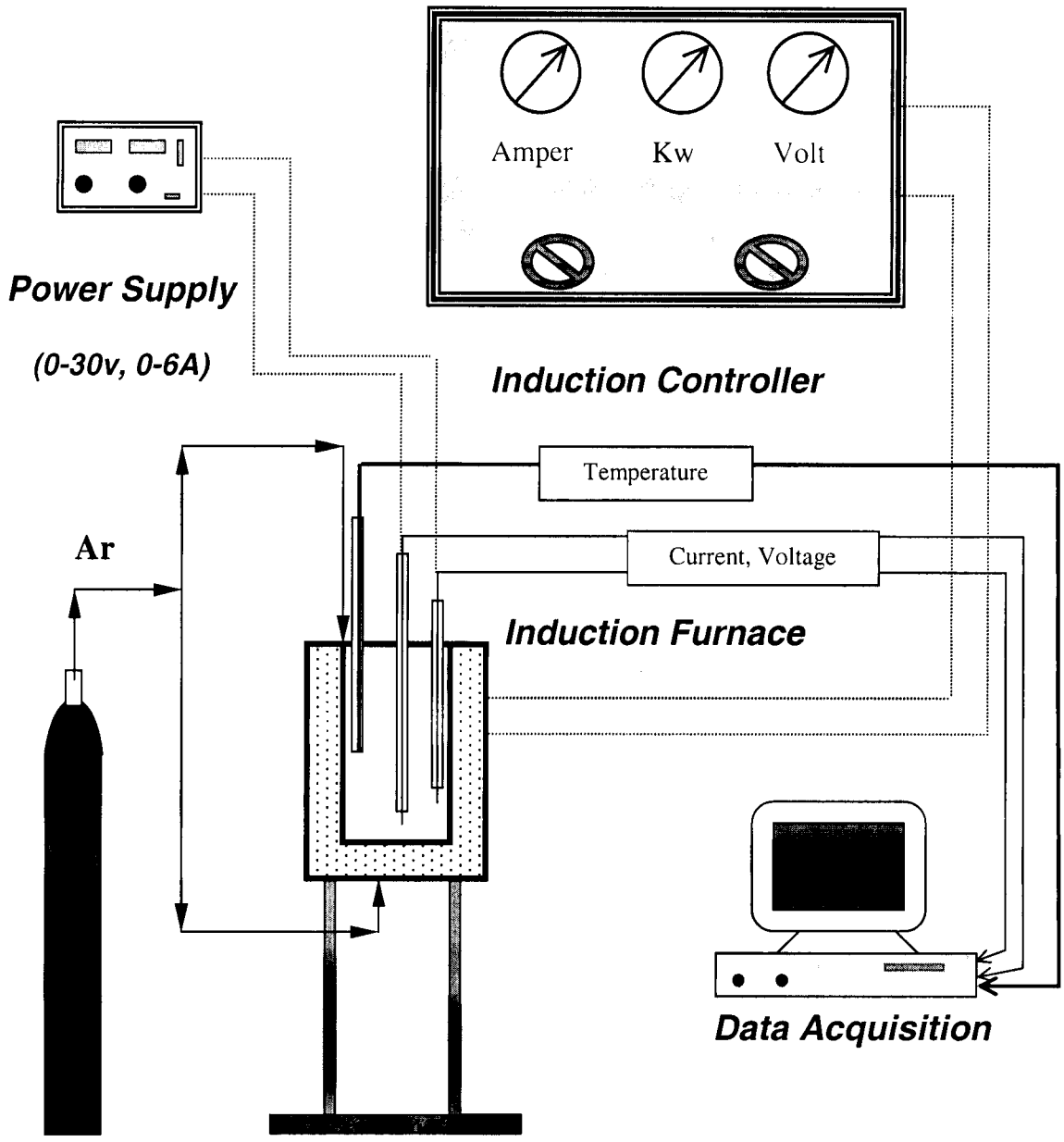

Fig. 27 — Schematic diagram of the experimental apparatus used for electrorefining experiments

Nearly all of the commercial fireclay crucibles are conical in shape while alumina crucibles are cylindrical in shape. In order to increase the cathode surface area for electrorefining experiments, a cylindrical crucible is preferred. For the sake of saving expense, all the electrorefining experiments were carried out in 400 gram fireclay crucibles 118 mm deep, with a diameter of 86 mm at the top and 56 at the bottom .

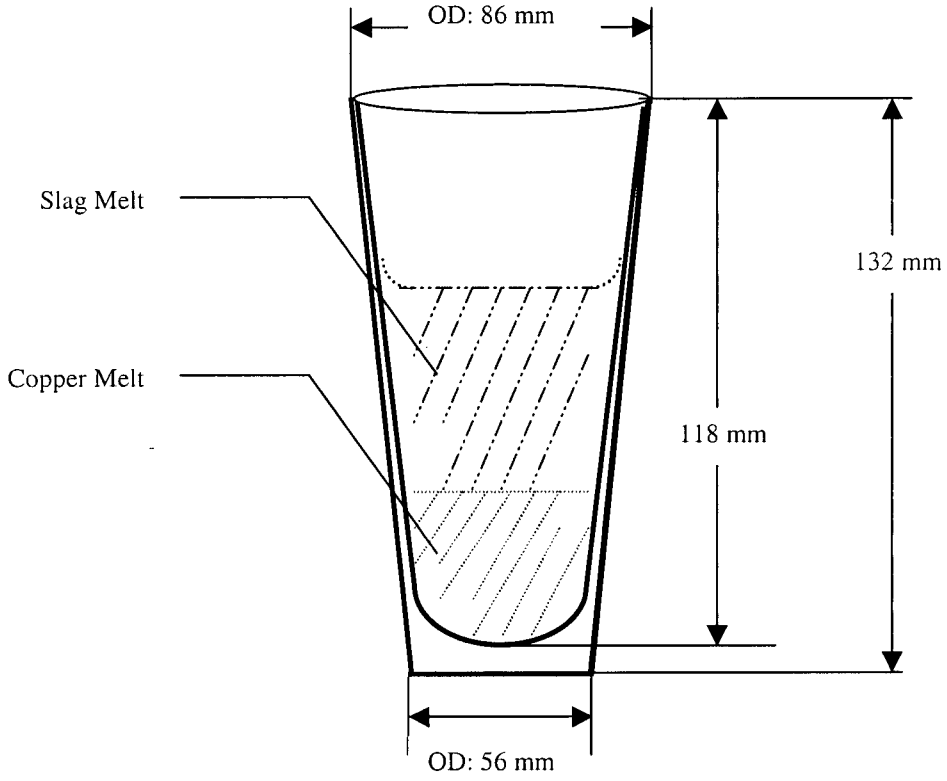

Fig. 28 — Schematic diagram of the crucible assembly with appropriate dimensions.

It was observed that even after the slag was melted in the crucible at 1350 °C and held at this temperature for two hours, there was very small corrosion of the crucible. As seen in Picture 29, there is a distinct interface between the synthetic slag and the fireclay crucible. Although the fireclay (right side) looks very porous, cross sectional examination showed that the synthetic slag did not diffuse into the holes in the crucible.

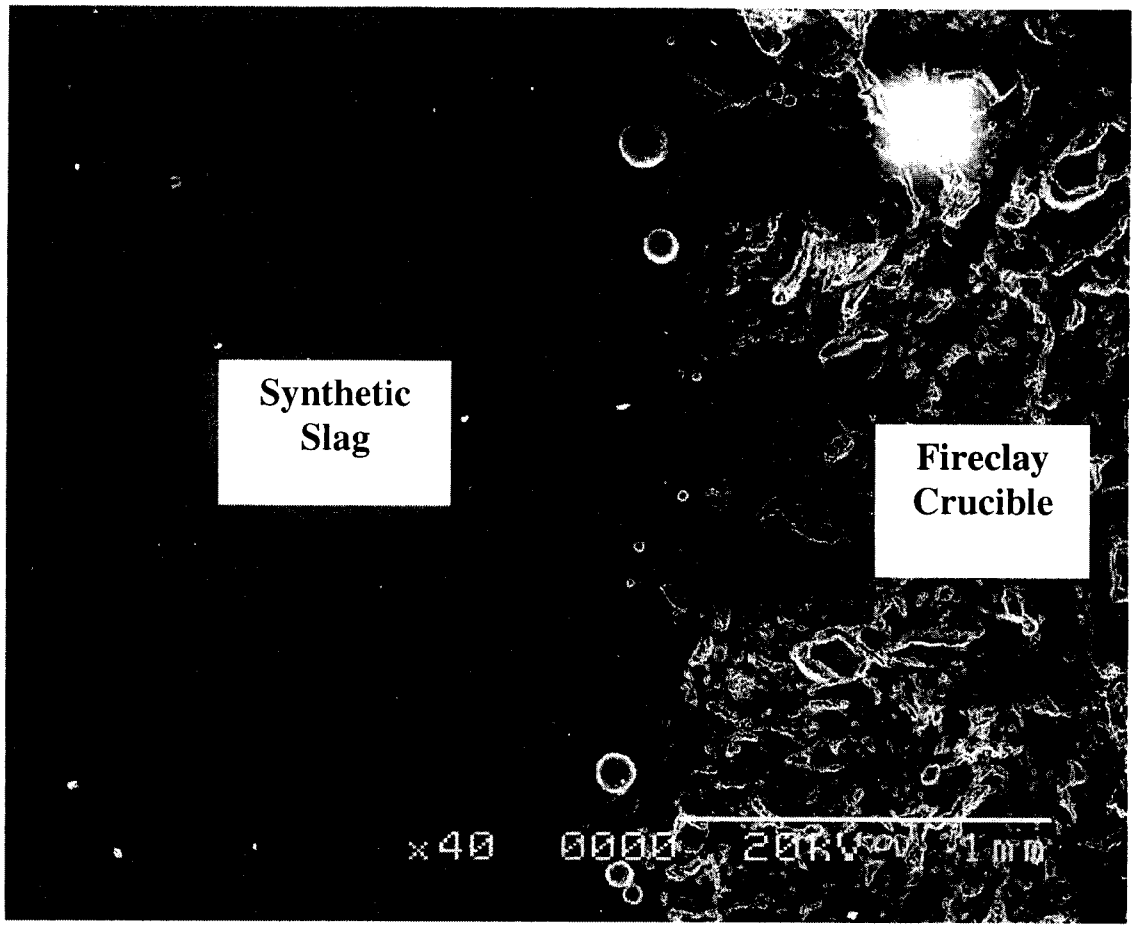

Fig. 29 — SEM picture shows that the interface between synthetic slag and fireclay crucible after slag was melted in crucible for two hours at 1250 °C

6.1.2. Electrode materials selection and dimensions

Materials chosen for the anode and cathode required the following special consideration:

- Anode:

Because the anode should stay inside the molten slag melt, the critical points for anode material selection were that

- it should resist the corrosion of slag;
- it should resist oxidation from the oxygen gas produced in electrochemical reaction at the anode;
- it should have the lowest overpotential(s) for the favored anode reaction(s).

Since our electrorefining process is very similar to the prime aluminum production process, the anode materials used there might also be applicable here. Much research has been done on the inert anode materials for aluminum production. These include metals and metallic alloys, cermets, oxides and cerium oxide coating[56,57], some of which have reached pilot scale tests[58] . Despite these tests, however, a consumable carbon anode is still the unique and irreplaceable choice in the production side.

At a working temperature of 1250 °C, if either carbon (graphite) or mild steel were used as the anode materials, it may behave as reductant to reduce zinc, iron or other metals in the slag melt, which also makes the anode process and cell reactions more complicated.

Platinum was finally chosen as the anode material because it is inert to molten slag and if there was oxygen involved in anode process, platinum would not be oxidized.

♦ Cathode:

Although molten aluminum itself is the cathode material for aluminum production, molten zinc can't be used as a cathode for electrorefining because the boiling temperature of zinc is only 907 °C. Also, a solid cathode is unacceptable because the deposited zinc will not be able to report to it. The ideal cathode candidate is a metal which has a melting temperature of below 1250 °C, and exists as an alloy element to zinc so that when zinc is deposited at the cathode, it will be dissolved into this metal melt.

The desired cathode metal should have the following properties:

- A melting temperature of below 1200 °C;
- A relatively high boiling temperature so that its vapor pressure at 1200 °C is reasonably low;
- A large solubility for zinc;
- A very limited solubility of iron;
- Limited solubility in the slag;
- Be more noble than iron or zinc;
- Reasonable price.

Based on the binary phase diagrams of Fe-Me (metal) and Zn-Me binary systems, metal copper, silver, lead and cadmium could be the possible cathode metals. Some of the important iron solubility data in Fe-Me and types of Zn-Me phase diagrams are summarized in Table IX.

Table IX. Possible Metals as Cathode

	Melting Point (°C)	Boiling Point (°C)	Fe-Me* (Fe solubility (wt.% at (°C))				Zn-Me
			1100	1200	1300	1400	
Cu	1084.87	2595	3	4.6	7.8	18.1	Several intermetallic compounds
Ag	961.93	2210	0.06	0.12	0.2	0.3	Several intermetallic compounds
Pb	320.85	1725	0.09	0.14	0.23	--	G + L above 907 °C
Cd	327.45	765	≅ 0	≅ 0	< 1	< 1	Eutectic relation

Me: ***representing any metal***

The phase diagram of Zn-Pb indicates that all of the zinc in liquid lead will vaporized into the gas phase at a temperature of above 907 °C. So, metallic lead is not suitable for cathode metal. Cadmium is also eliminated as a candidate cathode metal because it has a boiling temperature of only 765 °C. Silver is better than copper as a cathode metal but it is quite expensive. Finally, copper was chosen as the cathode material for the electrorefining process.

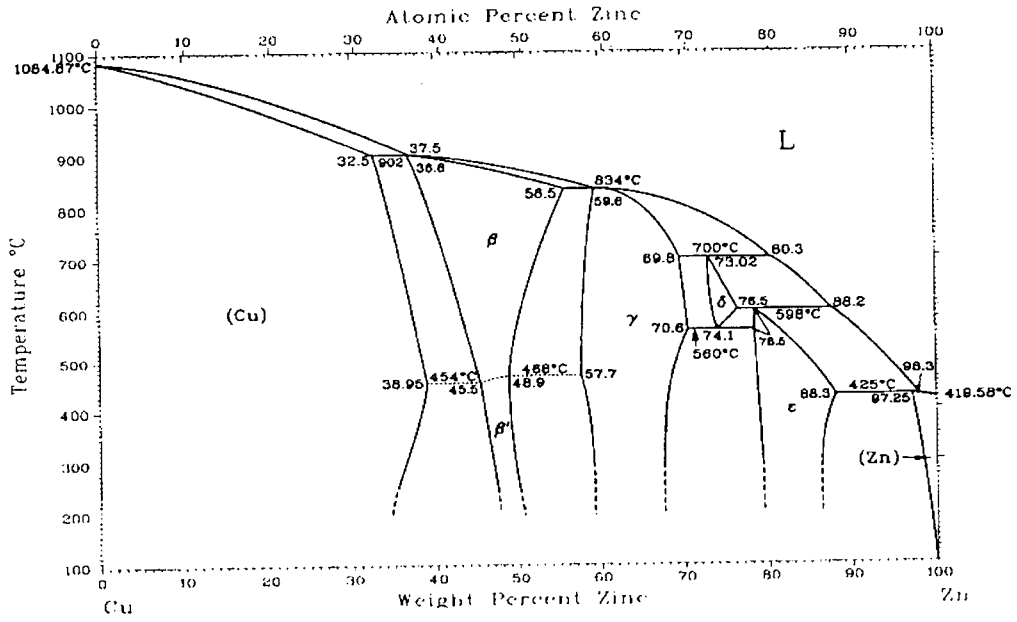

Fig. 30 — Phase diagramof Cu-Zn binary[59]

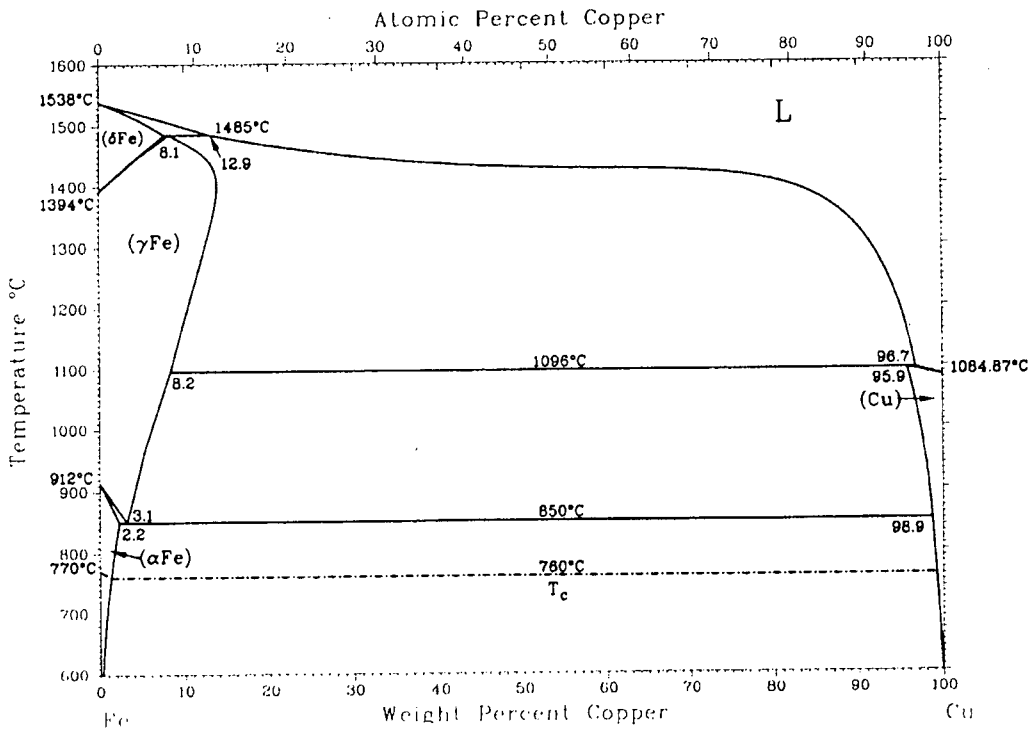

Fig. 31 — Phase diagram of Fe-Cu binary[59]

◆ Conduction-wires:

Adrian Fu[60] studied the suitability of materials for electrodes and conduction-wires. Four kinds of materials were tested in his experiments, namely molybdenum, platinum, molybdenum disilicide and silicon carbide. Molybdenum was burned into white fumes in air at a temperature of 1000 °C or over, and it also reacted with the zinc fuming slag. Molybdenum disilicide and silicon carbide, which are used widely as the materials for heating elements, were tested to determine their suitability as conduction-wire for the molten copper cathode. It was concluded that when contacted with liquid copper at 1300 °C, $MoSi_2$ was slowly dissolved into the liquid copper while SiC would melt.

Platinum wire, which can resist the erosion of molten slag, was chosen as the anode conduction wire which connects the platinum cylinder anode with the direct current power supply. As indicated in the binary phase diagram of Cu-Mo, Mo is nearly insoluble in copper melt at working temperature of about 1250 °C. Ahmad *et al.*[59] measured the solubility of molybdenum in liquid copper at 1350 °C for 7 hours under an argon atmosphere and showed very low concentration of Mo in copper, that is less than 0.01 weight percent. So, Mo wire, sheathed in alumina tubing, was selected as the cathode conduction wire.

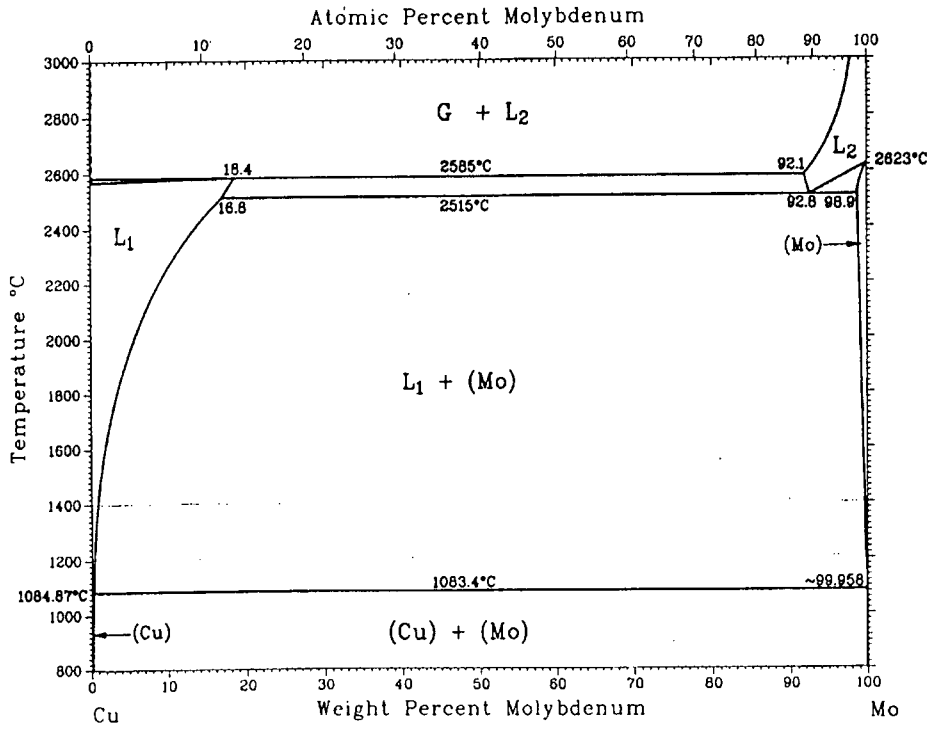

Fig. 32 — Binary phase diagram of molybdenum and copper[59]

A detailed sketch of the electrode assembly is shown in Figure 33. A molybdenum wire was used as a connection line to the liquid copper cathode. Platinum was chosen as the material for both the anode connection line and the anode cylinder. There were two concentrically fitted alumina tubes used for the protection of each electrode conduction-wire respectively. In order to prevent the molybdenum wire from burning away by combustion with air in the gap between the Mo wire and the alumina tube, a molybdenum wire of 0.85 mm diameter was used because it fitted the inner alumina protection tube exactly. A one ounce platinum coin (supplied by ***J&M Canada Coin and Stamp***, Vancouver, Canada), with a purity of 99.9%, was rolled into a thin plate for making the anode cylinder. There were two kinds of anodes: a bigger one with dimensions of diameter 39 mm, height 27 mm and thickness 0.01 mm, and a smaller one, with

dimensions of diameter 20 mm, height 10 mm and thickness 0.004 mm. The lower part of the alumina tube for the anode was wrapped by platinum foil of 0.025 mm thickness (supplied by Alfa@AESAR, Ward Hill, MA, USA) so that molten slag could not contact it directly. Two platinum wires with the same diameter of 0.35 mm were used as the anode conduction-wire, which connected the anode with the direct power supply.

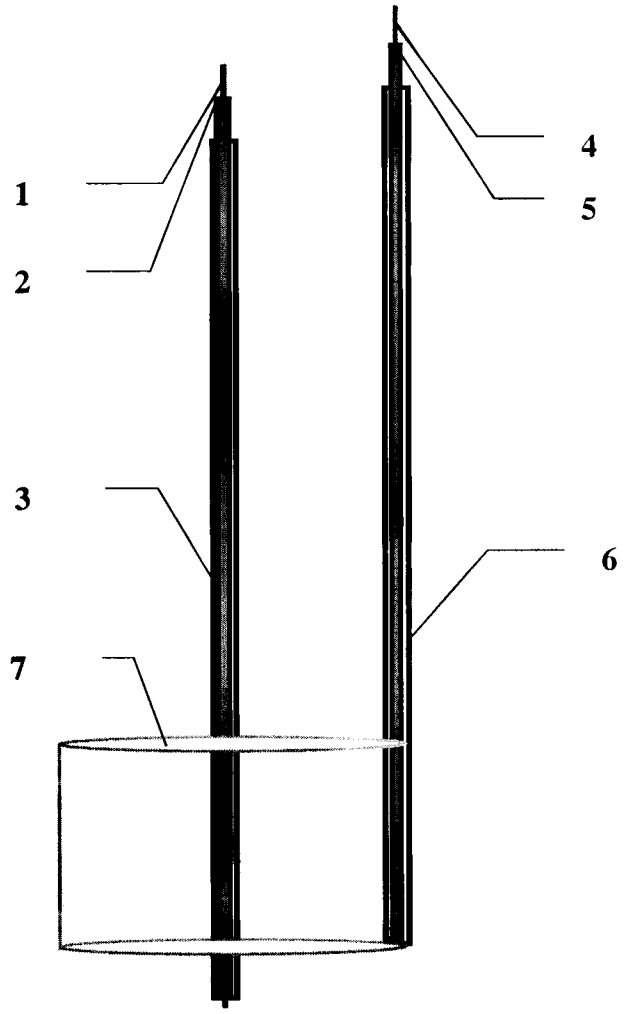

Fig. 33 — Electrodes. 1: cathode conduction-wire (Mo), 2: outer cathode protection tube (Al_2O_3), 3: inner cathode protection tube (Al_2O_3), 4: anode conduction-wire (Pt), 5: outer anode protection tube (Al_2O_3), 6: inner anode protection tube (Al_2O_3), 7: anode cylinder (Pt).

6.1.3. Furnace construction

All the experiments were carried out in a self-constructed induction furnace (Figure 34). A Graphite element (labeled "14" in Figure 34, Grade XG2000 Bushing, 5 ¼"(O.D.) x 3 ¾"(I.D.) x 9"(L), supplied by National Electrical Carbon Canada, Edmonton, AB, Canada, was used as the susceptor for induction. This element combined with the MgO ring (labeled "15") and the refractory ring (labeled "16"), separated the furnace into two parts: the inner chamber and the outer chamber. The inner chamber was the space inside the graphite element, which served as the working space for the crucible assembly and the electrodes. The outer chamber of the furnace was the space between graphite element and the outer one-end-closed refractory bucket (labeled "2"), which served as insulation and graphite element protection.

At the experimental temperature of about 1300 °C, the graphite element would be burned away after several runs if the atmosphere around it was air or if the oxygen potential was significantly high. Two methods were used to protect the graphite element from burning, one was to keep air away from it and the other was to flow argon around the wall.

The outer chamber was separated into two parts again by a mullite tube (labeled "12"), to prevent air flow from the outside of mullite tube to the inside. The gap between the mullite tube and refractory bucket was filled with fine alumina particles (about 50 mesh or 0.0117 ins.), and the gap between the mullite tube and graphite was filled with coarse alumina powder (diameter: about 2.1 mm).

Argon gas was introduced into the chamber between the mullite tube and the graphite element through three jets (labeled "9") located in the bottom fiber plate (labeled "7"). This argon flow was used solely to protect the graphite from oxidizing. A second stream of argon was introduced into the inner chamber through another three jets (labeled "10"); mixed with the argon gas from one argon jet in the top refractory cover; those argon flow exited the inner chamber through all the gaps of the inner chamber. This argon was for the furnace oxygen potential control and graphite element protection. All the argon streams were controlled at a predetermined flow rate, using a mass flow controller.

A graphite cup (labeled '13") was used to hold the working fireclay crucible (labeled "8"). As a protection, in case there was a leak of molten slag, or a slag overflow from the crucible or a melting of the fireclay crucible at an unreasonably high temperature, such as over 1450°C, this cup could hold the molten materials. Equipped with a moveable graphite shaft (labeled "11"), the graphite cup and the working crucible could be raised and lowered to move the crucible in and out of the furnace. The top of the furnace was covered by two pieces of porous fireclay bricks. The entire furnace was rested on a fiber plate (labeled "7"), which was supported by four steel posts to the ground.

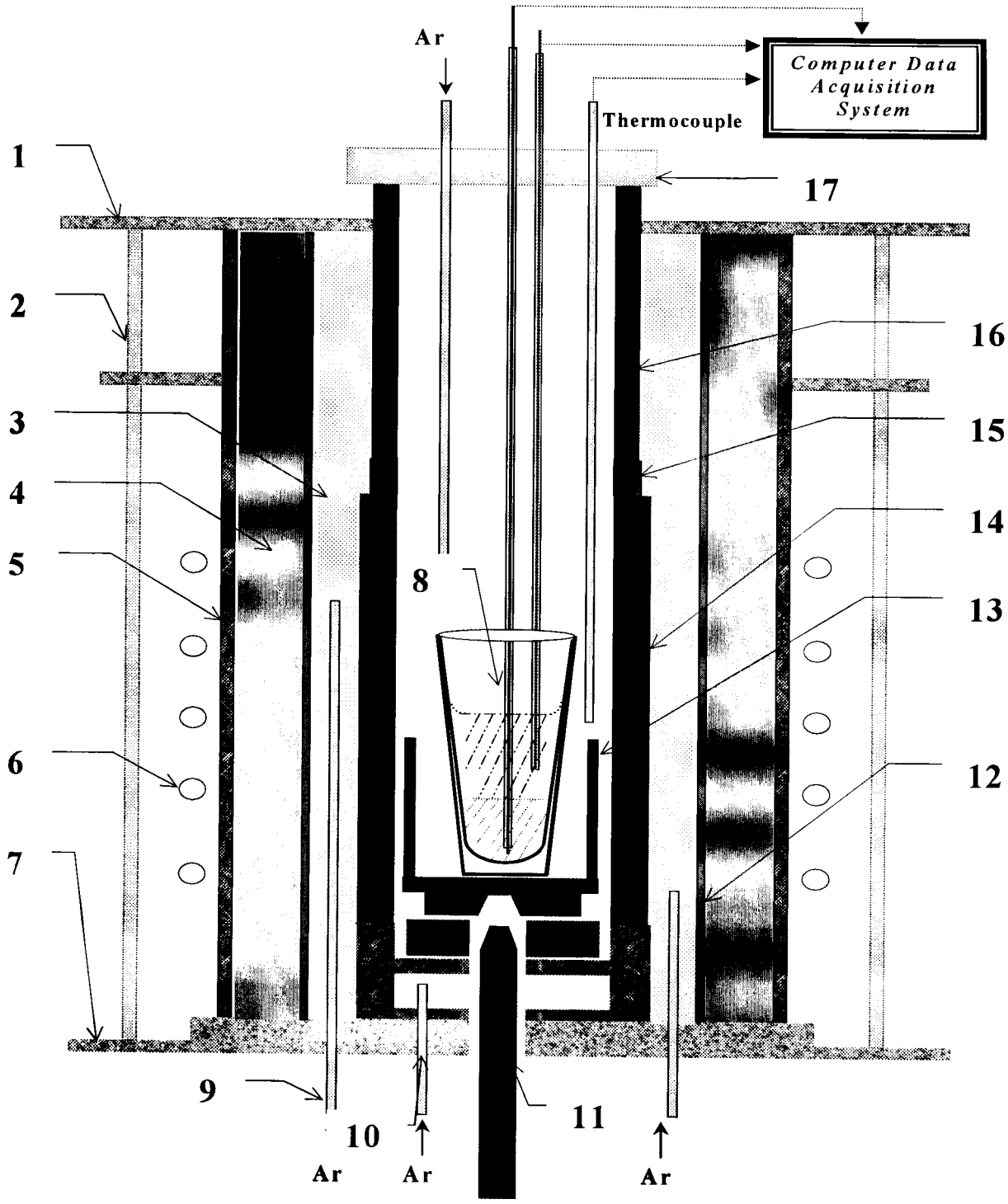

Fig. 34 — Induction furnace. 1:top plate (asbesto), 2: side support stands, 3: coarse alumina powder, 4: fine alumina powder, 5: refractory bucket, 6: induction coils, 7: bottom plate (asbesto), 8: crucible assembly, 9 & 10: argon inlet tubes, 11: graphite shaft, 12: mullite tube, 13: graphite cup, 14: graphite element, 15: MgO ring, 16: refractory tube, 17: furnace cover.

6.1.4. XYZ movement controller

The XYZ controller was designed to control the movements of the anode and cathode to the specified positions exactly. It was composed of two parts – The base and the height gauges. The Base was a XY movement controller which was capable of sliding horizontally in both X and Y directions; serving as a coarse adjustment. The Height Gauges allowed precise movements of electrodes in the vertical direction. A pair of steel disks, one for each electrode, controlled the tilt angle of the electrodes. Each of these disks contained three springs which were used for fine adjustment. By this mechanism, the tips of the electrodes could be precisely moved closer together or separated.

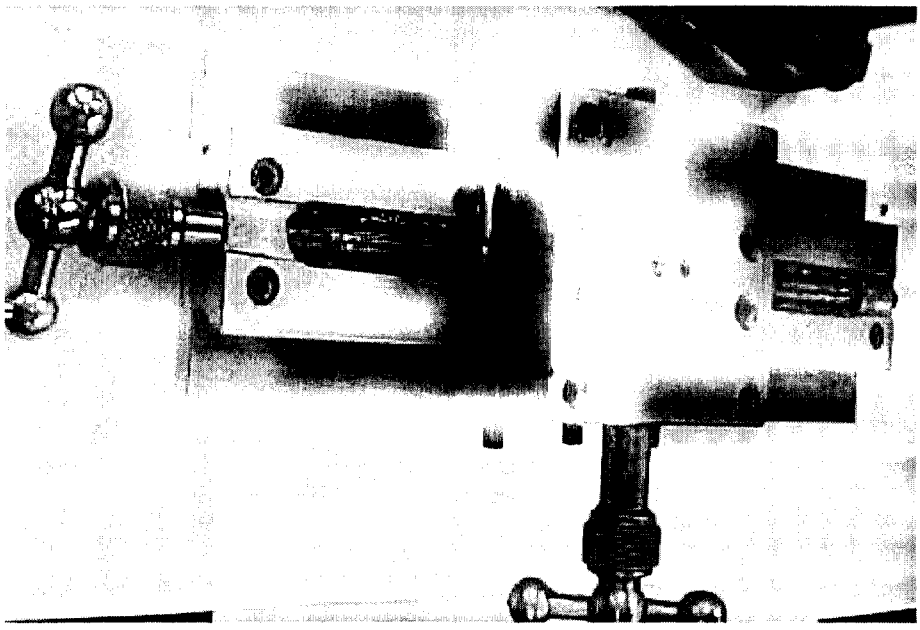

Fig. 35 — Base of XYZ movement controller

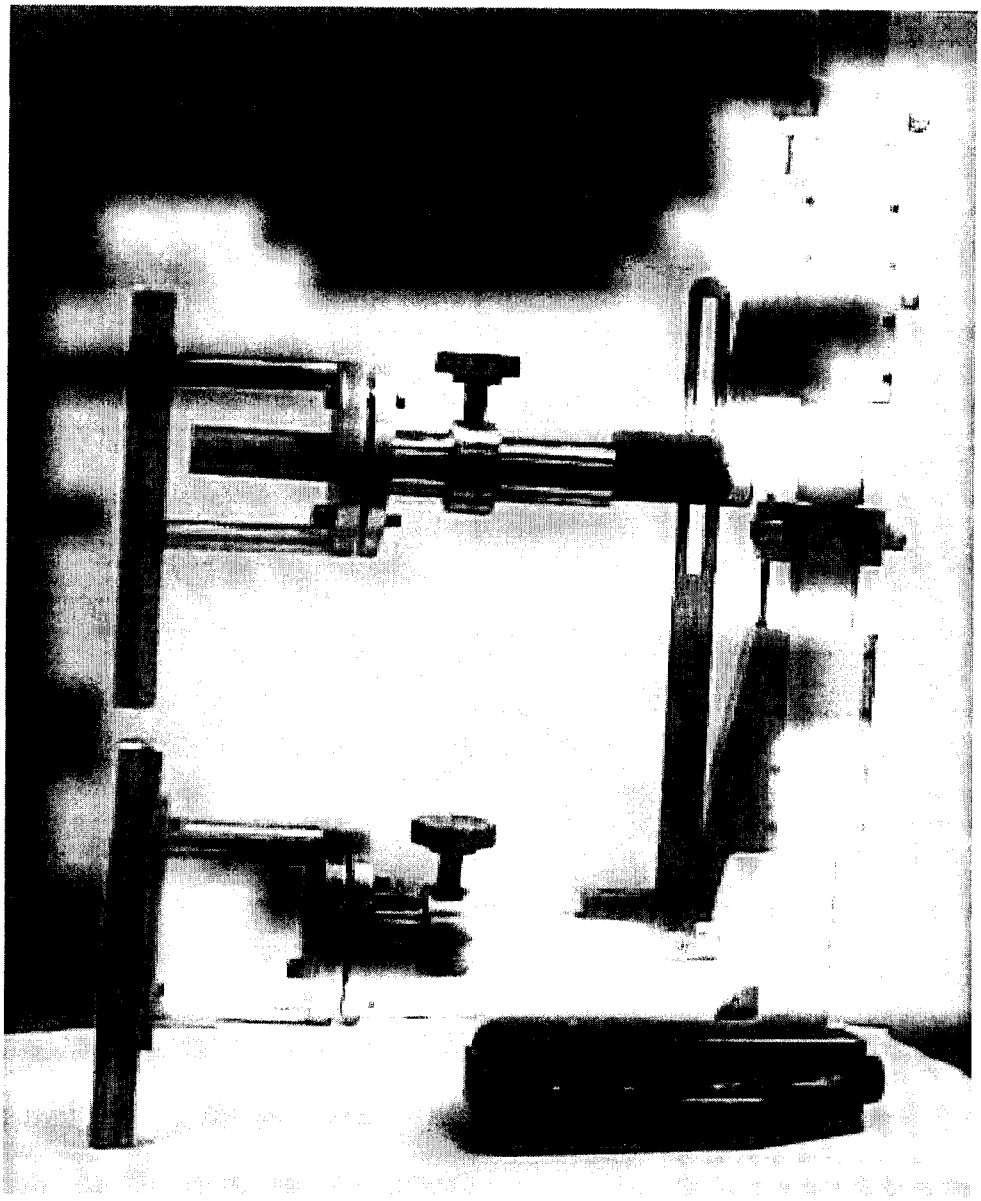

Fig. 36 — Height gauge modified for the electrode positions controlling

6.1.5. Data acquisition

A PC based data acquisition system was used to collect the temperature reading from the thermocouple, along with voltage and current readings from the power supply. The system was supplied by ***Keithley Instruments, Data Acquisition Division***, Taunton, MA, USA. The data acquisition card had 16 input channels with the flexibility of recording various types of input signals, i.e., temperature, voltage, and current signals. The card could obtain samples at different frequency, and saved the data in an ASCII format. The data thus obtained could be imported into Excel spreadsheets for further analysis.

6.2. Electrorefining Cell

6.2.1. Expected electrode reactions

Normally in an electroreduction cell the separation of the cation is aided thermodynamically by the oxidation of carbon at the anode. For example, in the cell cited by Pan[61] the half-cell reaction are

$$Mn^{2+} + 2e = Mn$$

$$C + O^{2-} = CO + 2e$$

In the cell contemplated in this work, the use of carbon would in all probability reduce the iron and cause it to precipitate. To avoid this problem, liquid copper was the cathode. Inasmuch as all of the metals of interest are completely soluble in copper at the temperature planned, there will be as additional thermodynamic driving force for the half-cell reduction reaction. Also, since the solubility of iron in copper at the temperature of 1200 °C is under 5 percent, the activity of iron in copper should reach a very high level quickly. The half cell reactions would be

Cathode:

$$\mathbf{Zn^{2+}_{(slag)} + 2e = Zn_{(diss.\ in\ Cu)}}$$

$$\mathbf{Pb^{2+}_{(slag)} + 2e = Pb_{(diss.\ in\ Cu)}}$$

$$\mathbf{Ge^{4+}_{(slag)} + 4e = Ge_{(diss.\ in\ Cu)}}$$

$$\mathbf{In^{3+}_{(slag)} + 3e = In_{(diss.\ in\ Cu)}}$$

Anode:

$$O^{2-} = \frac{1}{2}O_2 + 2e$$

It is also possible that at the cathode, some of the iron will be reduced to a lower valance state (or even metal), and at the anode, ferrous iron is reoxidized into its ferric form.

$$Fe^{2+}_{(slag)} + 2e = Fe_{(diss.\ in\ Cu)} \quad (1)$$

$$Fe^{3+}_{(slag)} + 3e = Fe_{(diss.\ in\ Cu)} \quad (2)$$

$$Fe^{3+}_{(slag)} + e = Fe^{2+}_{(slag)} \quad (3)$$

$$Fe^{2+}_{(slag)} = Fe^{3+}_{(slag)} + e \quad (4)$$

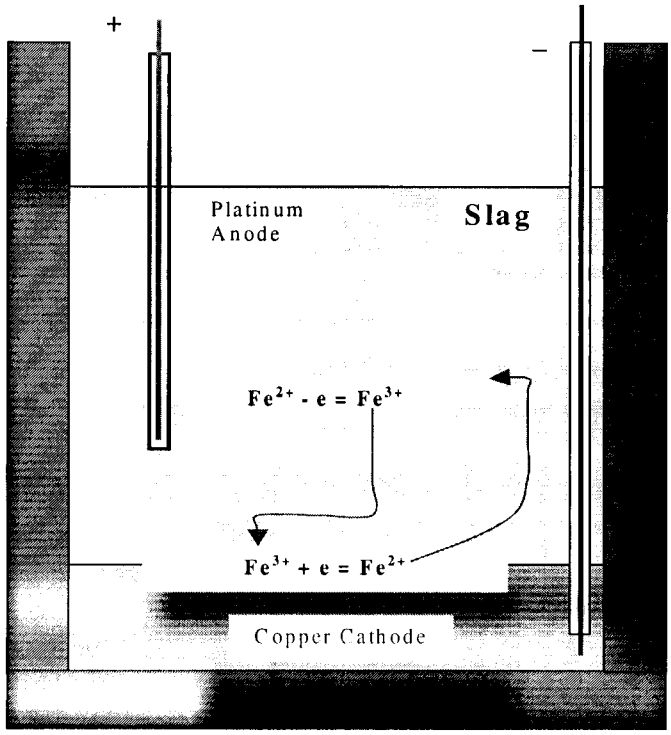

Fig. 37 — Picture shows possible iron circulation between anode and cathode

If the latter two reactions take place in the melt, between the anode and cathode, it would be the case that current can flow without the movement of ions. This is known as electronic conductivity and can markedly reduce current efficiency. However, if the silica content is above 30 per cent, the anode current efficiency should be more than 90 per cent. In other words, conduction in the slag should be mainly ionic.

Reactions (1) and (2) are undesirable since they lead to iron deposition into the cathode. Since the solubility of iron in the copper melt at the conceived working temperature is very limited, a small quantity of iron in copper will have a relatively high activity. Even if iron continues to deposit in the cathode, iron will reach its saturation point (at 1200 °C, 4.6 per cent). After that, the only way for iron to deposit on the copper cathode is in its solid form (the melting temperature of iron is 1536 °C). If iron is reduced into its solid form from the slag melt, it involves a process of new phase formation, which requires more energy. Thermodynamically, this process is more difficulty and unlikely.

Table X. Standard Reduction Potentials[62]

Reaction	E^0/V
$Zn^{2+} + 2e = Zn$	-0.7618
$Pb^{2+} + 2e = Pb$	-0.1262
$In^{2+} + 3e = In$	-0.3382
$Ge^{4+} + 4e = Ge$	0.124
$Fe^{2+} + 2e = Fe$	-0.447
$Fe^{3+} + e = Fe^{2+}$	0.771
$Fe^{3+} + 3e = Fe$	-0.037

The standard reduction potentials of the possible anode reactions are listed in Table X. The more negative the standard reduction potential of the reaction, the less likely the reaction will happen. It is clear that zinc reduction is the most negative one among all the reactions.

Because there is no reduction potential data for the reactions of interest in this research, the reduction potentials for zinc and iron were calculated from equations 3, 4, and 5. The results are listed in Table XI. At 1200 °C, the so-called standard reduction potentials of iron and zinc are nearly the same. When copper is used as the cathode and the corresponding activity of ratios of iron and zinc in copper and slag phase are placed into the equation, zinc oxide in slag becomes much easier to reduce and the difference between the so called standard reduction potentials is about 0.2 volt.

$$Me + \frac{1}{2}O_2 = MeO$$

$$\Delta G^0 = - ZFE_{Me}{}^0$$

$$E_{Me/v} = E_{Me}{}^0 + \frac{RT}{ZF} Ln \frac{a_{MeO}}{(a_{Me}) * (P_{O_2})^{\frac{1}{2}}}$$

where
Me: metal with valence of two
MeO: metal oxide
ΔG^0: standard free energy (calories)
Z: number of electron transfer in the reaction
F: Faraday constant (96500)
$E_{Me}{}^0$: standard reduction potential of metal Me
$E_{Me/v}$: real state reduction potential of metal Me
R: the gas constant (8.314 joules/K-mole or 1.987 calories/K-mole)
T: temperature, K

a_{MeO}, a_{Me} : activity of MeO and Me respectively

P_{O_2} : oxygen potential

Table XI. Reaction Potentials at 1200 °C

Element Reaction	ΔG^0 (kJ/mol Me)	E^0(v)
$Zn + \frac{1}{2}O_2 = ZnO$	-159.133	-0.8247
$Fe + \frac{1}{2}O_2 = FeO$	-166.026	-0.8604

State	ΔE(v)
$E^0_{Zn} - E^0_{Fe}$ *(Standard)*	0.0357
$E_{Zn} - E_{Fe}$ *(when a_{Fe}/a_{Zn} = 300, a_{FeO}/a_{ZnO} = 30, P_{O_2} = 1)*	0.1868

6.2.2. Estimation of cell voltage

It is estimated that the cell voltage of the zinc slag electrolysis should be about 4 volts. Each of the components is listed in Table XII. The anode overpotential of this study should be higher than that of alumina electrolysis, because the former uses inert anode and the later uses a consumable anode.

Table XII. Estimation of Cell Voltage of Zinc Slag Electrolysis

Component	*Volt(V)*
Decomposition voltage	0.77
IR Drop in electrolyte and connections	2.0
Anode overvoltage	0.5 – 1.0
Cathode overvoltage	0.1 – 0.5
Anode effect	0.15
Terminal voltage	3.52 – 4.42

6.3. Methodology

Two kinds of slags were used in the electrorefining experiments, namely ***Cominco*** *Fumer Slag* and *Synthetic Slag*. The former was provided by Cominco Research, Trail, British Columbia, Canada and its chemical composition was shown in Table I and V.

The synthetic slags were prepared by using laboratory grade oxides and metal iron powder. The composition of synthetic slag was based on the main components of Cominco Fumer Slag. The proportion was controlled as Fe 105(g), Fe_2O_3 295(g), CaO 230(g), SiO_2 370(g), plus the amount of zinc oxide. The chemical compositions of the two master synthetic slags are listed in Table XIII, one with a higher ZnO content of 4.33 percent and the other at 1.98 percent.

Table XIII. Chemical Compositions of Synthetic Slags Made in UBC (by Analysis)

	Fe^{2+} (Wt. %)	Fe^{3+} (Wt. %)	SiO_2 (Wt. %)	Al_2O_3 (Wt. %)	CaO (Wt. %)	Cu (Wt. %)	ZnO (Wt. %)
Slag1	24.52	3.01	37.91	4.74	17.98	0.03	4.33
Slag2	23.87	1.28	41.95	5.69	16.88	0.03	1.98

6.3.1. Sampling and analysis

For fuming or electrolysis, each run lasted for about two hours. Samples of the slag were obtained intermittently by dipping a 5 mm diameter stainless steel rod into the slag melt every fifteen minutes. The argon gas supply was increased to 15 l/minute just prior to sampling to prevent air flow into the furnace chamber. The rod was lowered carefully to the slag melt but not to the copper. After a few seconds, the rod was withdrawn carefully out of the melt and the furnace chamber, making sure to prevent any contact with the walls of the furnace, electrodes, argon inlet pipe and thermocouple protection tube. The frozen slag layer was then separated carefully from the rod and collected in appropriately labeled sample bags. About one minute elapsed between the time the gas supply was increased, and the argon flow was resumed to the normal flow rate of 5 l/minute after sampling was finished.

When a run was finished, the fireclay crucible and the melt inside it was taken out of the furnace as soon as possible, and air quenched. After cooling down, both a slag sample and a copper sample were taken. A handsaw was used to cut the cooled copper lumps and the saw dust was collected as the copper sample. The slag sample from the crucible and slag samples collected from the stainless steel rod were sent to ***Cominco*** Research, Trail, British Columbia, Canada for chemical analysis. Copper samples were sent to ***International Plasma Lab Ltd.***, Vancouver, Canada for zinc and iron analysis.

7. EXPERIMENTAL RESULTS

With using an induction furnace as the energy source for all the electrorefining runs, the question arises as to the impact of the electromagnetic field on the electrolysis experiments. Initial runs with a copper sulfate water solution were tested in the induction furnace with the objective of quantifying this influence. The copper sulfate was used as the electrolyte and the resistance of the solution was adjusted to approximately the same as that of the molten tail slag at 1250 °C. The electrolyzing testing cell was composed of a glass cup filled with the prepared solution and two iron plates with iron connection wires (One behaves as the anode and the other as the cathode. The plates were put into the solution as the electrodes and the corresponding connection wires were connected with the power supply). After the cell was put into the induction furnace, the voltage of the power supply was set to a desired constant value and the current passing in the cell was monitored with the furnace both on and off. Because the solution is aqueous, those tests could last for only several minutes before the temperature went too high to the boiling point of the solution. The results of those tests indicated that the effects of the induction field on the current and voltage of the working cell were small and tolerable.

In several electrorefining runs using synthetic slags, the current-voltage relationship was tested and the results were identical for the same synthetic slag. When induction was on, the current fluctuated in a limited range for a set voltage (Figure 38). When induction was off, the current and voltage were in good linear relationship (Figure 39) and the recorded current values were not as scattered as these of the previous one. A typical result for a run of 150 grams copper, 200 grams of slag, and with a large platinum anode, the current and

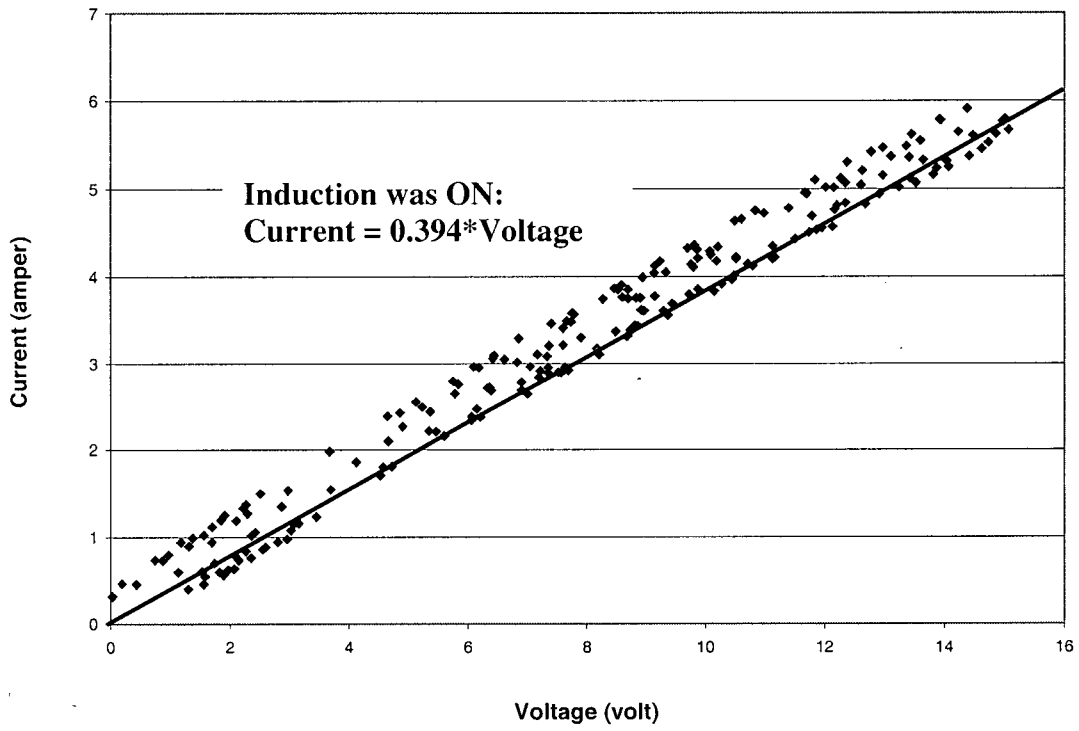

Fig. 38 — Current-voltage relationship for synthetic tail slag experiments at 1250 °C (Induction ON)

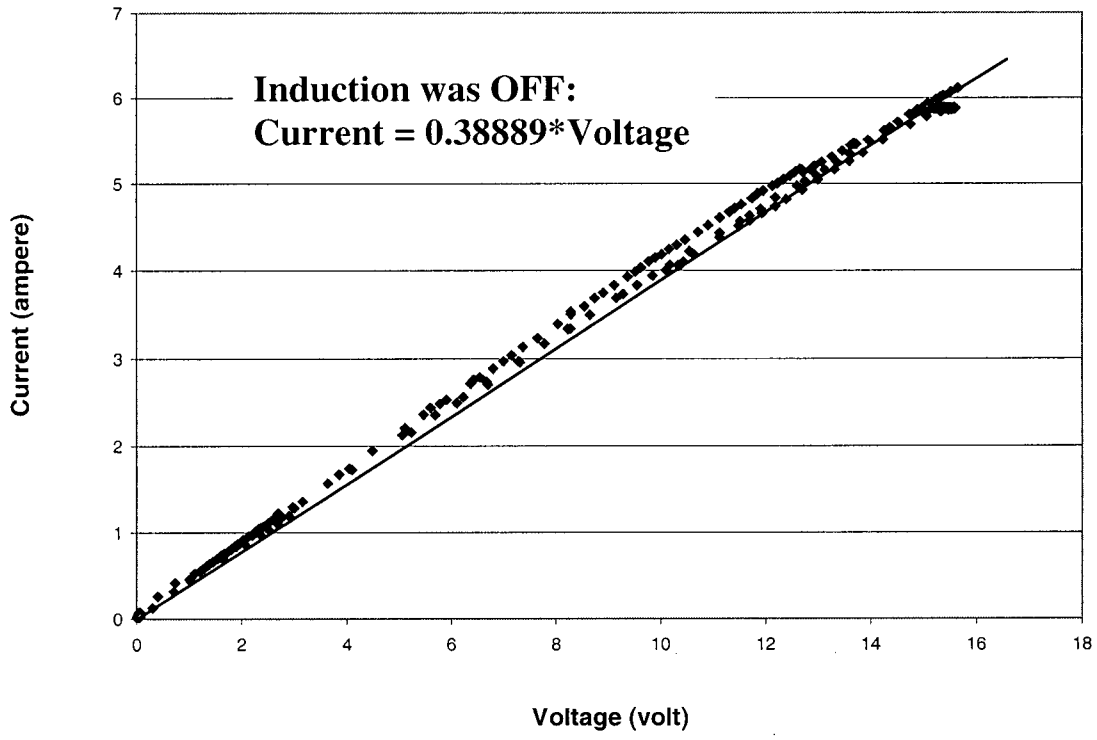

Fig. 39 — Current-voltage relationship for synthetic tail slag experiments at 1250 °C(Induction OFF)

voltage present a linear relationship with a slope of 0.394 and 0.3889 respectively while induction was run and off , as shown in Figure 38 and 39. Woolley and Pal[63] also observed the linear current-voltage relationship for their research in the cell of Fe-C anode, Mo (or graphite) cathode and slag with FeO as the melt.

The experiments were designed to examine the role of voltage and a copper "getter" on the recovery of zinc from tail slag, and to determine the suitable voltage for the electrorefining process. A secondary aim was to determine the effect of temperature and basicity on the recovery of zinc by electrolysis. Finally, the as-received ***Cominco*** tail slag was electrorefined at the voltage determined from previous experiments for synthetic slags.

7.1. The Effect of Voltage on Zinc Concentration in Slag

The initial experiments were carried out in a small fireclay crucible (15 grams) with a small platinum anode (diameter 19.20 mm, height 11.15 mm, thickness 0.1016 mm). Both the cathode copper and the synthetic slag weighed 60 grams for each of the experiments in this group. The heights of molten copper and slag were estimated from the solidified samples so that the distance between the top surface of the molten copper and the lower bottom of the platinum anode could be controlled. This distance was aimed at 2.50 mm. Because platinum softens at the working temperature of 1250 °C, the actual distance varied from 2.6 to 2.65 mm.

As estimated on page 74, the cell voltage to achieve electrolysis should be 4.0 volts or above. The experimental conditions and results of the first group of runs are listed in Table XIV. After electrolysis, the cathode copper contained some amount of iron and zinc. Although the results were quite scattered, there were some general relationships, such as

- The higher the voltage applied, the higher the iron and zinc concentrations in the cathode copper,
- The longer the eletrorefining time, the more metal was deposited,
- For all tests, no matter what the voltage applied or the elapsed time, the copper cathode contained more zinc than iron. The zinc concentration is roughly double that of iron for most experiments.

Table XIV. The Effect of Voltage and Time on the Copper Cathode Composition

Experimental Conditions	Fe %	Zn %
4.5v, 0.8A, 30min.	0.46	0.86
4.5v, 0.95A, 70min	0.51	1.09
5.0v, 0.9A, 30min.	0.33	0.86
5.0v, 1.12A, 121min.	0.83	1.43
6.0v, 1.1A, 30min.	0.63	1.04

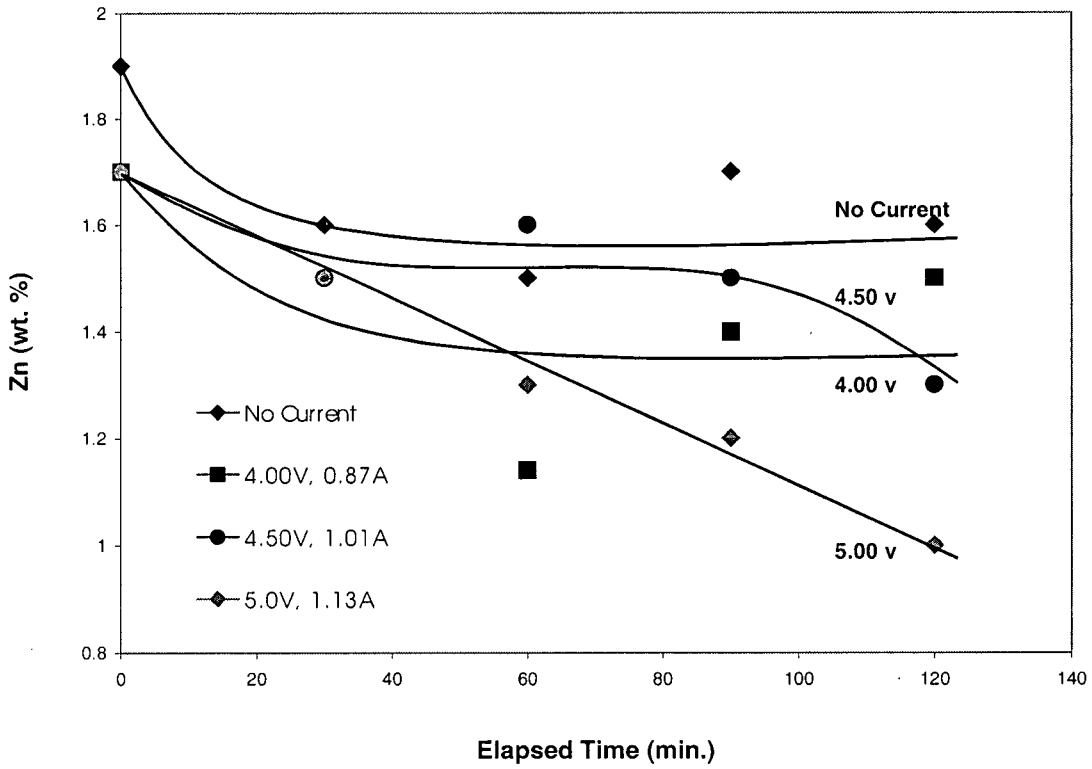

Fig. 40 —The effect of voltage on the zinc concentration of synthetic tail slag with higher initial zinc content, smaller electrodes (1250 °C)

In order to obtain more comparable values for further experiments, the second group of experiments were carried out at the same elapsed time, with only voltage as the variable. The voltage varied from 4.0 to 5.0 volts. One run, with no current passing, was carried out as a reference for all the electrorefining runs. As seen from Figure 40, without current passing, the zinc concentration was almost stable after 30 minutes. Apparently, zinc fuming reached chemical equilibrium after 30 minutes. Also, the experiments at 4.00 v and 4.50 v gave similar curves to that without current passing, except that zinc concentrations were lower. Only when the voltage was increased to 5 volts did the effect of voltage become obvious and an almost linear relationship existed between the zinc concentration and elapsed time.

7.2. The Effect of Copper, Direct Current on Zinc Concentration in Slag

Thermodynamical analysis and FACT simulation both indicate that the thermodynamic driving force for zinc is larger than that for iron if copper is used as the "getter" for zinc recovery from tail slag. In order to have a larger current flow, a bigger platinum anode (Diameter 39 mm, height 27 mm, thickness 0.11 mm), 150 grams of copper as cathode, and a bigger crucible (40 gram) were used for subsequent runs.

When a constant voltage of 4 volts was applied to the cell, the current was about 1.73 amperes. At this current, the zinc concentration changes in the synthetic slag are almost the same as those without current passing (Figure 41). When voltage was increased to 5 volts, the effect of voltage became obvious. All the later electrorefining runs were conducted at 5 volts.

For a pure fuming run (Figure 42) with an initial zinc concentration of 1.4 per cent, after about 30 minutes of fuming, there is no obvious decrease in the zinc concentration for a synthetic slag at 1250°C. The zinc concentration stabilized at about 1.1 per cent. When copper was employed as the "getter" for zinc (Figure 43), it was clear that the zinc concentration in the slag was much lower than that of the previous run. The zinc concentration stabilized again at a new value of about 0.78 per cent. When voltage was set to a constant of 5 volts, the direct current readout was about 2.10 amperes. With this current passing, the zinc concentration kept dropping continuously (Figure 44).

In both the fuming runs without copper or with copper, about 30 minutes appeared to being about equilibrium for zinc fuming. However, with current passing, the zinc concentration dropped continuously, as seen clearly in the run at 5 volts. An almost linear relationship between the zinc concentration and elapsed time existed (Figure 45). Although the same synthetic slag was used for the three experiments in Figure 45, there were some differences for the time needed to heat up and melt the synthetic slag. The initial zinc concentrations were different also.

For the run of 5 volts and 2.06 amperes (Figure 45), if the zinc concentration difference in the slag and the iron concentration difference in the copper are used to calculate the cathode current efficiency, the cathode current efficiency is 68 per cent.

It was found that the total zinc deposited in the copper (1.0275 gram, calculated by the concentration of zinc in copper) was less than that obtained from the difference of the zinc in the slag before and after electrolysis (1.52 grams). This difference might be due to some zinc reporting to the fume from the slag or from copper, while the electrorefining was in process. As shown in Figure 46 (by FACT calculation), the zinc vapor pressure in Cu-Fe-Zn is quite large, even when the zinc concentration is low. For each of the two-hour electrolysis, there was a continuous argon flow, which also behaves as a carrier for zinc fume and provides a path for zinc fuming. After each electro-reduction run, some white powder & film were observed around the top cover of the induction furnace, and further EDX examination confirmed this to be is zinc oxide.

If zinc is the only element that carries the current in the melt for the electrorefining reaction, it might be expected that with a decrease of zinc concentration in the melt, the current would decrease also. Figure 47 shows that the direct current did decrease in the 2-hour electrorefining run, but the drop was not significant.

An analysis of ferrous and ferric ions concentration changes in the slags under different conditions are summarized in Table XV. After two hours of fuming, the ferric ion concentration dropped to 1.13 from the original 1.87 per cent. When copper was used as the "getter", the ferric iron concentration increased to 1.94 per cent. With current passing, the ferric concentration increased to 3.10 per cent.

The air-quenched slag after electrolysis was examined by SEM (Figure 48). More dendrites in the slag matrix were observed than in the synthetic slag. Those dendrites, examined by EDX, were magnetite, which indicated qualitatively that there was an increase of the amount of ferric iron in the slag.

The zinc fuming and small amount of iron circulation in the melt are the two main reasons, which dropped the cathode current efficiency to 68%, less than the predicated value of around 90%.

Because the crucibles used in those experiments were fireclay crucibles, the slag dissolved some of the alumina and silica from the crucible in the electrorefining runs,

which led to a slight increase of alumina and silica concentration. The concentrations for iron and calcium were stable for all the runs (Figure 42, 43, 44).

Based on the experiments and analyzing results, possible reactions happened are proposed as follows:

- **Fuming without Copper:**

$$2Fe^{2+} + Zn^{2+} \rightarrow Zn_{(g)} + 2Fe^{3+}$$

- **Fuming with Copper:**

$$2Fe^{2+} + Zn^{2+} \rightarrow xZn_{(\text{in Cu})} + (1\text{-}x)Zn_{(g)} + 2Fe^{3+}$$

$$3Fe^{2+} \rightarrow Fe_{(\text{in Cu})} + 2Fe^{3+}$$

- **With Electrolysis:**

$$Zn^{2+} + 2e \rightarrow xZn_{(\text{in Cu})} + (1\text{-}x)Zn_{(g)}$$

$$O^{2-} - 2e \rightarrow {}^{1}/_{2}O_2$$

$$Fe^{2+} - e \rightarrow Fe^{3+}$$

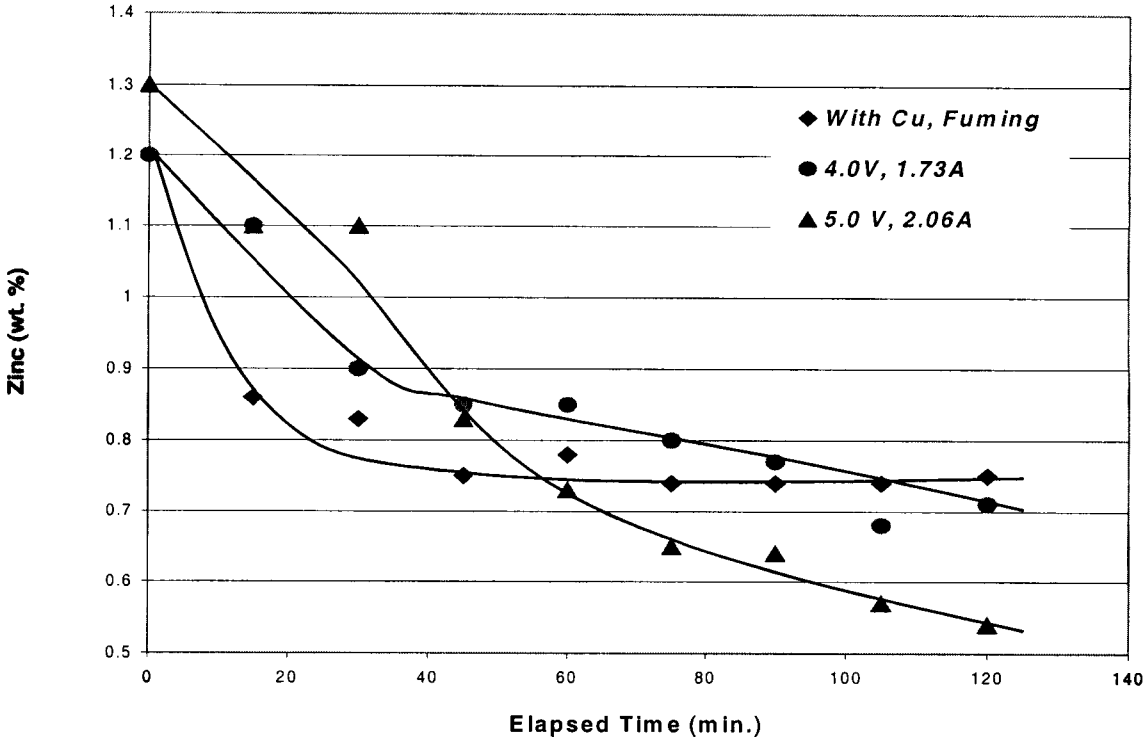

Fig. 41 — The effect of voltage on zinc concentration of synthetic tail slag (1250 °C)

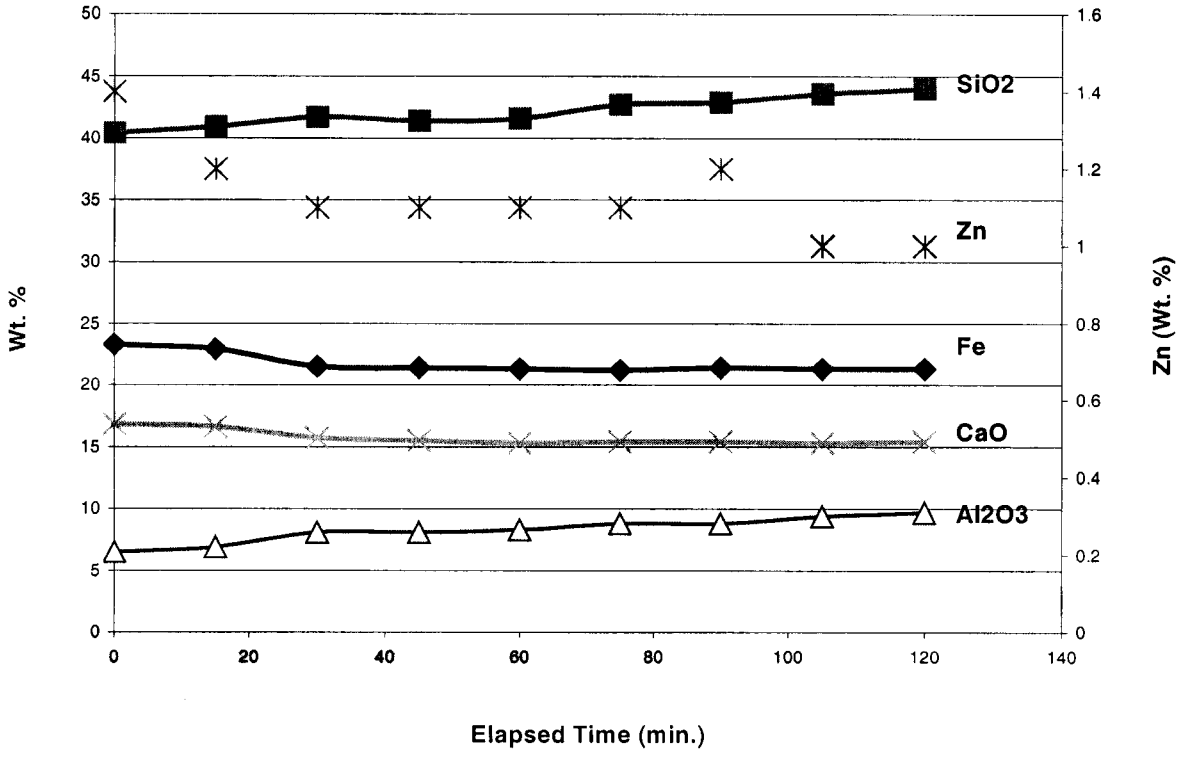

Fig. 42 — Synthetic zinc tail slag fuming run without copper, sampling data (1250 °C)

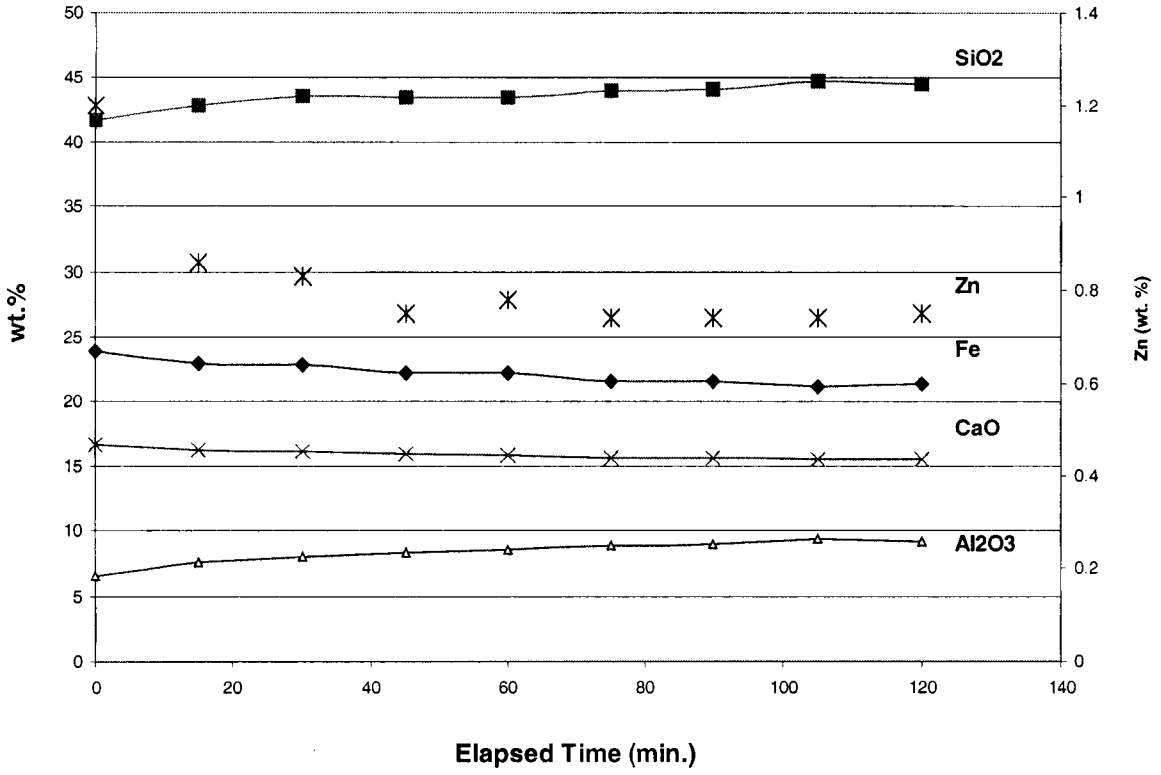

Fig. 43 — Synthetic zinc tail slag fuming run with copper, sampling data (1250 °C)

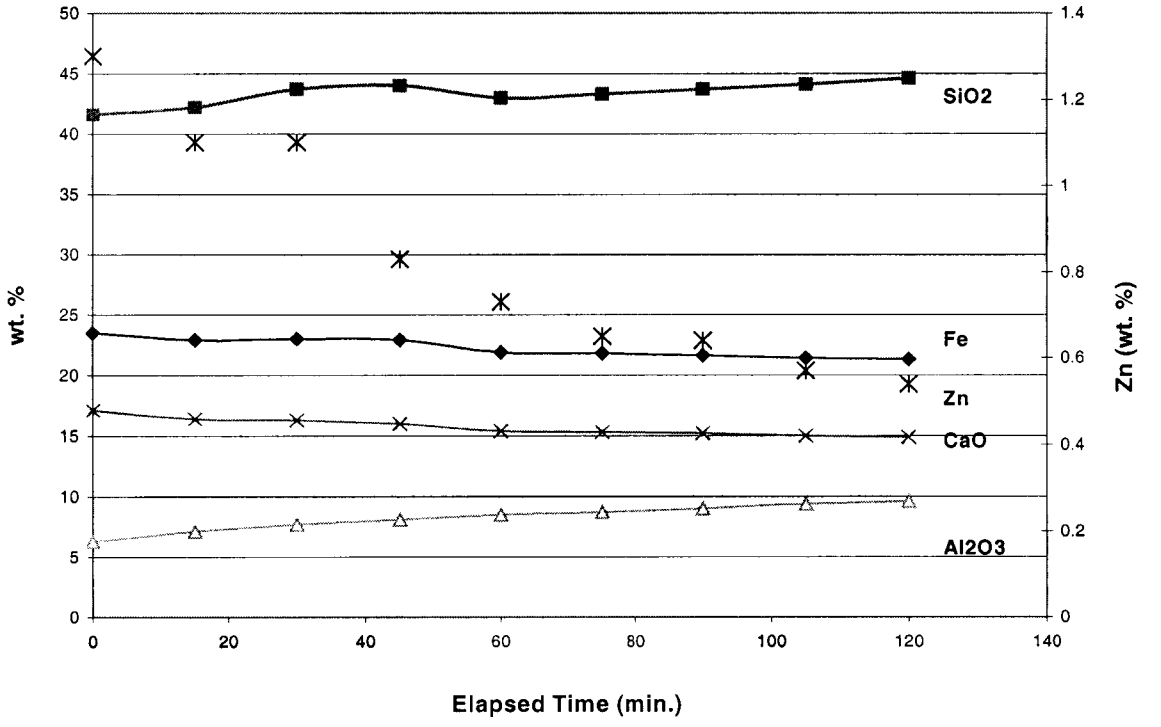

Fig. 44 — Synthetic zinc tail slag electrorefining run with copper cathode, sampling data (1250 °C)

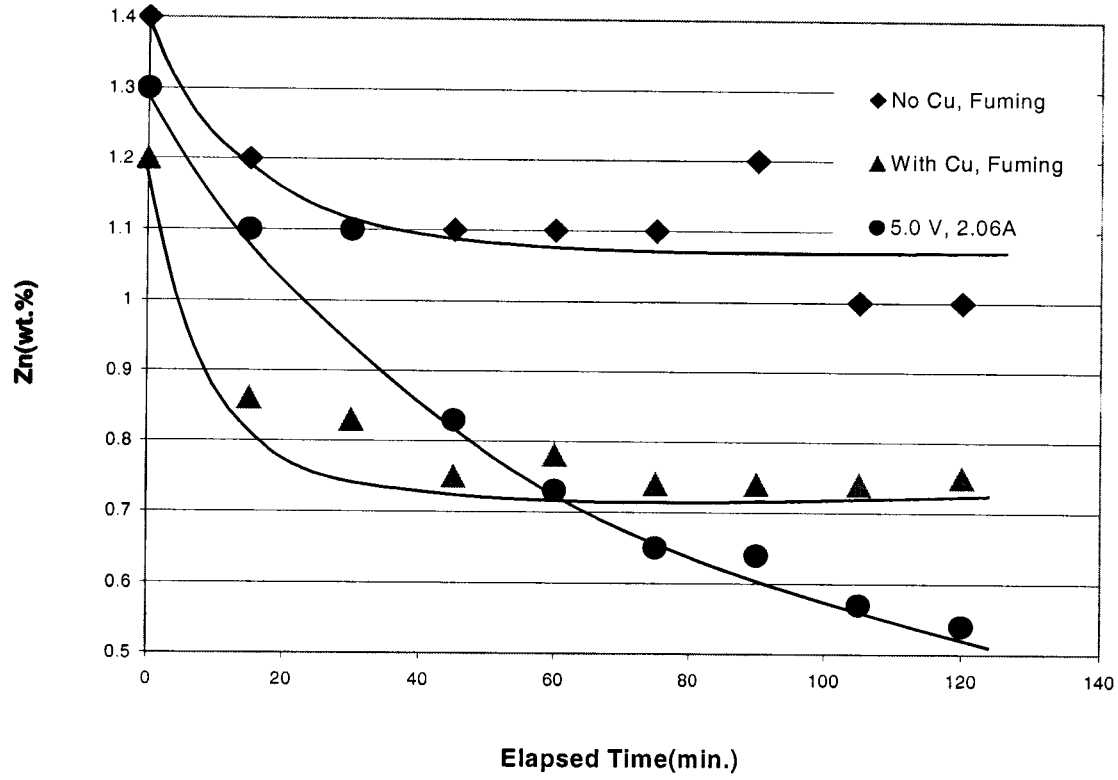

Fig. 45 — The effect of copper, current on the zinc concentration of synthetic tail slag (1250 °C)

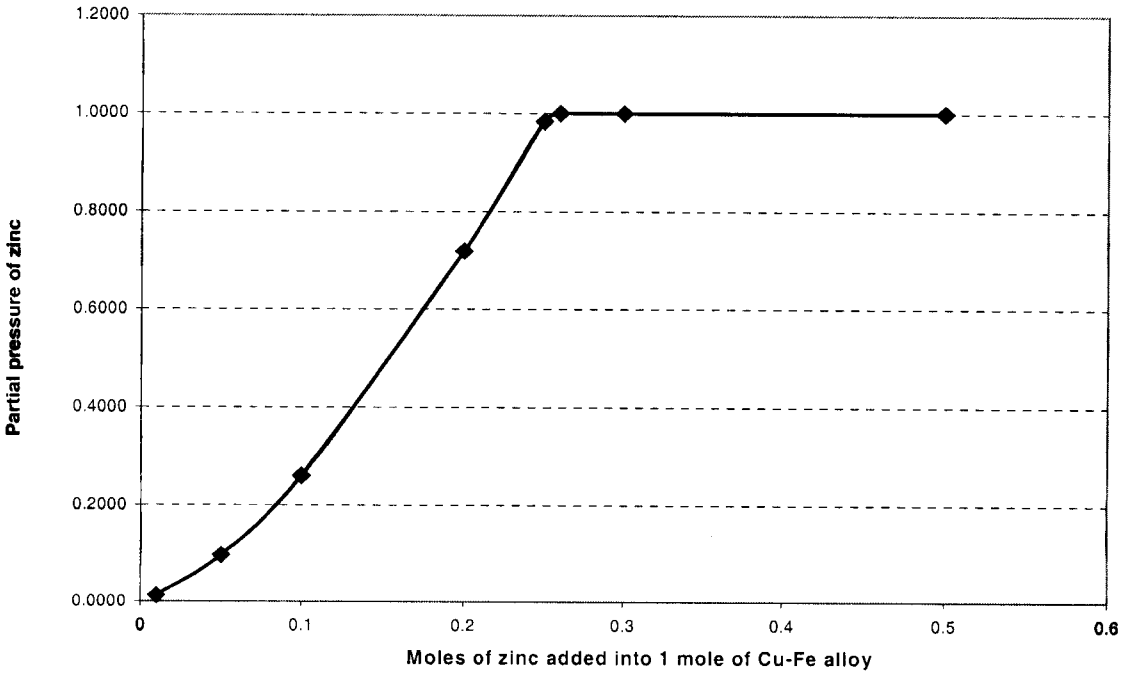

Fig. 46 — Zinc partial vapor pressure in Cu-Fe (0.95mole Cu + 0.05mole Fe) melt at 1250^0C

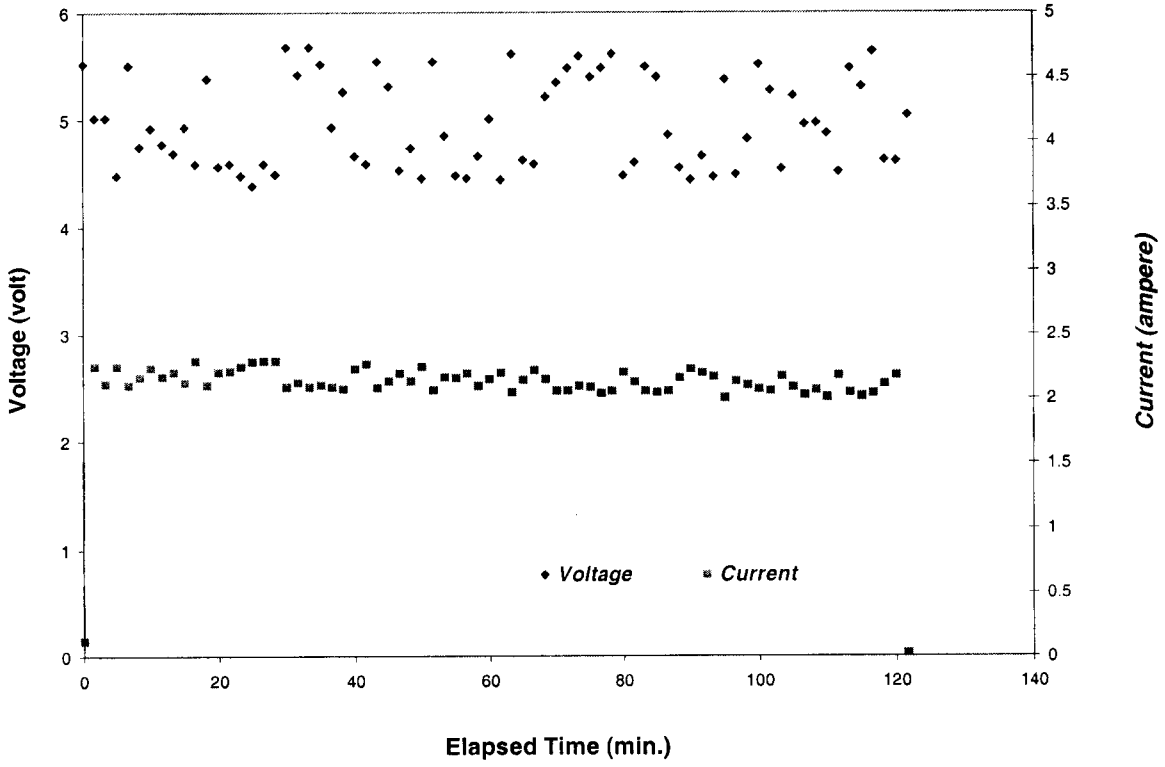

Fig. 47 — Current change during a synthetic tail slag run when voltage was set constant of 5 volt (1250 °C) and copper as cathode

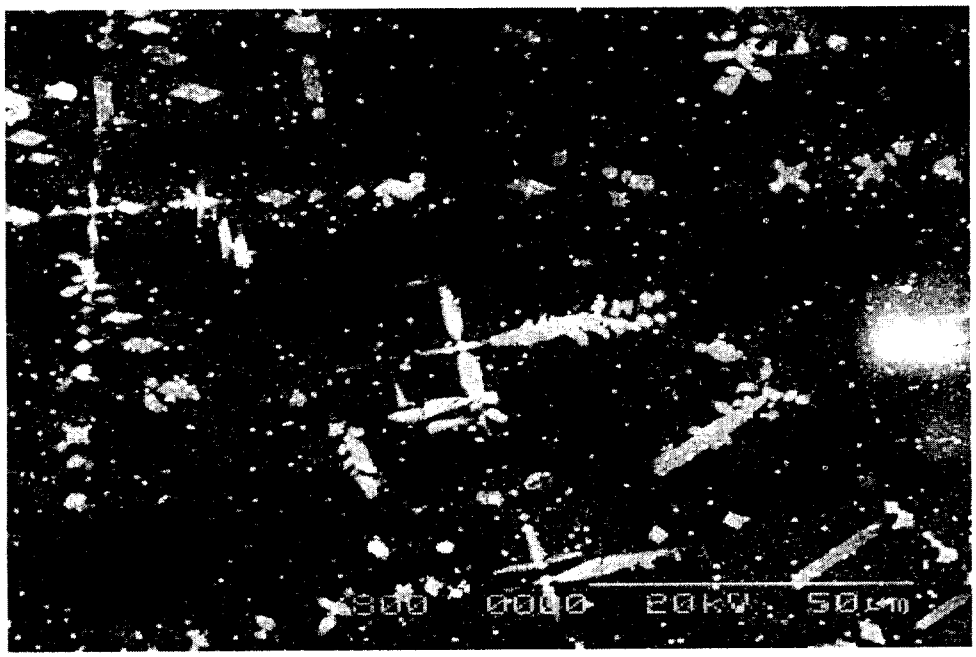

Fig. 48 — After electrorefining, some dendrites were observed in the slag matrix (slag air-quenched) (SEM, magnification 800, accelerating voltage 20kV)

Table XV. Fe^{2+} and Fe^{3+} Concentration Changes in Synthetic Slags

	Fe^{+2}	Fe^{+3}
Synthetic slag	23.84	1.87
Fuming, No Cu	23.11	1.13
Fuming, with Cu	22.41	1.94
5.00V, 2.08A, 2hrs	20.55	3.10

7.3. The Effect of Temperature on Zinc Concentration in Slag

Increased process temperature led to a higher fuming rate. With a temperature increase of 100 °C (from 1250 °C to 1350 °C) (Figure 49, 50), the zinc concentration decreases were faster than before. The patterns of the curves were kept the same for both the fuming and the electrorefining runs. For the fuming runs, about 20 minutes were needed for zinc fuming to reach equilibrium at 1350 °C, comparing that of 30 minutes for the run of 1250 °C. It was also observed that 0.44 % was the limiting zinc concentration for electrorefining run since after 90 minutes operation, there was no further zinc concentration drop. The identical electrorefining run of 1250 °C had not reached a limiting value. The fireclay crucibles were in good shape after the operation at 1350 °C, so, refractory attack is not a potential problem for higher temperature operation.

7.4. The Effect of CaO Concentration on Zinc Concentration in Slag

In order to compare the effect of basicity on the fuming and electrorefining of zinc from synthetic tail slag, two runs with increased CaO concentration were carried out. The CaO concentration increase was aimed at 5%. The CaO amount needed for this increase was weighed accurately and this CaO was well mixed with synthetic tail slag. The new slag with increased CaO concentration was tested for both the zinc fuming and electrolysis, while the operation temperature was kept constant at 1250 °C.

The Figure 51 and 52 show two set of fuming and electrorefining data for the CaO concentration of 16% and 21% respectively. When some CaO was added to the synthetic slag, there was no significant increase of the zinc-fuming rate. Comparing the electrorefining runs with different CaO concentration, the higher CaO concentration seems have some negative effects on the zinc deposition on the liquid copper cathode, because the curve follows the fuming pattern rather than electrorefining pattern. Because the calcium is a more electro-negative metal and the size of Ca^{2+} is much smaller than other ions such as Fe^{2+}, Zn^{2+}, *etc.*, Ca^{2+} can move much more freely in silicate melt. When electrorefining was in processing, Ca^{2+} could contribute to a large portion of the transfer number in the electrolysis. This makes the electrolysis of zinc less effective.

7.5. The Electrorefining of Cominco Tail Slag

A group of experiments with the as-received Cominco tail slag were carried out to test the effect of copper and direct current flow on the recovery of zinc (Figure 53). The data

showed that the effect of copper and current passing was not significant on the recovery of zinc from slag. No matter copper was used, current passed or just slag fumed, the zinc concentration was closing to about 2.5 per cent.

The results of cathode copper analysis indicated that 1) with current passing, more zinc and iron were deposited in the copper melt than without direct current flow, and the concentration of zinc was nearly double that of iron; 2) lead, germanium and indium can be collected in the copper melt besides zinc and iron, and there was no significant difference for the concentration of those metals (Table XVI).

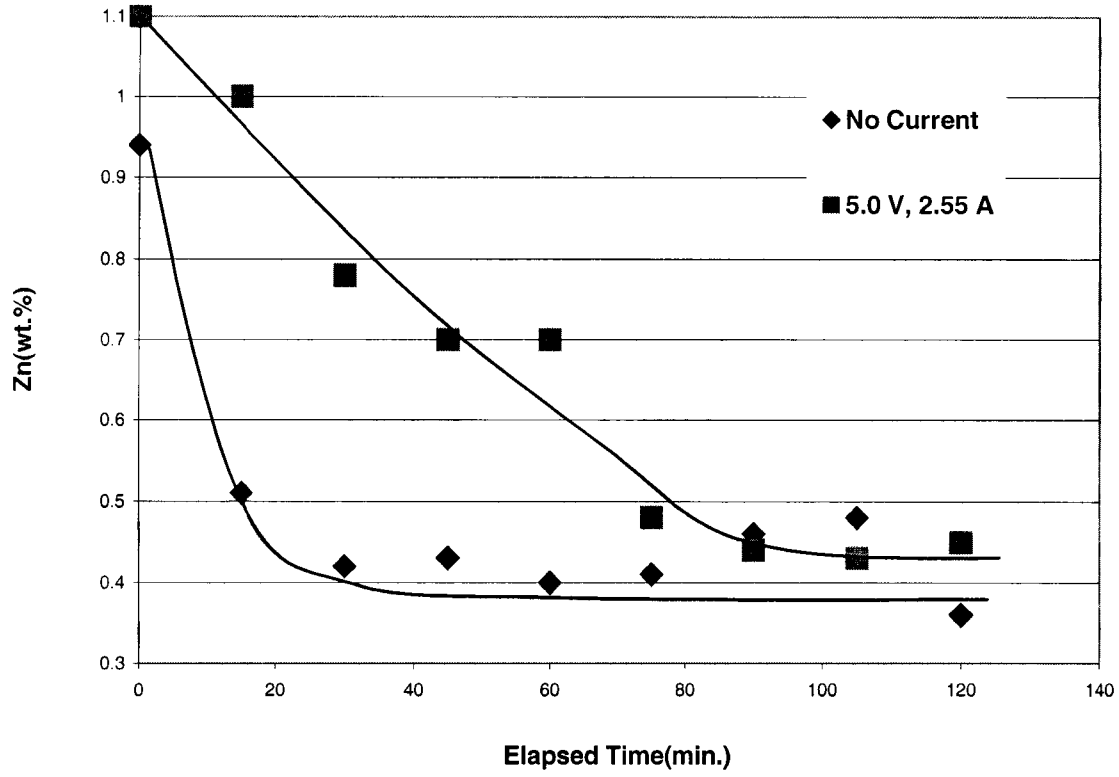

Fig. 49 — The zinc concentration change of synthetic tail slag at 1350 °C (with copper)

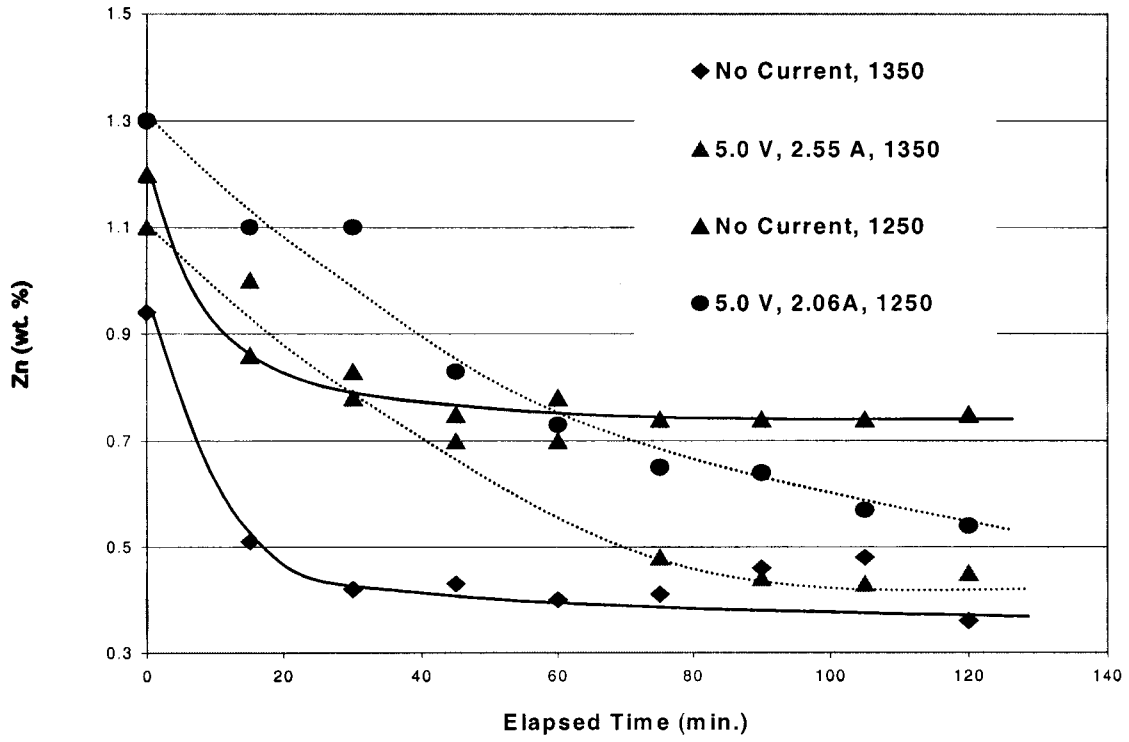

Fig. 50 — The effect of temperature on the zinc concentration in synthetic slag

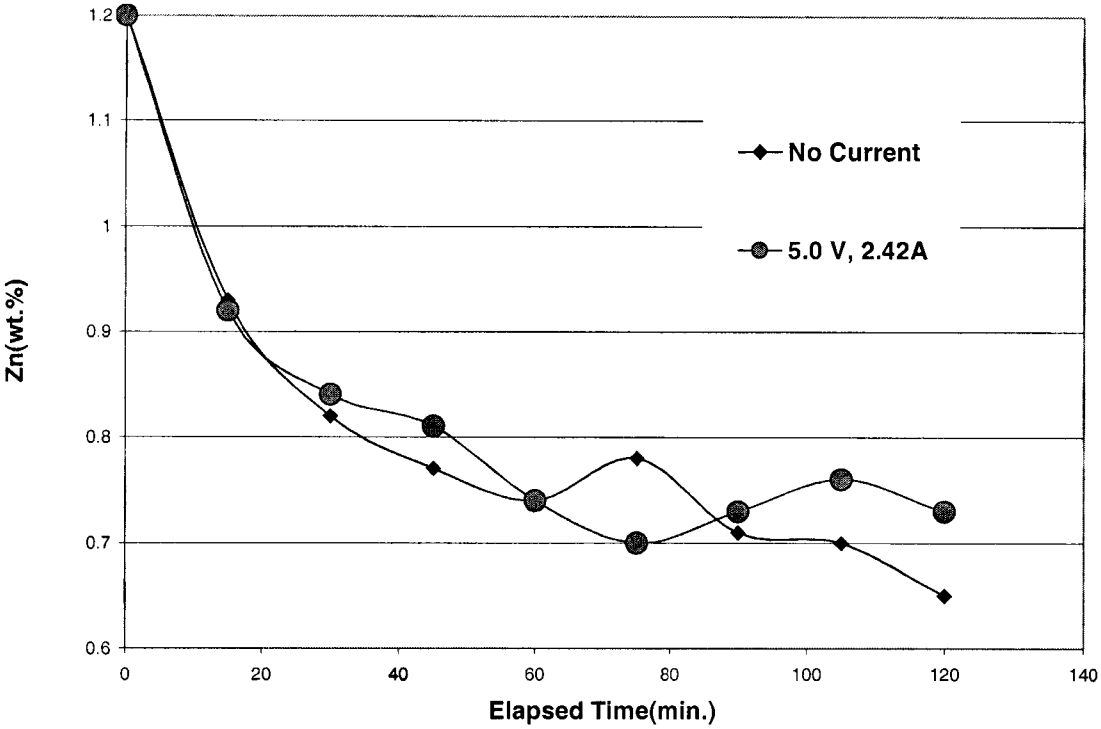

Fig. 51 — The zinc concentration change of synthetic tail slag when CaO ratio increased (with copper, at 1250 °C)

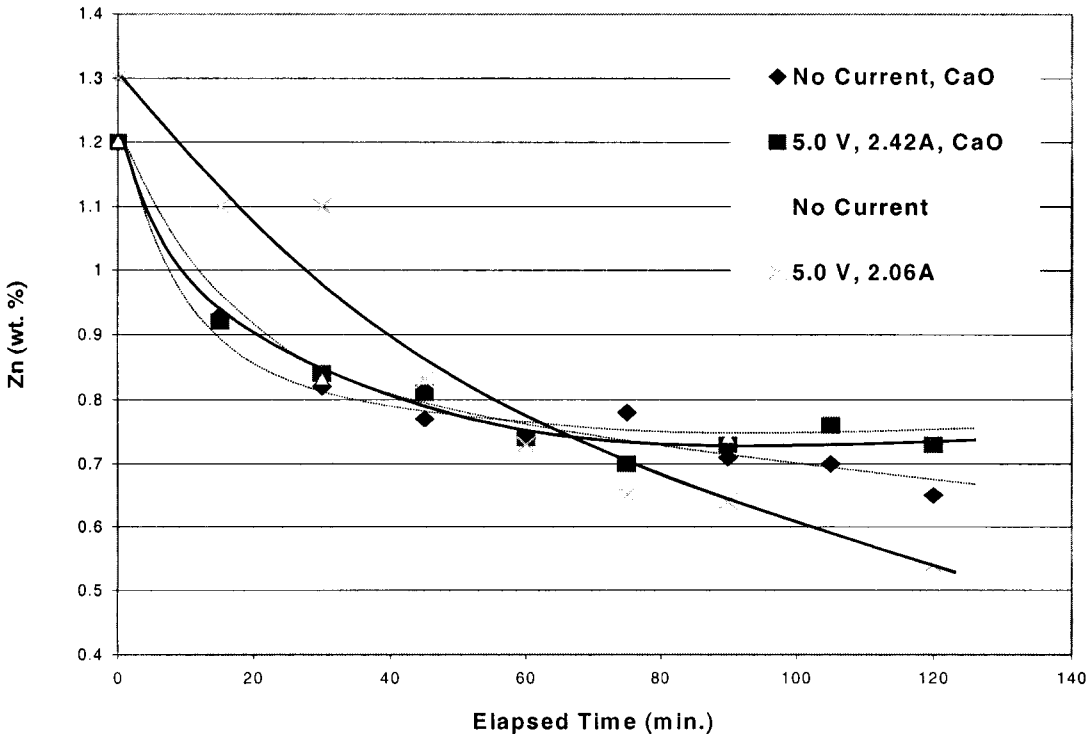

Fig. 52 — Comparing the zinc concentration changes when CaO concentration varies in synthetic tail slag at 1250 °C

Table XVI. The Concentrations for Some Metals of Interest in Copper Cathode (Cominco Slag)

	Fe (wt.%)	Zn (wt.%)	Pb (ppm)	Ge (ppm)	In (ppm)
No Current	0.06	0.27	5999	41	63
5.0 Volts	0.28	0.64	6569	43	67

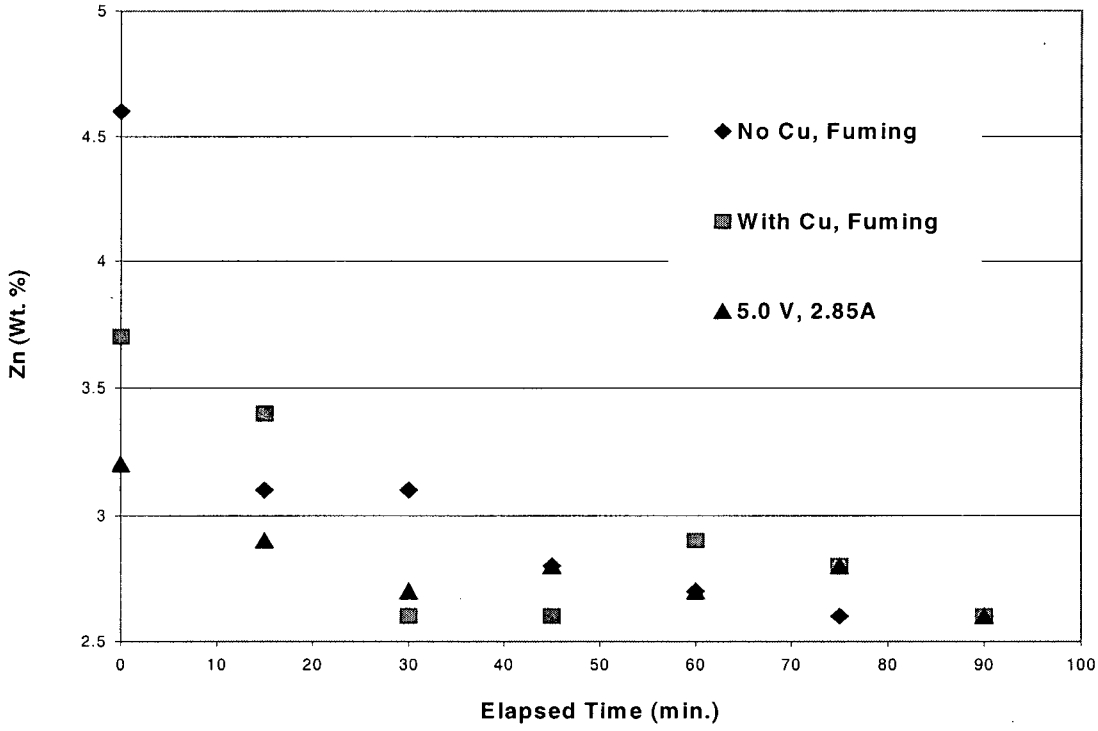

Fig. 53 — The effect of copper, voltage on the concentration of zinc of Cominco tail slag (1250 °C)

8. CONCLUSIONS

The present research work in The University of British Columbia has yielded valuable information that lead to several important conclusions:

1. Even without current passing, some zinc can be recovered from the slag to the copper melt by a thermodynamic driving force.
2. FACT calculation results indicated that, by introducing copper as the cathode, electrode potential difference of about 0.2 volts at the interface could effect electrolysis.
3. When the cell voltage was below 4 volts, the effect of current passing on the recovery of zinc from slag was negligible. When the voltage was 6 volts or over, more iron was deposited into the copper cathode. This is in agreement with the estimation that the cell voltage for the zinc slag electrorefining should be around 5 volts.
4. The cathode current efficiency was 68%, calculated from the concentration differences of zinc and iron in slag and copper; because of iron in the slag, some electronic conduction was anticipated.
5. Some of the zinc reported to fume and small amount of iron circulation between anode and cathode made the cathode current efficiency less than the expected value of around 90%.
6. The zinc concentration could be lowered to 0.5 per cent by a total voltage of 5 volts applied to the slag electrorefining cell, comparing the results for fuming (about 1.1 per cent without copper and 0.75 with copper).
7. The patterns of the zinc concentration evolution of the synthetic slag indicated that fuming without copper and with copper were chemically driven and, after about 30

minutes, they reached chemical equilibrium. However, the run with current passing had a constant zinc concentration drop, which indicated that an electro-chemical reaction was happening.

8. There was very limited decrease of current for the entire two-hour electrorefining runs with constant voltage of 5 volts.
9. When the working temperature increased from 1250 °C to 1350 °C, both of the fuming and electro-reduction became more effective for synthetic slags (page 96). After the zinc concentration was lowered to about 0.45 per cent, there was no more decrease with the same current flow.
10. The increase of CaO concentration (from 15 per cent to 20 per cent) in synthetic slags made the effect of electrorefining insignificant.
11. Some trace metals, such as Pb, In, Ge, and other precious metals could be collected in copper while electrifying zinc from slag, because copper is a good "getter" for these metals also.
12. With the as-received ***Cominco*** tail slag, the effects of copper for the fuming and the current passing for electrorefining were not as significant as that for synthetic. This might be due to the complexity of the slag and needs to be clarified in the future experiments.

9. RECOMMENDED WORK

- Measurement of the slag resistance, variation with composition, temperature;
- Electrode potential measurement for better understanding of the cell voltage and the current density, overpotential and reaction rate;
- Since the anode was Pt cylinder, for O_2 evolution consideration, bubbling of anode O_2 gas? Rotating anode disk research;
- Other anode material available, such as "mild steel" and graphite (consumable and sacrifice) to replace Pt for further commercial production operation. Also, the anode overpotential will decrease, and Fe => Fe^{2+} reaction provides a higher Fe^{2+}/ Fe^{3+} ratio, which is favorable for the electrorefining;
- The behavior of other elements, Pb, In, Ge, Au, Ag, etc. in slag? How effective is the proposed electrorefining for those metals?
- The surface properties of slag and metal copper, additives to decrease the surface tensions (which are not impairment the electrolysis), to increase the wetting ability between slag and metal copper?

REFERENCES

1. Personal communication, Cominco
2. J. M. Floyd and G. P. Swayn, "An update of Ausmelt technology for zinc and lead processing", Zinc and Lead Processing, The Metallurgy of CIM, 1998, pp. 861-74.
3. G. G. Richards, J.K. Brimacombe, and G. W. Toop, "Kinetics of the Zinc Slag-Fuming Process: Part I. Industrial Measurements", Metallurgical Transactions B, vol. 16B, 1985, pp 513-27.
4. G. G. Richards, J. K. Brimacombe, and G. W. Toop, "Kinetics of the Zinc Slag-Fuming Process: Part II. Mathematical Model", Metallurgical Transactions B, vol. 16B, 1985, pp 529-40.
5. G. G. Richards, J. K. Brimacombe, and G. W. Toop, "Kinetics of the Zinc Slag-Fuming Process: Part III. Model Predications and Analysis of Process Kinetics", Metallurgical Transactions B, vol. 16B, 1985, pp 541-49.
6. Albert F. S. Schoukens, Glen M. Denton, and Rodney T. Jones, "PILOT-PLANT PRODUCTION OF PRIME WESTERN GRADE ZINC FROM LEAD BLAST-FURNACE SLAGS USING THE ENVIROPLAS PROCESS", Third International Symposium on Recycling of Metals and Engineering Materials, Edited by P.B. Queneau and R.D. Peterson, The Minerals, Metals & Materials Society, 1995, pp. 857-68.
7. W. R. N. Snelgrove and John C. Taylor, "THE RECOVERY OF VALUES FROM NON-FERROUS SMELTER SLAGS", Canadian Metallurgical quarterly, vol. 20, No.2, 1981, pp. 231-40.
8. J. G. Peacey and P. J. Hancock, "REVIEW OF PYROMETALLURGICAL PROCESSES FOR TREATING IRON RESIDUES FROM ELECTROLYTIC ZINC PLANTS", IRON CONTROL AND DISPOSAL: PROCEDDINGS OF THE SECOND INTERNATIONAL SYMPOSIUM ON IRON CONTROL IN HYDROMETALLURGY, OTTAWA, CANADA, OCTOBER 20-23, 1996, pp. 17-35.
9. D. W. Ashman "A REVIEW OF ZINC LEACH RESIDUE TREATMENT OPTIONS FOR COMINCO'S OPERATIONS", IRON CONTROL AND DISPOSAL: PROCEDDINGS OF THE SECOND INTERNATIONAL SYMPOSIUM ON IRON CONTROL IN HYDROMETALLURGY, OTTAWA, CANADA, OCTOBER 20-23, 1996, pp. 37-48.
10. N. J. Themelis, J. G. Peacey and Q. Jiao, "RECOVERY OF ZINC IN A SLAG RESISTANCE ELECTRIC FURNACE", H. H. Kellogg International Symposium Quantitative Description of Metal Extraction Processes, Edited by N. J. Themelis and P. F. Duby, The Minerals, Metals & Materials Society, 1991, pp. 331-47.
11. Dhiren Kumar Panda, Ph.D Dissertation, The University of Missouri-Rolla, USA, 1997.
12. Ismail, DAL, "THE MECHANISM AND KINETICS OF REDUCTION OF ZINC OXIDE FROM SLAGS AND THE EFFECT OF SULPHUR", Ph.D. dissertation, University of Melboune, Australia, Oct. 1995.
13. G. Courtney, Proc. Australas., I.M.M., N.S., no. 38, 1920, pp. 75-84.
14. R. B. Caples, J. Amer. Zinc Inst., vol. 14, 1931, pp. 81-85.

15. G. E. Murray, Trans. Canadian I. M. M., vol. 36, 1933, pp. 90-92.
16. C. Mattich, K. Hasselwander, H. Lommert and A. N. Beyzavi, "Electrolytic zinc manufacture with Waelz treatment of neutral leach residues", Zinc and Lead Processing, 1998, pp. 561-78.
17. J. D. Mackenzie, "Oxide Melts", Advance in Inorganic Chemistry and Radiochemistry, 1962, pp. 293-317.
18. Carlos Diaz, "THE THERMODYNAMIC PROPERTIES OF COPPER-SLAG SYSTEMS", INCRA SERIES ON THE METALLURGY OF COPPER, 1974, pp.67-73.
19. R. H. Aiken, U. S. Patent 816142, March 27, 1906.
20. C. Doelter, Monatshette für Chemie, 1907, vol. 28, pp. 1313-79.
21. F. Sauerwald and G. Neuendorff, Zisch. Elektrochem., 1925, vol. 31, pp. 643-46.
22. F. Rarup, W. Fleischer, and E. Holtan: Chem. Und Industrie, 1924, vol. 12, pp. 11-15.
23. A. Wejnarth, Trans. Amer., Electro-Chem. Soc., 1934, vol. 63, pp. 177-87; vol. 66, pp. 329-43.
24. A. E. Martin and G. Derge, Trans. AIME, 1943, vol. 154, pp. 104-15.
25. Henry Inoury, J. W. Tomlinson and John Chipman, "THE ELECTRICAL CONDUCTIVITY OF WÜSTITE MELTS", Trans. Faraday Soc., 49, 1953, pp. 796-801.
26. M. T. Simnad, G. Derge, and I. George, "Ionic Nature of Liquid Iron-Silicate Slags", AIME Trans., 1954, vol. 200, pp. 1386-90.
27. D. A. Dukelow and G. Derge, "Electrochemistry Characteristic of FeO-MnO-SiO_2 Melts", AIME Trans.,1960, vol. 218, pp. 136-41.
28. Walter R. Dickson and Edward B. Dismukes, "The Electrolysis of FeO-CaO-SiO_2 Melts", AIME Trans., 1962, vol. 224, pp. 505-11.
29. J. O'M. Bockris, J. A. Kitchener, S. Ignatowicz and J. W. Tomlison, "Electric Conductance in Liquid Silicates", Transactions of the Faraday Society, 1952, vol. 48, pp. 75-90.
30. A. A. Hejia, Doctoral Thesis, The University of Witwatcrarand, Sept. 1975.
31. K. S. Goto, Proceesings of International Symp. On Metall. Slags, AIME, 1984, pp. 839-61.
32. K. S. Goto, M. Sasabe, and M. Kawakami, Trans. ISIJ, 1977, vol. 17, pp. 212-14.
33. Q. Jiao and N. J. Themelis, "Correlation of Electrical Conductivity to Slag Composition and Temperature", Metallurgical Transactins B, vol. 19B, 1988, pp. 133-40.
34. C. R. Masson, "Application of Temkin's Law to Polyionic Melts", presented at International Symp. On Metall. Slags, held by Metall. Soc. Of CIM, Aug. 1980.
35. A. Fontana, L. Segers, K. Twite and R. Winand, "Electrical Conductivity of Ferrous Silicate Melts from Slag Cleaning Operations", TMS-AIME Paper Selection, Paper No. A 84-38, 1984.
36. G. S. Victorovich, C. Diaz, and D. K. Vallbacka, Proceedings of International symp. On Metall. Slags, TMS-AIME, 1984, pp. 907-25.
37. Philip Gray, "Zinc Production – The Warner process", Mining Magazine(UK), vol. 166, no. 1, pp. 14-17, Jan. 1992.
38. P. M. J. Gray, "the Warner Zinc Process", World Zinc '93, Hobart, TAS, Australia, 10-13 Oct. 1993, pp. 483-89.

39. Noel A Warner, "Method of recovery zinc", US Patent No US5358544, 15rd Oct. 1994.
40. Supachai Surapunt, Y Takeda, and K. Itagaki, "Dissolution of zinc in $CaO-SiO_2-FeO$ slag coexisting with liquid Cu-Zn-Fe", Journal of the Mining and materials Processing Institute of Japan, vol. 111, issue: 8, July 1995, pp: 553-8.
41. K. Azuma, S. Goto, and O. Ogawa, "Thermodynamic studies on zinc oxide in slag", J. Fac. Eng. Univ. Tokyo, Ser. A, 5, 1967, pp: 8-22.
42. A. W. Richards and D. F. J. Thorne, "The Activities of zinc Oxide and Ferrous Oxide in Liquid Silicate Slags", Physical Chemistry of Process Metallurgy, Part I (ed. G. R. St. Pierre), 1961, pp: 177-91.
43. S. Wright, W. T. Denholm and W. J. Rankin, "The Activity of Zinc and Lead Oxides in Lead Blast Furnaces Slags", Non-ferrous Smelting Symposium, Port Pirie South Australia, September 1989, pp: 79-85.
44. Yoichi Takeda, "ACTIVITIES OF LEAD AND ZINC OXIDES IN $CAO-SiO_2-FeO$ SLAG", ZINC & LEAD '95, Proceedings of the International Symposium on the Extraction and Applications of Zinc and Lead, Sendai, Japan, pp:766-76.
45. Supachai Surapunt, Rodriguez R. Vazquez and K Itagaki, "Activity measurements in liquid Cu-Zn-X(X=lead, silver, gold) ternary alloys", Journal of the Mining and materials Processing Institute of Japan, vol. 110, issue: 8, July 1994, pp. 631-5.
46. Supachai Surapunt and M. Hiro, "Activity of zinc in molten Cu-Zn-Fe ternary system", Journal of the Mining and materials Processing Institute of Japan, vol. 111, issue: 8, June 1995, pp. 495-9.
47. David R. Gaskell, "Introduction to Metallurgical Thermodynamics", 1973.
48. N. J. Filipovska and H. B. Bell, "Activity measurements in $FeO-CaO-SiO_2$ and $FeO-CaO-Al_2O_3-SiO_2$ slags containing zinc oxides saturated with iron at 1250 °C", Inst. Min. Metall. Trans. C, 87, pp: 94-8.
49. K. Grjotheim, C. Krohn, M. Malinovský, K. Matiašovský and J. Thonstad, "Aluminum Electrolysis – The Chemistry of the Hall-Héroult Process", 1977.
50. Harold R. Larson and Thomas w. Eagar, "The Plasma-Enabled Recovery of Titanium by the Electrolysis of Titanate Slags", JOM, September 1998, pp. 56-7.
51. Warren Geoffry Frank, Horstik Alfred, Corbetta Alberto, Malpas Richard Edward, Honders Antonie and Van Eijden Gerbrand Jozef, "Process for the electrolytic production of metals", EP0219157, 22th Apr. 1987.
52. Blander Milton (US), Wai Chien M (US), and Nagy Zoltan (US), "Extraction of trace metals from fly ash", US4475993, 9th Oct. 1984.
53. Sergei A. Degterov, Yves Dessureault and Arthur D. Pelton, "THERMODYNAMIC MODELING OF ZINC DISTRIBUTION AMONG MATTE, SLAG AND LIQUID COPPER", Canadian Metallurgical Quarterly, vol. 39, No 1, pp. 43-54, 2000.
54. C. W. Bale, W. T. Thompson, A. D. Pelton, G. Eriksson and P. K. Talley and J. Melancon, "Recent developments in the F*A*C*T system", COMPUTER SOFTWARE IN CHEMICAL AND EXTRACTIVE METALLURGY: PROCEEDINGS OF THE 2^{ND} INTERNATIONAL SYMPOSIUM ON COMPUTER SOFTWARE IN CHEMICAL AND EXTRACTIVE METALLURGY, QUEBEC CITY, QUEBEC, AUGUST 29-SEPT. 1993, pp. 73-86.
55. Steven S. Zumdahl, "Chemistry, second Edition", 1989, pp. 328.

56. Donald R. Sadoway, "A materials systems approach to selection and testing of nonconsumable anodes for the Hall cell", Light Metals 1990, pp. 403-7.
57. Rudolf P. Pawlek, "INERT ANODES FOR THE PRIMARY ALUMINUM INDUSTRY: AN UPDATE", Light Metals 1996, pp. 243-7.
58. T. R. Alcorn, A. T. Tabereaux, N. E. Richards, C. F. Windisch, Jr., D. M. Strachan, J. S. Gregg, and M. S. Frederick, "OPERATIONAL RESULTS OF PILOT CELL TEST WITH CERMET "INERT" ANODES", Light Metals 1993, pp. 433-43.
59. Thaddeus B. Massalski, "Binary Alloy Phase Diagrams", 1990.
60. Adrian Fu, "REFINING OF A COMINCO TAIL SLAG", Research Report, Department of Metals and Materials Engineering, The University of British Columbia, 1997.
61. X. W. Pan, "Electrochemical effects of direct current on the reduction of manganese oxide from molten MnO-SiO2-CaO-Al2O3 slag", Journal of the South African Inst. Of Mining and Met. Sept., 1995, pp: 221-224.
62. Peter Vanýsek, "Electrochemical Series", Handbook of Chemistry and Physics, (David R. Lide, Edit-in-chief), 75th Edition, 1994-1995, pp. **8**-21-**8**-26.
63. David E. Woolley and Uday B. Pal, "Experimental Evidance for Electrochemical Nature of the Reaction between Iron Oxide in Calcia-Silica-Alumina Slag and Carbon in Liquid Iron", Metallurgical and Materials Transactions B, vol. 30B, oct. 1999, pp. 877-89.

APPENDIX I — Process Conditions and Results for Zinc Fuming Runs[3-5,10]

Company	Zinc Concentration		Fuming Time (min)	Bath Temp. (^{0}C)
	Initial Pct	Final Pct		
A	**11.0**	**5.0**	**80**	-
	4.5	**0.8**	**60**	-
	4.3	**0.8**	**60**	-
B	**14.5**	**2.6**	**100**	-
	13.4	**1.4**	**95**	-
	12.5	**1.8**	**90**	-
C	**8.5**	**3.4**	**60**	**1170 - 1210**
	12.1	**2.2**	**150**	**1230 - 1315**
D	**11.7**	**1.9**	**79**	**1190 - 1250**
	10.1	**3.1**	**70**	**1165 - 1194**
E	**7.8**	**2.3**	**105**	-
Asarco, El Paso[10]	**12**	**2**	**65**	-
Cominco, Peters	**10**	**2**	**100**	-
Port Pirie, Grant , #198	**10.5**	**3.8**	**50**	-
Port Pirie, Grant , #207	**8.4**	**3.0**	**50**	-
Boliden, Lehner	**9.0**	**2.0**	**100**	-
Portovesme, continuous	**14.9**	**7.0**	-	-
Hoboken, continuous	**7.2**	**5.7**	-	-
AMAX, continuous	**4.7**	**1.9**	-	-

Ave. = 2.3

APPENDIX II — Operating conditions for commercial Ausmelt plants[2]

No	Company	Location	Year Started	ID (m)	Cont. or Batch*1	Feed Type	Design Feed Rate(tpa)	Product	Temp Range (^{0}C)	Fuel	Reductant	Air or Oxygen*2	Lance Tip*3
1	Broken Hill Associated Smelter	Port Pirie, South Australia	1988	0.9	B2	Lead Refinery Retort Bullion	1000	Silver/Gold Metal	900 - 1100	Light Oil	Coal	0.21	(1) O (2) O
2	Rio Tinto Zimbabwe	Eiffel Flats, Zimbabwe	1992	1.5	B2	Lead Residue	7700	Desulph Ni/Cu matte	1250 - 1350	Coal	Coal	0.21	(1) O (2) R
3	Korea Zinc(1)	Onsan, Korea	1992	3.2	C1	QSL Furnace Slag	100000*4	Zn/Pb Fume	1300	Coal	Coal	0.35	N or R
4	Mitsui	Hachinohe, Japan	1993	2.4	C1	ISF Slag	80000	Zn Fume	1300 - 1350	Heavy Oil	Heavy Oil/Coke Breeze	0.21	R
5	Anglo American Corp.	Bindura Zimbabwe	1995	2.2	B3	Leach Residue	10000	Blister Copper	1250 - 1300	Coal	Coal	0.21	(1) N (2) O (3) R
6	Korea Zinc(2) F1	Onsan, Korea	1995	3.9	C2	Zinc Leach Residue	120000	Zinc/Lead Fume	1250 - 1300	Coal	Coal	0.35	N
7	Korea Zinc(2) F2	Onsan, Korea	1995	3.2	C2	F1 Slag (liquid)	100000	Zinc Fume	1250 - 1300	Coal	Coal	0.21	R/N
8	Metaleurop	Nordenham, Germany	1996	3.4	C1/B2	Battery Paste High Pb Conc.	122000	Lead Bullion	950 - 1250	Natural Gas	Coal/Pet Coke	0.21-0.40	N/O/R
9	Minsur/Funsur	Pisco, Peru	1996	3.4	B2	Tin Conc.	30000→40000	Tin Metal	1150 - 1300	Light Diesel Oil	Coal	0.21-0.40	N/R

10	Consolidated Gold Fields	Tsumeb, Namibia	1997	4.4	B2	Low Pb Conc./Second	120000	Lead Bullion	1150 - 1250	Heavy Furnace Oil	Coal	0.21	O/N/R
11	Portland Aluminium Alcoa	Portland, Australia	1997	-	B2	Spent Pot Lining	12000	AlF_3	1250	Natural Gas	-	0.40	O/N
12	Hindustan Copper Limited	Ghatsila, India	1998	0.5	B2	Anode Slimes	72	Silver-Gold Doré	1000 - 1100	Light Diesel Oil	-	0.21	(1) N (2) O
13	Zhong Tiao Shan F1	China	1998	4.4	C	Copper Conc.	200000	Copper Matte (60%)	1200	Coal	-	0.40	O
14	Zhong Tiao Shan F2	China	1998	4.4	B	Copper Mattw	67000	Blister Copper	1300	Coal	-	0.21	O
15	SASE *6	Whyalla, Australia	1998	*5	C	Iron Ore	15000	Pig Iron	1450	Coal	Coal	0.60	R
16	Korea Zinc(3)	Onsan, Korea	1999	*7	C	Lead Secondaries	100000	Lead Bullion	1000	Coal	Coal	0.4	R

Notes for the Table:

*1 Continuous stage = C1, Continuous two stage = C2, Batch one stage = B1, Batch two stage = B2, Batch three stage = B3

*2 Fraction oxygen Air = 0.21, Oxygen =>0.21

*3 Oxidizing = O, Neutral = N, Reducing = R

*4 100,000 for liquid slag, 50,000 for solid slag

*5 Elliptical furnace = 5m x 3m

*6 Demonstration plant under design

*7 Under design at present

Typical Composition of Slag and Fume

	Zn (wt%)	Pb (wt%)	Cu (wt%)	Ag (g/t)	S (wt%)	FeO (wt%)	SiO_2 (wt%)	CaO (wt%)
ISF Slag	6.5	0.5	0.4	30	2.7	37	20	14
Fumer Slag	3.0	0.1	0.5	25	2.6	40	19	13
Fume	60	12	0.1	100	0.5	0.3	0.1	0.1

APPENDIX III — The activity coefficient of zinc oxide determined by several investigators [43]

Temp (^{0}C)	CaO/SiO_2	$\%Al_2O_3$	%FeO	N_{ZnO}	γ_{ZnO}
Azuma (1967) 1200	**1.17**	**-**	**47.0**	**0.026**	**3.0**
	0.93	**-**	**50.0**	**0.040**	**3.0**
	1.0	**-**	**45.9**	**0.052**	**2.9**
	0.83	**-**	**50.4**	**0.085**	**3.3**
	0.85	**-**	**50.9**	**0.118**	**2.7**
Richards (1961) 1250	**0.93**	**8.5**	**36.1**	**0.008**	**2.6**
	1.11	**-**	**37.4**	**0.008**	**2.8**
	0.93	**8.5**	**35.9**	**0.010**	**2.8**
	0.93	**8.5**	**35.7**	**0.012**	**2.8**
	1.11	**-**	**37.2**	**0.014**	**3.1**
Grant (1980) 1200	**1.10**	**9-10**	**20-26**	**0.02-0.1**	**3.4**
Filipovska (1978) 1250	**1.10**	**10.0**	**32.0**	**0.04-0.08**	**1.7**
	1.0	**10.0**	**35.0**	**0.04-0.08**	**1.5**
	0.95	**10.0**	**30.0**	**0.04-0.08**	**1.5**
Levin (1966)	**1.15**	**-**	**31.1**	**0.022**	**2.1**
1300	**1.31**	**-**	**31.0**	**0.010**	**3.2**
Wright (1989) 1300	**1.10**	**7-9**	**28.5**	**0.02-0.1**	**3.4**

APPENDIX IV — Warner Process

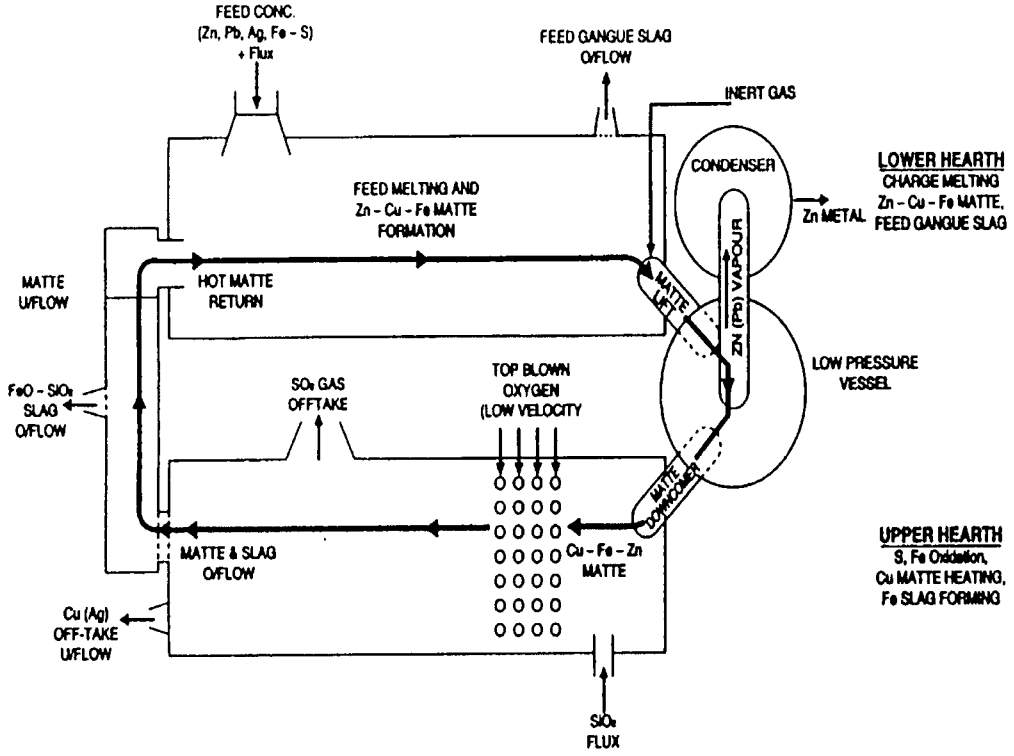

APPENDIX V — Schematic illustration of a high pressure zinc extraction process